University of Naples "FEDERICO II"

Department of Biology

Ph.D. in Advanced Biology

Section: Molecular Systematic
XXV Cycle

New Dehydrogenase/Reductase as Biocatalysts for Stereoselective Reduction of Prochiral Ketones

Ph. D.

Pennacchio Angela

Coordinator

Prof. Gaudio Luciano

Tutors

Dott. Carlo A. Raia

Prof.ssa Serena Aceto

April 30th, 2013

TABLE OF CONTENTS

Abbreviations

ADH	Alcohol dehydrogenase
BMIMBF4	1-Butyl-3-methylimidazolium tetrafluoroborate
BSA	Bovine serum albumin
BsADH	ADH from *Bacillus stereothermophilus*
ClMBF	Methyl *o*-chlorobenzoylformate
ClMM	Methyl (*R*)-*o*-chloromandelate
CMA	*trans*-Cinnamaldehyde
CMO	Cinnamyl Alcohol
DNA	Deoxyribonucleic acid
EDTA	Ethylenediaminetetraacetic acid
ee	Enantiomeric excess
EMO	Ethyl 3-methyl-2-oxobutyrate
IPTG	Isopropyl β-D-1-thiogalactopyranoside
LB	Luria Bertani medium
MBF	Methyl benzoylformate
MES	2-(N-morpholino) ethanesulfonic acid
MM	Methyl (*R*)-mandelate
$NAD(P)^+$	Nicotinammide adenine dinucleotide (phosphate),oxidized form
NAD(P)H	Nicotinammide adenine dinucleotide (phosphate), reduced form
NEB	New England Biolabs
PCR	Polymerase chain reaction
PMSF	Phenylmethylsulfonyl fluoride
SaADH	ADH from *Sulfolobus acidocaldarius*
SDR	Short-chain dehydrogenase
TaGDH	Glucose dehydrogenase from *Thermoplasma acidophilum*
TtADH	ADH from *Thermus thermophilus*

Abstract

Biocatalysis is well-matched to chemical synthesis in the pharmaceutical as well as the agrochemical and flavours industry. A significant number of products are chiral in at least one center, and many of them have multiple chiral centers. These compounds are usually manufactured in single isomer form since the current Food and Drug Administration regulations demand proof that the non-therapeutic isomer is non-toxic. The synthesis of a chiral center requires enantio and regioselective catalysts, and enzymes are consistently the most selective catalysts available being able to perform reactions under mild conditions of pH value, temperature, and pressure in aqueous solutions, a greener approach to chemistry, with remarkable chemo-, regio-, and stereoselectivity. Chiral alcohols are very important precursors for a large number of drugs, agrochemical and flavours. Their production by asymmetric bioreduction of a prochiral carbonyl precursor is becoming well-established in the field of biocatalysis. Enzymes that catalyze ketone reductions (known as ketoreductases) are a reliable source of high enantiomeric excess chiral alcohols.

The aim of the present PhD research is to characterize new alcohol dehydrogenases (ADHs) for the synthesis of chiral secondary alcohols and the structural study of the isolated enzymes for the understanding of the structure-function relationships.

The basic approach was to identify oxidoreductases with these distinctive features, operational stability and NAD dependency, by looking for in the genome of thermophilic microorganisms for genes coding putative short-chain dehydrogenases/reductases (SDR) with an acidic residue which determines NADH specificity in a particular position of the sequence.

In the present work an applicative development of *Thermus termophilus* ADH in the asymmetric synthesis of two valuable chiral building blocks methyl (*R*)-mandelato and methyl (*R*)-*o*-chloromandelate at lab scale was carried out, and adaption of two different enzyme-coupled systems for the cofactor regeneration system was studied.

Two novel NADH dependent-ADHs identified in the crenarchaeon *Sulfolobus acidocaldarius* SaADH and SaADH2 were biochemically characterized, a suitable cofactor regeneration system for the analytical study of the stereoselectivity both enzymes was utilized, moreover, the solved SaADH2 3D structure was discussed.

Finally, an applicative utilization of *Bacillus stearothermophilus* ADH both as an isolated enzyme, and in recombinant *E. coli* whole cells in the synthesis of cinnamyl alcohol, a versatile fine chemical, by chemoselective reduction of cinnamaldehyde at gram scale was described.

Sintesi

La biocatalisi ha di recente assunto una crescente importanza nella sintesi chimica di prodotti nel settore agroalimentare, delle fragranze e soprattutto nel settore farmaceutico per la preparazione di composti enantiomericamente puri. Un numero significativo di farmaci sono chirali in almeno un centro e devono essere prodotti come singolo isomero, poiché la regolamentazione internazionale (Food and Drug Administration) richiede la certificazione che l'isomero non terapeutico sia non tossico.

La sintesi di un centro chirale richiede catalizzatori enantio e regioselettivi, e gli enzimi sono i catalizzatori più selettivi disponibili per poter effettuare queste reazioni in condizioni blande di pH, temperatura e pressione in soluzione acquosa, un più verde approccio per la chimica, e con notevole chemo-, regio-e stereoselettività. Gli alcoli chirali sono precursori molto importanti per un gran numero di farmaci, agrochimici ed aromi.

La produzione di alcoli chirali mediante riduzione asimmetrica di un precursore carbonilico prochirale è ben consolidata nel campo della biocatalisi. Gli enzimi che catalizzano la riduzione di chetoni, le ossidoriduttasi, sono in grado di fornire alcoli dall'elevatissima purezza ottica. Lo scopo del presente progetto di ricerca è la caratterizzazione di nuove alcol deidrogenasi (ADH) per la sintesi di alcoli secondari chirali e lo studio della relazione struttura-funzione degli enzimi isolati. L'approccio

di base è stato identificare ossidoriduttasi con due caratteristiche distintive, stabilità operativa e dipendenza dal NAD(H), cercando nel genoma di microrganismi termofili geni codificanti putative deidrogenasi/riduttasi a catena corta avente un residuo acidico in una particolare posizione della sequenza che determina la specificità per il NADH.

Nel presente lavoro è stata realizzata la sintesi asimmetrica in scala di laboratorio di due precursori di notevole interesse applicativo, (*R*)-mandelato di metile e (*R*)-*o*-cloro-mandelato di metile, mediante l'ADH di *Thermus termophilus*, e lo sviluppo di due diversi sistemi enzimatici per la rigenerazione del cofattore.

Inoltre, due nuove ADH NADH-dipendenti individuate nel crenarchaeon *Sulfolobus acidocaldarius*, SaADH e SaADH2, sono state caratterizzate biochimicamente; per lo studio analitico della stereoselettività di entrambi gli enzimi è stato utilizzato un adeguato sistema di rigenerazione del cofattore. La struttura 3D di SaADH2 è stata risolta a 1.75 Å e discussa.

Infine, un efficiente sistema di sintesi dell'alcol cinnamilico per riduzione chemoselettiva della cinnamaldeide è stato sviluppato, utilizzando l’alcol deidrogenasi di *Bacillus stearothermophilus* (BsADH), sia come enzima isolato sia in cellula intera.

INTRODUCTION

Biocatalysis

Biocatalysis is increasingly being used in synthetic routes to complex molecules of industrial interest. Biocatalysts not only commonly work under ambient conditions of temperature, pH value, and pressure in aqueous solutions, a greener approach to chemistry but, most importantly, are highly chemo-, regio-, and stereoselective and therefore of great interest in fine chemical synthesis. The main role for biocatalysis is in the agrochemical, flavours and pharmaceutical sector for the preparation of enantiomerically pure compounds. Compounds with a chiral centre are usually manufactured in single isomer form since the current Food and Drug Administration regulations demand proof that the non-therapeutic isomer is non-toxic. Many of these molecules are also structurally complex and contain multiple chiral centres.

Chirality and drugs

Chirality is a key factor in the efficacy of many drugs. The classic case of failure to take account of chirality concerned the drug thalidomide, a mild analgesic prescribed for pregnant women in the 1960s (Fig. 1). This relatively simple compound contains only one chiral centre yet the chirality proved crucial to the biological effects of the drug. Since the working environment of drugs in nature is chiral, enantiomers are not identical

chemical entities. With respect to their receptor complexes they have a diastereoisomeric relationship. In the case of thalidomide, no heed was taken of the potential consequences of this relationship and the drug was manufactured and sold as a racemic mixture. Tragically, women who had taken the drug gave birth to deformed offspring. Further research showed that only the *S* isomer was teratogenic and the *R* isomer was safe.

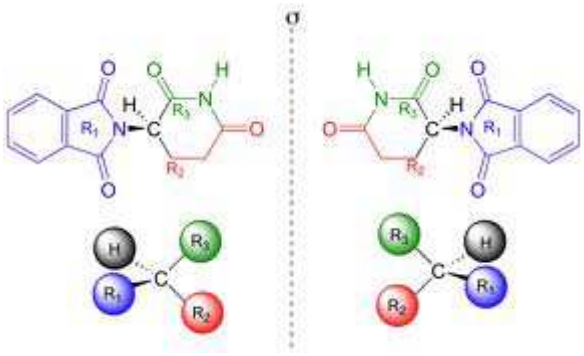

(*S*)-(-)-N-(2,6-dioxo-3-piperidyl)phthalimide
or
(*S*)-thalidomide
Teratogenic

(*R*)-(+)-N-(2,6-dioxo-3-piperidyl)phthalimide
or
(*R*)-thalidomide
Safe Analgesic

Figure 1. Representation of the enantiomers of thalidomide.

Drugs are compounds that in small amounts trigger a response in living organisms. Many processes within an organism sensitive to the action of a drug, such as the inhibition of an enzyme, the process of transport across the membrane, the binding of receptors, depend on the stereochemistry of the molecule-drug (Jamali et al. 1989; Sundby 2003). Biological activity, toxicity, or the metabolism of the drug can be very different for the

enantiomers of a chiral drug. In fact, there are many examples in which one enantiomer of a chiral drug has a therapeutically useful action and the other enantiomer but no, one enantiomer is toxic and the other is safe (see the case of thalidomide), one is agonist and the other is antagonistic (Table 1).

Table 1. Enantiomers may confer benefits over racemates for therapeutic uses

Properties of racemate	**Potential benefits of enantiomer**
One enantiomer is exclusively active	Reduced dose and load on metabolism
The other enantiomer is toxic	Increased latitude in dose and broader use of the drug
Enantiomers have different pharmaco-kinetics	Better control of kinetics and dose
Enantiomers metabolized at different rates in the same person	Wider latitude in setting the dose; reduction in variability of patients' responses
Enantiomers metabolized at different rates in the population	Reduction in variability of patients' responses; greater confidence in setting a single dose
One enantiomer prone to interaction with key detoxification pathways	Reduced interactions with other common drugs
One enantiomer is agonist, the other antagonist	Enhanced activity and reduction of dose
Enantiomers vary in spectra of Pharmacological action and tissue specificity	Increased specificity and reduced side effects for one enantiomer; use of other enantiomer for different indication

It is now established that the enantiomers of racemates longer confer benefits in therapeutic use and, consequently, the production of single

enantiomer has become increasingly important and is currently performed by chemical synthesis or enzymatic. Enantiomers of chiral drugs may differ both quantitatively and qualitatively in their biological response. At one extreme, one enantiomer might have no effect. At the other extreme, both enantiomers have potent, but distinct, biological activity.

Ways of producing enantiomers

There are several ways to produce enantiomerically pure products, but still the most used techniques in industry are based on chirality of natural origin, the so-called *chirality pool* (Sundby 2003). In order to produce "new" chirality, it is common to distinguish between methods that are based on resolution of building blocks with a racemic origin and asymmetric synthesis. In the latter case, a prochiral starting material is converted to an optically active product using a chiral additive *via* an asymmetric reaction step. The different routes to enantiomerically pure building blocks are outlined in Scheme 1. It is important to emphasize the difference between asymmetric synthesis and kinetic resolution. The latter case involves a racemic chiral compound with a chiral reagent or an achiral reagent/chiral catalyst system. In either case, the two different enantiomers undergo reaction with different rates, thereby leading to a chiral enrichment

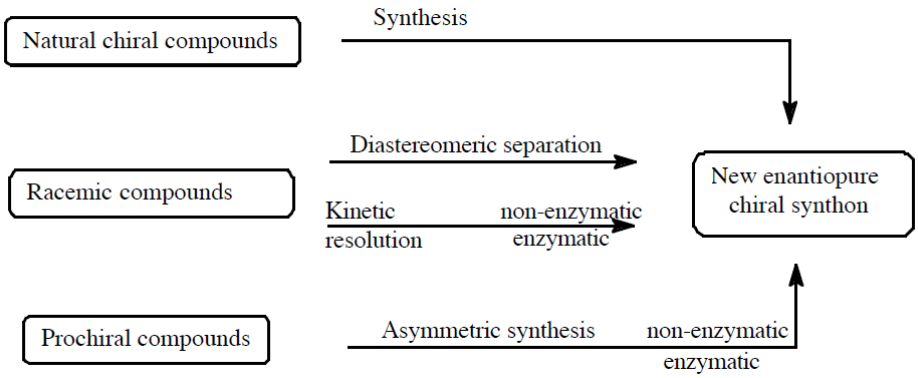

Scheme 1. Different routes to enantiomerically pure building blocks.

in the product. In an ideal case, one enantiomer is converted to the product while the other stays intact.

This means that the enantiomeric excess of both product and substrate changes as the reaction progresses. Moreover, maximum yield in this reaction is 50%. On the other hand, asymmetric synthesis has a prochiral starting point, which ensures a theoretical yield of 100%. A chiral reagent or an achiral reagent/chiral catalyst system introduces chirality to the prochiral center, and the enantiomeric excess is constant during the reaction.

The more classes of enzymes used in the enantioselective synthesis are the following: lipase, esterase, alcohol oxidase, nitrilase, transaminases, amino acid oxidase, and dehydrogenase/reductase (ADH).

Dehydrogenases/Reductases (ADHs)

Dehydrogenases/Reductases, classified under E.C.1.1.1., are a group of dehydrogenase enzymes that occur in many organisms and facilitate the interconversion between alcohols and aldehydes or ketones with the reduction of nicotinamide adenine dinucleotide (NAD^+ to NADH). These enzymes are ubiquitous in nature: *Eucarya*, *Bacteria* and *Archaea*, they play considerable process and production roles, for example in generation of potable alcohol, solvents and acetic acid. ADHs also support the growth of methylotrophs, oxidize alcohols and catalyse lignin degradation (Radianingtyas and Wright 2003). More recent studies have shown that mammalian ADH catalyzes retinol oxidation to provide retinal for retinoic acid synthesis, the active metabolite which controls a nuclear receptor signaling pathway (Duester 1996). Many studies have been addressed to characterize ADHs, mainly to understand their evolution and structure/function/stability relationship (Radianingtyas and Wright 2003) and develop their biotechnological potential mainly in the synthesis of the (*S*) or (*R*) enantiomers of alcohols from prochiral ketones (Hummel 1999). Fig. 2 shows an example of asymmetric bioreduction of an aromatic ketone.

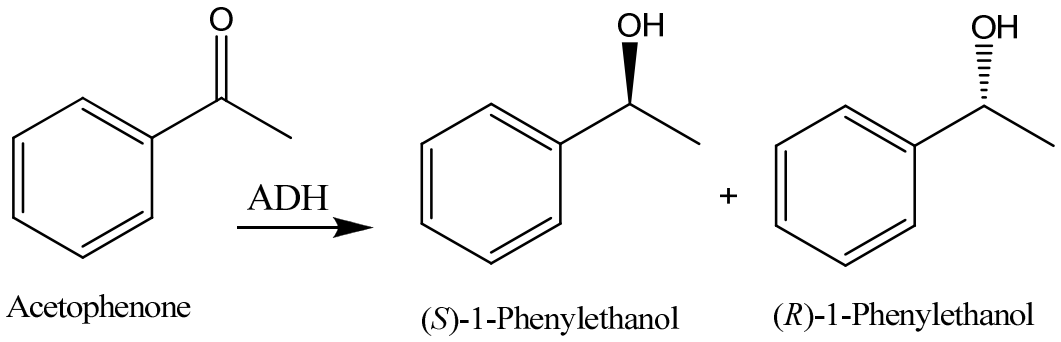

Figure 2. Highly *S*-enantioselective ADH that produces 99% of (*S*) isomer and 1% of (*R*) will have an enantiomeric excess of 98%. The enantiomeric excess = ([*S*]-[*R*]/[*S*]+[*R*]) × 100

Recently, enzymatic processes using whole cell fermentation or isolated ADHs have attracted a growing interest for the commercial production of chiral alcohols (Breuer et al. 2004; Liese et al. 2000).

Production of chiral alcohols with whole cells

The biotechnological processes for the production of chiral alcohols by reducing prochiral ketones with whole cells are known since many decades. Enzymes utilized as whole cells are usually more stable due to the surrounding of their natural environment. Furthermore, the use of whole-cell biocatalysts is sometimes desirable, as there is no need for downstream processing and purification of enzymes. Furthermore, especially in fermentative processes, the cells have internal cofactor regeneration, so that the addition of cheap co-substrate is sufficient to drive the reaction (Nakamura and Matsuda 2002; Faber 2004). On the other hand, when wild-type microorganisms are used as biocatalysts, insufficient values for

selectivity and, in particular, enantioselectivity may occur due to the presence of multiple reductases in the cell that display different enantiopreferences or even modify the substrate in other undesired position (Faber 2000; Kaluzna et al. 2004; Johanson et al. 2005). Furthermore, the cellular content of the carbonyl reductase giving a desired enantiomer may be relatively low, because the enzyme gene might be weakly expressed. However, cloning and overexpression of the gene encoding the enzyme of interest are powerful tools in the solution of this problem.

Production of chiral alcohols with isolated enzyme

Since early application of ADHs in asymmetric synthesis using horse liver and yeast ADHs (Jones and Beck 1976) and *Thermoanaerobacter brockii* ADH (TbADH) (Keinan et al. 1986), screening efforts have been directed at various species of microorganisms, which has resulted in new ADHs that have distinctive substrate specificity, good efficiency, and high enantioselectivity.

ADHs from thermophilic microorganisms

Representative examples of ADHs from thermophilic microorganisms are medium-chain enzymes, including TbADH (Korkhin et al. 1998), the ADH from *Bacillus stearothermophilus* (BsADH) (Ceccarelli et al. 2004), and

two archaeal enzymes, the ADH from *Aeropyrum pernix* (Guy et al. 2003) and the well-known ADH from *Sulfolobus solfataricus* (SsADH) (Raia et al. 2001; Giordano et al. 2005; Friest et al. 2010). The latter is a tetrameric, *S*-specific, NAD-dependent zinc enzyme, which is more active on primary alcohols than on secondary alcohols and is poorly active on arylketones. By contrast, the thermophilic *S*-specific enzyme TbADH is NADP dependent and complements horse liver ADH by preferentially accepting acyclic ketones and secondary alcohols rapidly (Keinan et al 1986).

ADHs from mesophilic microorganisms

Representative examples of enzymes from mesophilic microorganisms are the NADP-dependent (*R*)-specific ADH from *Lactobacillus brevis* (LB-RADH), which is active on aryl ketones and whose crystal structure has been solved (Schlieben et al. 2005), the NAD-dependent (*S*)-specific 1-phenylethanol dehydrogenase from the denitrifying bacterium strain EbN1 (PED), which was characterized and crystallized (Höffken et al. 2006), and the NAD-dependent ADH from *Leifsonia* sp. strain S749 (LsADH), which was found to be active on (*R*)-*sec* alcohols, aryl ketones, aldehydes, and keto esters and whose gene has recently been cloned for protein expression in *Escherichia coli* (Inoue et al. 2006). These enzymes are homotetrameric and belong to the short-chain NAD(P)(H)-dependent

dehydrogenase/reductase (SDR) superfamily (Kallberg et al. 2002). SDR enzymes have critical roles in lipid, amino acid, carbohydrate, cofactor, hormone and xenobiotic metabolism as well as to play a role as scaffolds for an NAD(P)(H) redox sensor system, of importance to control metabolic routes, transcription and signalling. SDRs are characterized by ~250 residue subunits, a Gly motif in the coenzyme-binding regions, and a catalytic triad formed by the highly conserved residues Tyr, Lys, Ser, to which an Asn residue has been added according to the proposal of Filling et al. (2002) later supported by the LB-RADH structure (Schlieben et al. 2005). Typically SDRs enzymes are non metal. However, LB-RADH contains Mg^{2+} having a structural role (Niefind et al. 2003). An important feature within the amino acid sequence will be discussed below.

Research project aim

The aim of my PhD research is to characterize new ADHs for the synthesis of chiral secondary alcohols as well as the structural study of the isolated enzymes for the understanding of the structure-function relationships. In particular, my attention was focused mainly on thermophilic ADHs belonging to the SDR superfamily.

Lines of activity

The activity for my research project covers the following lines:

- Identification of thermophilic ADHs belonging to the short-chain dehydrogenase/reductase (SDR) superfamily by genome sequence analysis.

- Cloning and expression in *E. coli* of the selected gene and purification of the protein. These issues can be achieved using the conventional techniques of molecular biology, biochemistry and enzymology.

- Enzyme purification at laboratory scale and characterization of substrate specificity, kinetic properties and stability. Extensive screening of alcohols, aldehydes and ketones is needed, with particular attention to bulky aromatic ketones, since many of the corresponding chiral alcohols are important intermediates in the synthesis of pharmaceuticals and agrochemicals.

Following the individuation of the most efficient substrate, it is necessary to determine:

- the optimal parameters for the enzyme oxidation and reduction reaction, such as buffer, pH and temperature
- determination of the k_{cat}/K_m values for the more interesting substrates
- the enzyme thermophilicity and thermostability and its resistance to organic solvents

- the optimal reaction conditions to develop an efficient bioreduction system for producing chiral alcohols of interest.

Characterization of the crystal structure of the purified proteins by X-ray diffraction studies

The structural analysis of the enzyme-cofactor-substrate complex allows to identify residues involved in the binding of the alcohol and/or ketone and in particular those determinants the stereo-preference, to design mutants to improve substrate specificity, stereospecificity and enzyme stability. (Schlieben et al. 2005; Zhang et al. 2008). The availability of detailed structural information has provided guidance on the possible enzyme action mechanisms. This work has been performed in close collaboration with Dr. Luciana Esposito of IBB, CNR, Naples.

The cofactor regeneration

The vast majority of dehydrogenases used for ketone reduction require nicotinamide cofactors, such as NADH and NADPH that are converted in equimolar amounts compared to the substrate. Due to the high costs of NAD(P)H, a suitable cofactor regeneration is required (van der Donk and Zhao 2003). An efficient bioreduction system requires a simultaneous and valid coenzyme-regenerating step and an appropriate reaction engineering

technique. To achieve an efficient recycling, two strategies are feasible (Fig. 3).

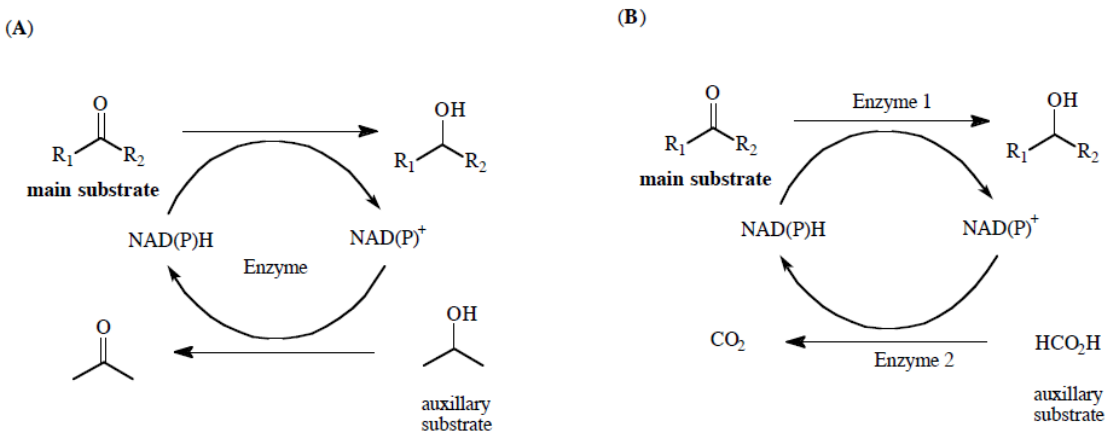

Figure 3. Regeneration of cofactors by (**A**) coupled-substrate and (**B**) coupled-enzyme strategies.

The most elegant and simple approach makes use of a single enzyme, which simultaneously transforms substrate plus co-substrate. A very common system consists in using 2-propanol as co-substrate. The latter, however, must be applied in large excess to drive the equilibrium into the desired direction. As a consequence, these so-called 'coupled-substrate' systems are commonly impeded by cosubstrate-inhibition. To circumvent these drawbacks, cofactor-recycling can be performed by using a second (and preferably irreversible) enzymatic reaction, for example using formate dehydrogenase or glucose dehydrogenase.

Formate dehydrogenase (FDH) is a promising enzyme for cofactor regeneration, because the substrate formate is very cheap and the by-

product through cofactor regeneration is carbon dioxide, which is volatile and makes the reaction irreversible. Glucose dehydrogenase (GDH) can also be utilized as a cofactor regeneration enzyme. This enzyme is rather inexpensive, highly active, and stable. Since GDH can regenerate both NADH and NADPH via glucose oxidation, it could be used with various kinds of carbonyl reductases, independent of their cofactor specificities.

Genome sequence analysis of SDRs

As noted above, a typical SDR is characterized by ~250 residue subunits, a Gly-motif in the coenzyme-binding regions and a catalytic triad formed by the highly conserved residues Tyr, Lys, Ser (Kallberg et al. 2002). Interestingly, analysis of the LB-RADH sequence based on multiple-sequence alignment with other well-known SDRs had suggested (Kallberg et al. 2002) an important role in the aspartate residue (D37) located 18 amino acids C terminal of the third glycine residue (see Fig. 4). Structural studies on the LB-RADH mutant G37D have shown that this residue plays a critical role in determining the preference of SDRs for NAD(H) (Schlieben et al. 2005). Further evidence of this role is provided by the LsADH (Inoue et al. 2006) and PED (Höffken et al. 2006) proteins, both being strictly NAD-dependent SDRs possessing an aspartate residue at position 37.

Thus, SDRs possessing an aspartate residue at position 37 are expected to show preference of NAD(H) over NADP(H), the proper being 5 to 6-fold less expensive than the latter. This preference as well as an intrinsic thermal/long term stability and tolerance of organic solvents are the features that make an oxidoreductase more attractive from an application perspective (Hummel 1999; Kroutil et al. 2004; Zhu et al. 2006). Therefore, our first aim was to identify genes coding for putative oxidoreductases with these distinctive features, NAD dependency and structural stability, in the genome of thermophilic microorganisms such as *Thermus termophilus*, *Sulfolobus acidocaldarius*, *Thermotoga maritima* MSB8, *Thermoanaerobacter ethanolicus* and *Bacillus licheniformis*.

Next sections deal with:

i) an applicative utilization of *Thermus termophilus* ADH

ii) the complete characterization of two ADHs from *Sulfolobus acidocaldarius*

iii) an applicative utilization of *Bacillus stearothermophilus* ADH.

RESULTS and DISCUSSION

Asymmetric reduction of α-keto esters with *Thermus thermophilus* NADH dependent carbonyl reductase

Thermus thermophilus alcohol dehydrogenase (TtADH)

Perusal of the genome of *Thermus thermophilus* HB27, an extremely thermophilic, halotolerant gram-negative eubacterium (Henne et al. 2004), available in the Gene Bank Data Base revealed the presence of one gene coding for a putative oxidoreductase. The amino acid sequence (Fig. 4) shows an aspartate residue (D37) located 18 amino acids C-terminal of the third glycine residue, suggesting that the putative dehydrogenase/reductase was expected to display a preference for NAD(H) rather NADP(H).

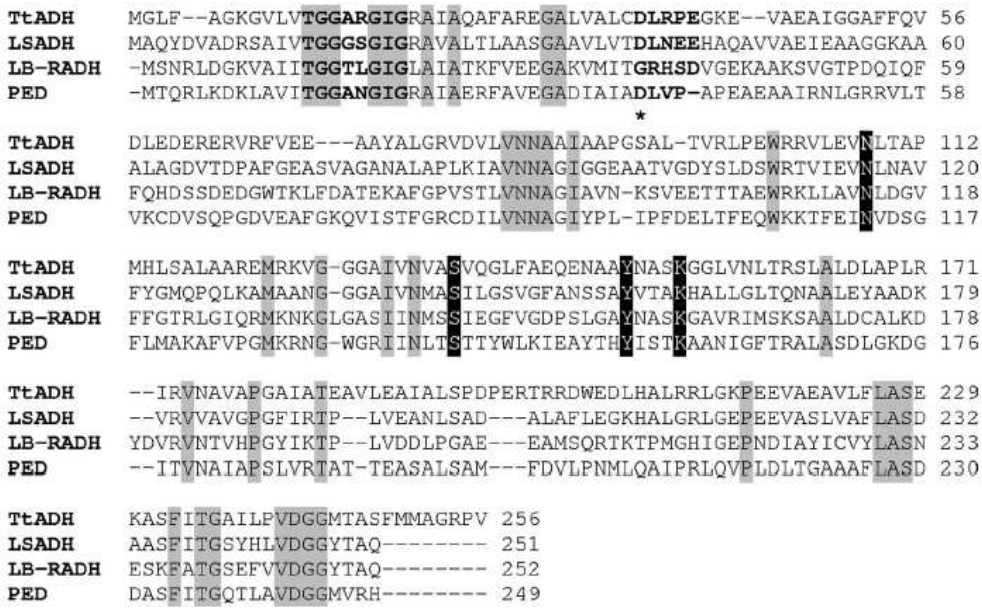

Figure 4. Multiple-sequence alignment of the *T. thermophilus* ADH (TtADH) and ADHs belonging to the SDR family, including *Leifsonia* sp. strain S749 ADH (LsADH) (NCBI accession no. BAD99642), *L. brevis* ADH (LB-RADH) (PDB code 1ZK4), and (*S*)-1 phenylethanol dehydrogenase from denitrifying bacterial strain EbN1 (PED) (PDB code 2EWM). The sequences were aligned using the BioEdit program. Gray shading indicates residues highly conserved in the SDR family. The four members of the catalytic tetrad are indicated by a black background. The following positions are indicated by bold type: the glycine-rich consensus sequence and the sequence motif Dhx(cp) that (in all SDRs) have a structural role in coenzyme binding (Kallberg et al. 2002). The star indicates the major determinant of the coenzyme specificity. The LB-RADH G37D mutant shows preference for NAD^+ over $NADP^+$ (Schlieben et al. 2005).

This prompted us to isolate and study the novel enzyme mainly to characterize its substrate specificity and stereoselectivity. The purification to homogeneity and the complete characterization of the *T. thermophilus* ADH recombinant form (TtADH) appeared in a paper prior to this doctoral thesis (Pennacchio et al. 2008).

Briefly, TtADH is a tetrameric enzyme consisting of identical 26,961-Da subunits composed of 256 amino acids. The enzyme has remarkable thermophilicity and thermal stability, displaying activity at temperatures up

to ~73°C and a 30-min half-inactivation temperature of ~90°C, as well as good tolerance to common organic solvents. TtADH has a strict requirement for NAD(H) as the coenzyme, a poor activity on aromatic alcohols and aldehydes and a preference for reduction of aromatic ketones and -keto esters.

Two interesting substrates of TtADH

The enzyme was found to catalyze the reduction of methyl benzoylformate (MBF) to methyl (*R*)-mandelate (MM) and methyl *o*-chlorobenzoylformate (ClMBF) to methyl (*R*)-*o*-chloromandelate (ClMM), two valuable synthons used in organic synthesis.

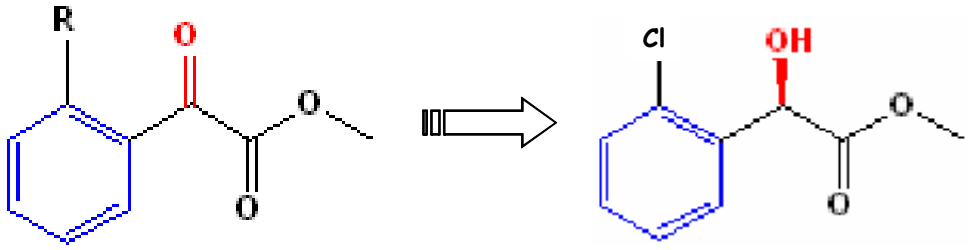

R = **H** Methyl Benzoylformate (MBF)

R = **Cl** Methyl *o*-chlorobenzoylformate (ClMBF)

R = **H** Methyl (*R*)-mandelate (MM)

R = **Cl** Methyl (*R*)-*o*-chloromandelate (ClMM)

O-protected MM is used as an intermediate for the synthesis of pharmaceuticals (Kobayashi et al. 1990; Pousset et al. 2001) and ClMM is an intermediate for the *anti*-thrombotic agent, (*S*)-clopidogrel,

commercialized under the brand name Plavix (clopidogrel sulfate) (Bousquet and Musolino 1999).

These interesting applicative properties prompted us to develop a system for the enzymatic synthesis of MM and ClMM by TtADH evaluating the use of glucose dehydrogenase as well as BsADH for cofactor regeneration as **Scheme 2** shows:

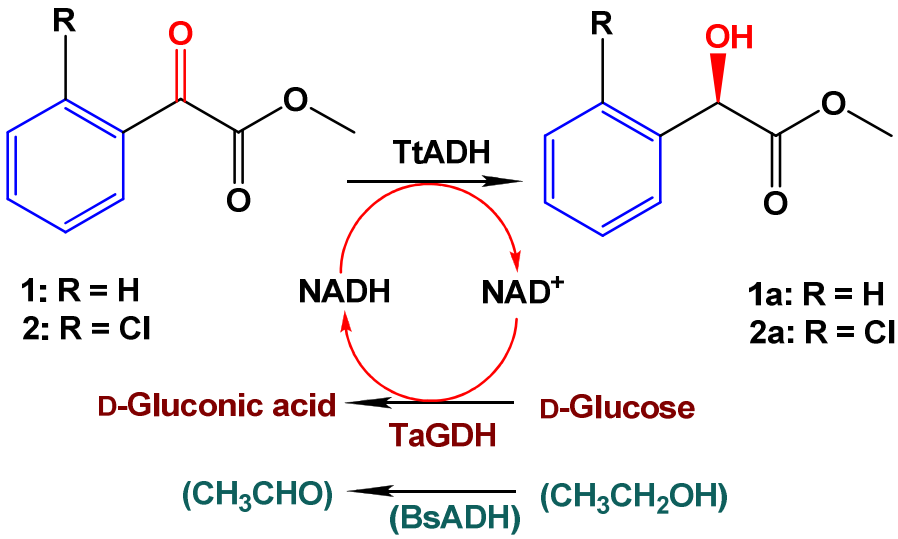

The development includes a) the determination of the optimal reaction time and substrate concentration in the absence and presence of organic solvents and b) the choice of the suitable alcohol as co-substrate for the TtADH/BsADH system.

Enzymatic synthesis of MM and ClMM by TtADH using glucose dehydrogenase for cofactor regeneration

Glucose dehydrogenase from *Thermoplasma acidophilum* (TaGDH), a thermophilic and stable enzyme possessing dual cofactor-specificity (John et al. 1994) was utilized for the in situ NADH-regeneration system together with glucose as the hydride source (Scheme 2). Biosynthesis experiments in analytical scale were undertaken to combine the optimum values of pH, temperature, substrate concentration, stirring speed, and reaction time.

Optimal pH

Previous studies showed that the optimal pH for the reduction reaction catalyzed by TtADH is approximately 6.0 (Pennacchio et al. 2008) and that for glucose oxidation catalysed by TaGDH is 7.0 (Woodward et al. 2000). Due to the instability of the reduced cofactor under acidic conditions, neutral pH was chosen as a compromise taking into account cofactor stability and TtADH activity at suboptimal pH.

Optimal reaction time and temperature

TaGDH retains full catalytic activity after 9 h at 55°C (Smith et al. 1989), while TtADH is highly efficient and selective at 50°C (Pennacchio et al. 2008). To establish the optimal reaction time the conversion of MBF was

carried out at 50°C, at low substrate concentration (1 g L^{-1}, 6.2 mM) in aqueous solution and by letting the reactions proceed for 1, 3, 6 and 24 h. Fig. 5 shows the conversion of MBF proceeded in 99% after 6 h, affording the (*R*)-α-hydroxy ester MM with 95% *ee*.

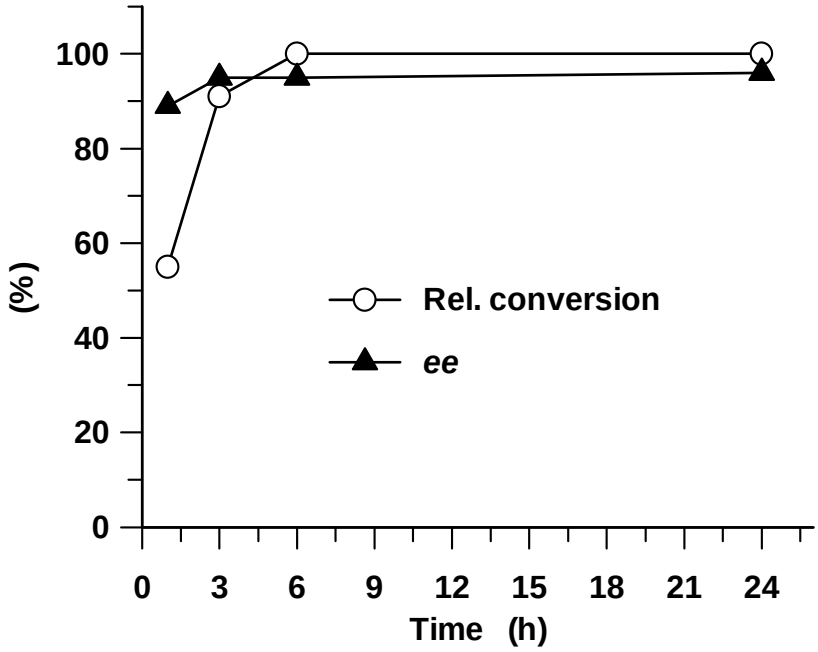

Figure 5. Time course of the bioreduction of MBF by TtADH. The reactions were carried out at 50°C in 50 mM sodium phosphate, pH 7.0, 100 mM KCl and NADH regeneration system of TaGDH and glucose. Reaction volume, 0.2 mL; TtADH and TaGDH 25 and 5.5 µg, respectively; NAD^+, 1.0 mM; MBF, 1.0 g L^{-1}; glucose, 50 mM. The reactions were stopped by addition of ethyl acetate at the times indicated. The dried extracts were analysed by chiral HPLC and the relative conversion calculated as the area of alcohol products divided by the total area.

The degree of conversion and *ee* of the biotransformation was unchanged at reaction times as long as 24 h. The high conversion is noteworthy, considering that TaGDH has a marked preference for NADP(H) over NAD(H) (John et al. 1994).

Optimal substrate concentration

Bioconversions were then carried out using increasingly higher concentrations of MBF for a reaction time of 24 h. The conversion proceeded with ~99% at MBF to 10 g L^{-1} MBF, but decreased to ca. 10% and ca. 1% yields at 30 and 50 g L^{-1} substrate, respectively. However, the *ee* of MM was 95% over the whole range of concentrations for MBF that were examined (see Fig. 6). The decrease in conversion could be due to a decrease in solubility of the substrate, enzyme inactivation by substrate or product, or both factors.

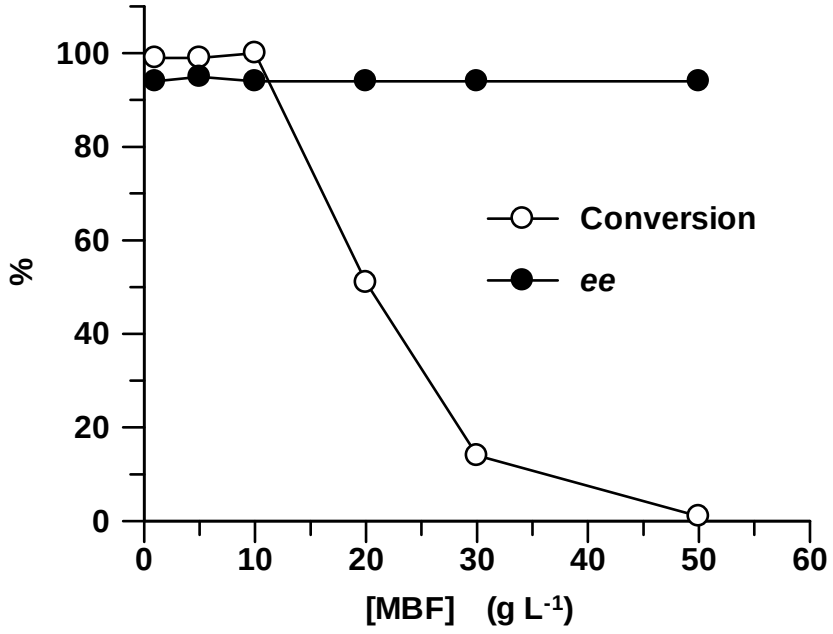

Figure 6. Production of MM at different MBF concentrations. The reactions were carried out at 50°C in 50 mM sodium phosphate, pH 7.0, 100 mM KCl and NADH regeneration system of TaGDH and glucose. Reaction volume, 1 mL; TtADH and TaGDH 25 and 5.5 µg, respectively; NAD^+, 1.0 mM; MBF, 1.0 g L^{-1}; glucose, 50 mM. The reactions were stopped by addition of ethyl acetate after 24 h of reaction. The dried extracts were analysed by chiral HPLC and the relative conversion calculated as the area of alcohol products divided by the total area.

TtADH stability in organic solvent

The next step was to develop a suitable solvent system to improve bioconversions at higher substrate concentrations. TtADH possesses a remarkable tolerance to common organic solvents. Indeed, it even showed a significant increase in activity in the presence of various organic solvents, reaching 150% and 180% of the initial value with 5% v/v acetonitrile and 10% v/v 2-propanol, respectively, after 24 h of incubation at 50°C and 182% with 10% v/v hexane after 65 h at 25°C (see Pennacchio et al. 2008).

TaADH stability in organic solvent

The stability of the archaeabacterial glucose dehydrogenase in the presence of organic solvents was investigated to evaluate its tolerance to organic solvents (Fig. 7). TaGDH was inactivated by 34% and 28% following 24 h incubation at 50°C, in the absence and presence of 20% v/v hexane, respectively. Moreover, the enzyme was inactivated by over 50% in the presence of 5% v/v and 10% v/v DMSO, 10% v/v acetonitrile or 10% v/v methanol. However, incubation in the presence of 5% and 10% v/v 2-propanol, 5% v/v methanol or 5% v/v acetonitrile resulted in activities that were similar to those measured in aqueous buffer after 6 h and 24 h.

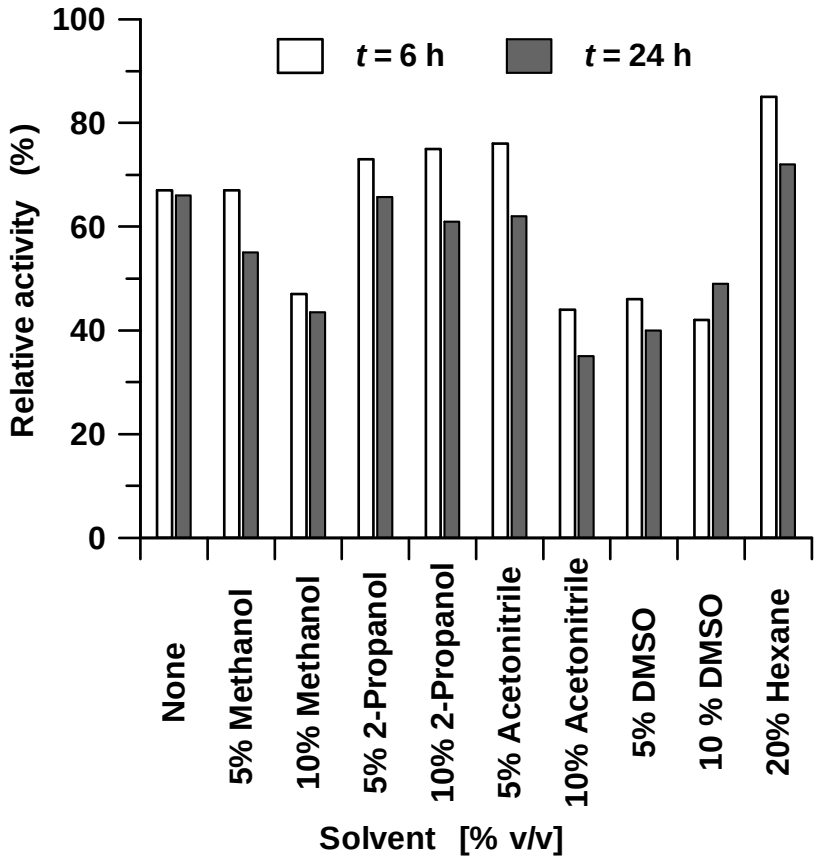

Figure 7. Effects of organic solvents on TaGDH. Samples of enzyme (0.025 mg mL^{-1}) in 50 mM sodium phosphate, pH 7.0 were incubated at 50°C in the absence and presence of the organic solvents at the indicated concentrations, and assays were performed after 6 h and 24 h. The activity assays were performed as described in Material and Methods using glucose as the substrate. The data obtained in the absence and presence of organic solvents are expressed as percentage activity relative to the value determined prior to incubation.

Bioconversions at higher substrate concentrations

Bioconversions were carried out at different concentrations of MBF in the presence of acetonitrile or hexane at concentrations of 5% and 20% v/v, respectively; these concentrations fulfilled the majority of the criteria for a solvent system in which both enzymes retained activity. As shown in Fig. 8, the presence of water-miscible or immiscible organic solvents did not

improve conversion at concentrations of MBF higher than 10 g L^{-1}, since the profiles of the conversion with acetonitrile and hexane were similar to those obtained in aqueous buffer (Fig. 6).

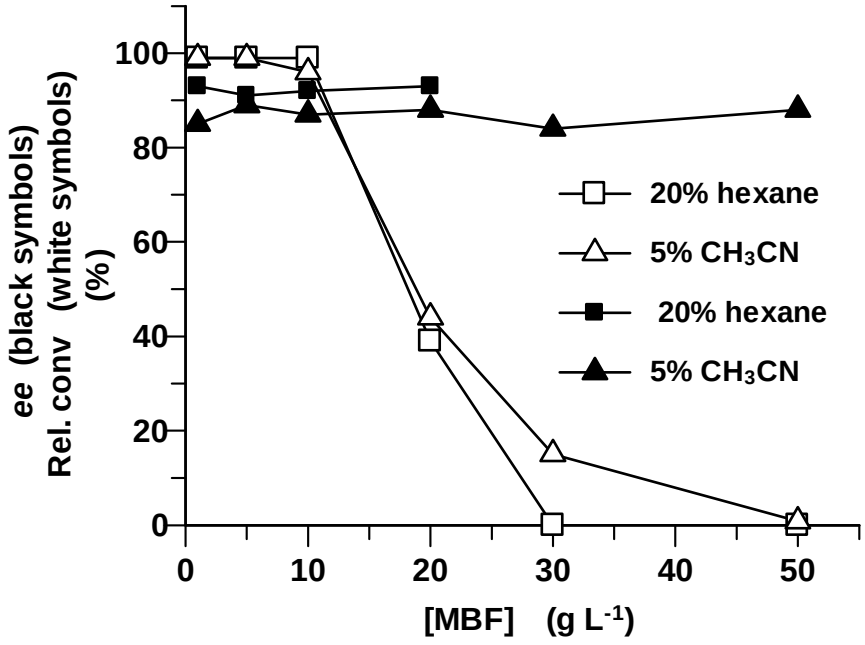

Figure 8. Production of MM at different MBF concentrations. The reactions were carried out for 24 h at 50°C under the same conditions as for Fig. 6 at increasing substrate concentrations and in the presence of 5% v/v acetonitrile and 20% v/v hexane.

Nevertheless, the good levels of conversion obtained between 1 and 10 g L^{-1} substrate was accompanied by a slight decrease in enantioselectivity in the presence of acetonitrile (*ee* = 85%–89%) as well as in the presence of hexane (*ee* = 92–93%) compared to the 95% *ee* obtained in aqueous buffer. The decrease in enantioselectivity could be related to the solvent-mediated

enhancement of catalysis as a result of increased flexibility of the enzyme active site (Pennacchio et al. 2008).

Optimal conditions for bioconversions at lab-scale

In light of our findings related to enantioselectivity and concentration, optimum conditions for the bioconversion of MBF as well as ClMBF were determined to involve a temperature of 50°C, substrate concentrations up to 10 g L^{-1}, in the presence of 1 mM NAD^+ in pH 7.0 aqueous buffer.

Table 2 summarizes the results of a study carried out for the two α-hydroxy esters.

Table 2. Reduction of MBF and ClMBF to MM and ClMM with TtADH by the TaGDH/glucose-NADH regeneration system [a]

Entry	MBF (mg)	[MBF] (g L^{-1})	TtADH (mg mL^{-1})	TaGDH (mg mL^{-1})	Conversion[b] (%)	*ee*[b] (%)
1	100	10	0.05	0.010	100 (74) [d]	95
2 [c]	100	2	0.10	0.010	78 (77) [d]	96
	ClMBF (mg)	[ClMBF] (g L^{-1})				
3	100	10	0.125	0.0275	28 (nd) [d]	88
4	100	2	0.100	0.020	96 (86) [d]	93
5	100	5	0.125	0.0275	100 (62) [d]	95

[a] The reactions were carried out for 24 h at 50°C.
[b] Determined by HPLC [Chiralcel OD-H, hexane/i-PrOH [(9:1)].
[c] The reaction was carried out in 6 h.
[d] Isolated yield in parentheses. nd, not determined.

The bioreduction of 100 mg of MBF at 50°C for 24 h gave 74 mg of MM with *ee* = 95% (Table 2, entry 1). The same reaction carried out in 6 h with a 5-fold lower substrate and 2-fold higher TtADH concentrations yielded slightly better results (Table 2, entry 2). However, the conversion and optical purity of ClMM were somewhat lower when the concentration of ClMBF was 10 g L^{-1} (Table 2, entry 3). Nevertheless, the bioreduction of 100 mg of ClMBF gave 86 and 62 mg of ClMM with similar *ee* (Table 2, entries 4 and 5) at substrate concentrations of 2 and 5 g L^{-1}, respectively. This suggests that greater insolubility of the halogenated keto ester and/or enzyme inactivation alters the efficiency of the biotransformation. It is noteworthy that, although the affinities of the two substrates are quite different, the presence of the halogen in substrate ClMBF did not affect TtADH enantioselectivity.

Enzymatic synthesis of MM and ClMM by TtADH using BsADH for cofactor regeneration

Early bioconversion processes performed to establish TtADH enantioselectivity were carried out on analytical scale by way of an in situ NADH-recycling system involving a second thermophilic NAD-dependent ADH, the recombinant ADH from *Bacillus stearothermophilus* (BsADH) (Pennacchio et al. 2008). The bacillary enzyme is active with 2-propanol

which was therefore used as both co-solvent and substrate. The enzyme is inactive on aliphatic and aromatic ketones, including the carbonyl substrates of TtADH and the corresponding alcohols. However, TtADH does not accept 2-propanol or acetone as substrates. These features allowed the reaction to proceed almost to completion for reduction of 3 mg of MBF to MM with 99% conversion and *ee* = 91%, in 24 h at 50°C, and in the presence of 2% v/v 2-propanol (Pennacchio et al. 2008).

Bioconversions at lab-scale

The scaled-up bioreduction of MBF involving 100 mg of substrate was performed by increasing the amount of 2-propanol to 4% v/v and using different enzyme concentrations. The data summarized in Table 3 indicate

Table 3. Asymmetric reduction of MBF with TtADH by the BsADH/2 propanol-NADH regeneration system [a]

Entry	TtADH (mg mL^{-1})	BsADH (mg mL^{-1})	Time (h)	2-propanol (% v/v)	Conversion [b] (%)	*ee* [b] (%)
1	0.050	0.010	6	4	81	84
2	0.050	0.010	24	4	97	86
3	0.265	0.024	6	4	96	87

[a] Conditions: MBF concentration, 10 g L^{-1}; TtADH and BsADH at the indicated concentrations; 1 mM NAD^+; buffer, 0.1 M sodium phosphate pH 7.0, 0.1 M KCl, 5 mM 2-mercaptoethanol. Reaction volume, 10 mL. Temperature, 50°C.
[b] Determined by HPLC [Chiralcel OD-H, hexane/i-PrOH [(9:1)].

that the improved conversion was obtained either in a short reaction time (6 h) using higher amounts of the two enzymes (Table 3, entry 3) or using lower amounts of enzymes at a reaction time which was four times longer (Table 3, entry 2).

Notably, the yields of 96–97% were similar to those obtained from bioreductions using 3 mg substrate (Pennacchio et al 2008), but with a lower optical purity (86–87% *ee* relative to 91% *ee*), suggesting that the change in TtADH selectivity could be related to 2-propanol concentrations.

Choosing the most suitable alcohol

In addition to 2-propanol (k_{cat}/K_m = 9 s^{-1} mM^{-1}), BsADH oxidizes other alcohols with even greater efficiency. Examples include ethanol (k_{cat}/K_m = 64 s^{-1} mM^{-1}), 1-propanol (286 s^{-1} mM^{-1}), 1-butanol (437 s^{-1} mM^{-1}), 1-pentanol (64 s^{-1} mM^{-1}), and 1-hexanol (64 s^{-1} mM^{-1}) (Raia, unpublished data) and these were therefore tested as alternative hydride sources for NADH recycling. Moreover, these alcohols and their respective aldehydes are not substrates of TtADH (Pennacchio et al. 2008). Thus, only the cofactor is the co-substrate of TtADH and BsADH.

Bioreductions of 100 mg of MBF were carried out in the presence of each alcohol at a concentration of 4% v/v, which corresponds to 700 mM for ethanol down to 310 mM for 1-hexanol. All values were over-saturating for

the bacillary ADH. The data obtained were plotted against the respective log*P* values to correlate conversions and the TtADH enantioselectivity with the hydrophobicity of the alcohol added (Fig. 9).

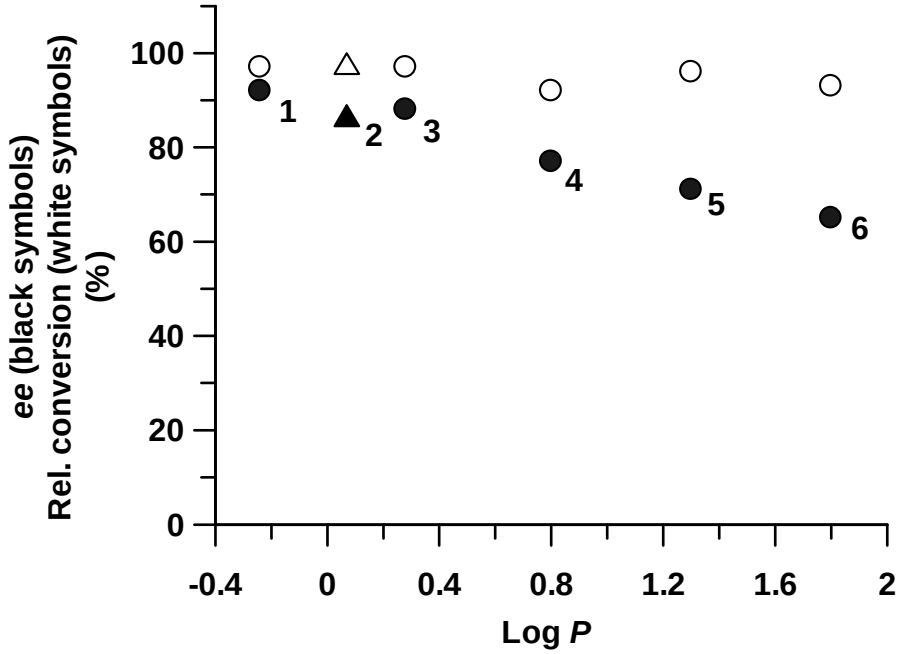

Figure 9. Effect of the BsADH alcohol substrate on the enantioselectivity and efficiency of the reduction catalysed by TtADH. **1**, ethanol (log *P* = –0.24); **2**, 2-propanol (0.07); **3**, 1-propanol (0.28); **4**, 1-butanol (0.8); **5**, 1-pentanol (1.3); **6**, 1-hexanol (1.8). The reactions were carried out for 24 h at 50°C under the same conditions as for Table 3 in the presence of 4% v/v alcohol. TtADH and BsADH concentrations, 0.050 and 0.010 mg mL^{-1}, respectively; vol = 10 mL. Data for 2- propanol were from Table 3, obtained after 24 hours of reaction (entry 2). Error limit, 2% of the stated values.

The TtADH enantioselectivity decreased as the hydrophobicity of the medium increased. However, the level of conversion remained high and near constant for all of the alcohols tested, emphasizing the versatility and high efficiency of the BsADH/alcohol substrate system in recycling the

reduced cofactor. An increase in conversion rate with increasing log *P* with no effect on enantioselectivity was recently reported for the 2-octanone to (*R*)-2-octanol reduction with *Oenococcu oeni* cells in a biphasic system (Hu and Xu 2006). Moreover, *Lactobacillus brevis* ADH enantioselectivity was recently shown not to be altered by the presence of an organic phase (Villela Filho et al. 2003). Instead, *Thermoanaerobium brockii* ADH enantioselectivity was seen to increase proportionally to increasing water composition (Jönsson et al. 1999). In general terms, the stereoselectivity of enzymes decreased as solvent hydrophobicity increased (Carrea and Riva 2000) and enantiofacial selectivity was also significantly affected by the reaction medium (Klibanov 2001). Although the examples mentioned describe biphasic systems, including high concentrations of an apolar solvent, the effect of relatively low concentrations of polar protic solvents on the TtADH enantiofacial selectivity is rather remarkable. Docking calculations using the TtADH structure explain the selective formation of the methyl (*R*)-mandelate (Pennacchio et al. 2010b) by showing that the methyl benzoylformate molecule assumes the lowest energy orientation by fitting the phenyl ring into a hydrophobic pocket, with the two carbonyl groups staggered by about 78° and the methoxy group pointing toward the carboxyamide group of the cofactor. Moreover, the docking analysis showed that the keto ester molecule can also assume another conformation,

less energetically favourable compared to that described above, which has the opposite face of the carbonyl group directed to the nicotinamide ring, and therefore leading to the (*S*)-enantiomer of the alcohol product. Importantly, there is no major steric constraint preventing the positioning of this alternative conformation in the enzyme active site (Pennacchio et al. 2010b). A change in polarity occurring in the active site may induce a structural rearrangement that facilitates the positioning of this alternative conformation. Since the TtADH/BsADH system showed higher enantioselectivity with ethanol than with 2-propanol, the next step was to examine the synthesis of MM using concentrations of ethanol lower than 4% v/v (Table 4).

Table 4. Asymmetric reduction of MBF with the TtADH/BsADH system at different ethanol and cofactor concentrations [a]

Entry	Ethanol (% v/v)	NAD^+ (mM)	TtADH (mg mL^{-1})	BsADH (mg mL^{-1})	Conversion (%)	*ee* (%)	Isolated yield (%)
1	0.6	1 (2)	0.05	0.01	60 (89)	90 (90)	nd
2	1	1 (2)	0.05	0.01	79 (98)	89 (92)	nd
3	2	1 (2)	0.05	0.01	92 (98)	90 (93)	nd
4	3	1 (2)	0.05	0.01	91 (98)	92 (92)	nd
5	4	1 (2)	0.05	0.01	91 (99)	91 (93)	nd
6	4	2	0.10	0.02	99	94	81

[a] Conditions reaction and chiral analysis as in Table 1. Amount of MBF = 100 mg MBF concentration, 10 g L^{-1}, except for # 6: 2 g L^{-1}. Values in parentheses refer to data obtained with 2 mM NAD^+. nd, not determined.

The keto ester reduction was limited by the cofactor recycling rate when the ethanol percentage was 0.6% or 1% v/v and the cofactor concentration was 1 mM (Table 4, entries 1 and 2). This concentration is much lower than the cofactor K_m (13±2 mM) and is therefore far below that required for saturation of the BsADH active sites. However, by doubling the cofactor concentration, the conversion increased from 60 to 89% (Table 4, entry 1) and from 79 to 98% (Table 4, entry 2) in the presence of 0.6% and 1% v/v ethanol, respectively. Conditions employing 4% v/v ethanol and 2 mM NAD^+ (Table 4, entries 5 and 6) and a substrate concentration of 2 g L^{-1} (as in Table 2, entry 2) were shown to be ideal for achieving asymmetric reduction of 100 mg of MBF with 81% isolated yield and *ee* = 94% (Table 4, entry 6). The bioconversion of ClMBF to ClMM occurred with the same enantioselectivity as the non-halogenated compound and with good productivity (Table 5).

Table 5. Reduction of ClMBF to ClMM with TtADH by the BsADH /ethanol - NADH regeneration system [a]

Entry	ClMBF (mg)	[ClMBF] (g L^{-1})	TtADH (mg mL^{-1})	BsADH (mg mL^{-1})	Conversion[b] (%)	*ee*[b] (%)
1	1	1	0.05	0.01	100	91
2	2	2	0.05	0.01	100	92
3	100	2	0.10	0.02	98 (78) [c]	92

[a] The reactions were carried out for 24 h at 50°C. Ethanol, 4% v/v.
[b] Determined by HPLC [Chiralcel OD-H, hexane/i-PrOH [(9:1)].
[c] Isolated yield in parentheses.

Using relatively low substrate concentrations 78 mg of ClMM (*ee* = 92%) was obtained from 100 mg of ClMBF in 24 h at 50°C (Table 5, entry 3). As in the case for the TtADH/TaGDH system (Table 2, entry 3) the substrate concentration of 2 g L^{-1} was found to be optimal for scaling up production of ClMM. However, the formation of the more reactive acetaldehyde could limit the use of ethanol as a regeneration reductant. Nevertheless, new applications for ethanol as a tunable nicotinamide reductant under four-electron redox conditions for the chemoenzymatic synthesis of important synthons (Broussy et al. 2009), as well as solvent and reductant in the enantioselective synthesis of (*S*)-profens using *Sulfolobus solfataricus* ADH (Friest et al. 2010) and (2*S*)-2-arylpropanols using horse liver and yeast ADHs (Galletti et al. 2010) have been recently reported.

Conclusion

The enzymatic synthesis of methyl (*R*)-mandelate (MM) and methyl (*R*)-*o*-chloromandelate (ClMM), two important pharmaceutical building blocks, has been developed in a one-phase system, using a carbonyl reductase and two different dehydrogenases to recycle the NADH. The two regeneration modes gave similar yields and optical purities. BsADH displayed two distinct advantages: feasibility of purification and high efficiency at suboptimal pH. For the TaGDH method, the hydride source was glucose, which constitutes cheap biomass whereas for the BsADH method, ethanol was the cheap sacrificial substrate. Both methods are characterized by favourable thermodynamics since alcohol/aldehyde, and glucose/gluconic acid do not interfere with the synthesis reaction. Only a few examples are known for enzyme-coupled cofactor regeneration involving a second ADH (Goldberg et al. 2007) and the present study represents a successful application of the bacillary ADH.

Two short-chain NAD(H)-dependent dehydrogenase/reductase from *Sulfolobus acidocaldarius*: SaADH and SaADH2.

Two amino acid sequences with typical features of the SDRs were found in the genome of *S. acidocaldarius*, an aerobic thermoacidophilic crenarcheon which grows optimally at 80°C and pH 2 (Chen et al. 2005). Both the putative archaeal oxidoreductases were expected to be NAD dependent based on the presence of an Asp residue at position 42, and a glutamic acid residue at position 39 of the first and second sequence, respectively.

Biochemical characterization of a recombinant short-chain NAD(H)-dependent dehydrogenase/reductase from *Sulfolobus acidocaldarius*

The first gene, *saadh*, encoding a putative NAD(H)-dependent oxidoreductase has been heterologously overexpressed in *Escherichia coli*, and the resulting protein (SaADH) purified to homogeneity and characterized in terms of substrate specificity, kinetics and stability as well as enantioselectivity.

Expression and protein purification

Analysis of the *Sulfolobus acidocaldarius* genome (Chen et al. 2005) for genes encoding short-chain ADHs resulted in identification of a putative oxidoreductase gene. The oxidoreductase protein, named SaADH, was expected to be NAD(H)-dependent on the basis of the presence of an aspartic residue at position 42, whose critical role in determining the preference for NAD(H) (Kallberg et al. 2002) has been shown through kinetic and structural studies of the LB-RADH G37D mutant (Schlieben et al. 2005), and recently supported by kinetic studies (Pennacchio et al. 2008) and structural characterization of TtADH (Asada et al. 2009).

SaADH is a 28,978-Da protein whose sequence shows the greatest identity to four typical SDRs, LB-RADH (30% identity), LsADH (29%), PED

(28%), and TtADH (27%), as well as the archaeal AdhA (25% identity). The *saadh* gene was successfully expressed in *E. coli* cells, yielding an active enzyme accounting for more than 20% of the total protein content of the cell extract (Table 6).

Table 6. Purification of recombinant SaADH [a]

Step	Total protein (mg)	Total activity (U)	Specific activity (U/mg)	Yield (%)	Purification (fold)
Crude extract	294	750	2.5	100	1
Thermal step	184	618	3.3	82.4	1.3
DEAE FF	119	578	4.8	77.0	1.9
Gel filtration	68	452	6.6	60.3	2.6

[a] The data are for a 2-liter culture. Activities were measured at 65°C as described in Materials and Methods, using cycloheptanol as substrate.

Host protein precipitation at 75°C was found to be the most effective purification step. An overall purification of 2.6-fold was achieved from crude, cell-free extracts with an overall yield of 60%. The enzyme was shown to be homogeneous by denaturing and non-denaturing PAGE (data not shown). Protein separation by SDS-PAGE resulted in a single band corresponding to a molecular mass of ~30 kDa (see below). Gel filtration performed in 50 mM Tris–HCl buffer, pH 9.0 containing 150 mM NaCl yielded a profile consisting of a single peak corresponding to molecular mass ~65 kDa (data not shown). The quaternary structure of SaADH was

further investigated by chemical crosslinking using dimethyladipimate (DMA, N–N distance 8.6 Å) and dimethylsuberimidate (DMS, N–N distance 11.0 Å) as bifunctional reagents. SDS-PAGE of the DMAcross-linked enzyme resulted in the appearance of four bands decreasing in intensity from monomer to tetramer (Fig. 10).

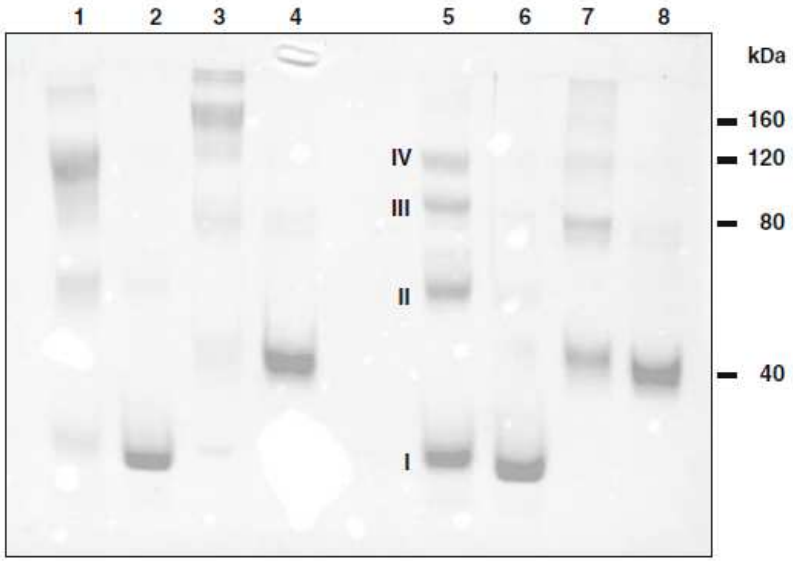

Figure 10. SDS-PAGE analysis of cross-linked SaADH. Lanes **1** and **5** DMS- and DMA-cross-linked and denatured enzyme, respectively. Lanes **2** and **6** non-cross-linked denatured enzyme. Lanes **3** and **7** DMS- and DMA-cross-linked and denatured aldolase, respectively. Lanes **4** and **6** non-cross-linked denatured aldolase. The kDa values refer to Mr of monomer, dimer, trimer, and tetramer of cross-linked aldolase, used as molecular mass markers. I, II, III, and IV indicate the monomer, dimer, trimer, and tetramer of DMS-cross-linked SaADH. Cross-linking reaction and SDS-PAGE were carried out as described in Materials and Methods.

However, the longer cross-linking reagent, DMS, resulted in a pattern predominantly consisting of crosslinked tetramer and smaller amounts of the other species (Fig. 10). These data suggest that SaADH has a tetrameric

structure which adopts a more compact structure in the presence of salt, resulting in greater permeation into the packing pores of the gel matrix. However, it is not excluded that a tetramer to dimer dissociation occurs in the presence of relatively high salt concentration. The molecular mass of the subunit determined by ESIMS analysis proved to be 28,978.0 Da (average mass), in agreement with the theoretical value of the sequence.

Optimal pH and thermophilicity

Fig. 11 shows the pH dependence of SaADH in the reduction and oxidation reactions.

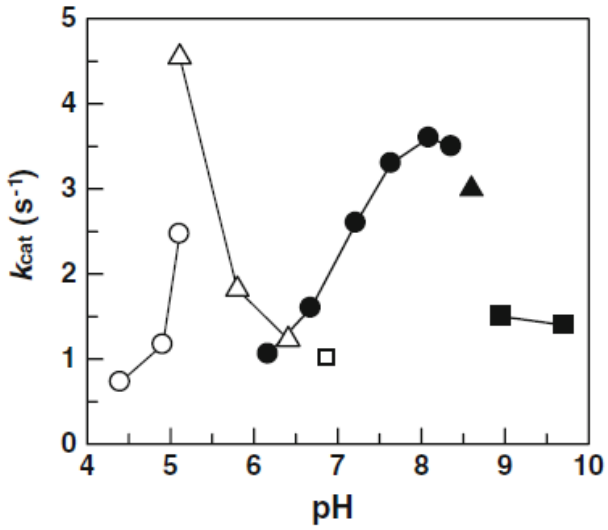

Figure 11. SaADH activity as a function of pH in the reduction and oxidation reactions. The following 50 mM buffer solutions were used: sodium acetate (open circles), MES (open triangles), and sodium phosphate (open square) in the reduction reaction, and sodium phosphate (filled circles), Tris–HCl (filled triangle), and glycine–NaOH (filled squares) in the oxidation reaction. The mixture for the reduction reaction contained 25 mM methyl benzoylformate and 0.1 mM NADH, and the mixture for the oxidation reaction contained 25 mM cycloheptanol and 5 mM NAD^+. The assays were performed at 65°C under the conditions described in Materials and Methods.

The SaADH activity was found to be closely dependent on pH in the reduction reaction, displaying a narrow peak of maximum activity at approximately pH 5.1. The oxidation reaction showed a less marked dependence on pH, displaying a peak with a maximum at around pH 8.2.

The effect of temperature on SaADH activity is shown in Fig. 12.

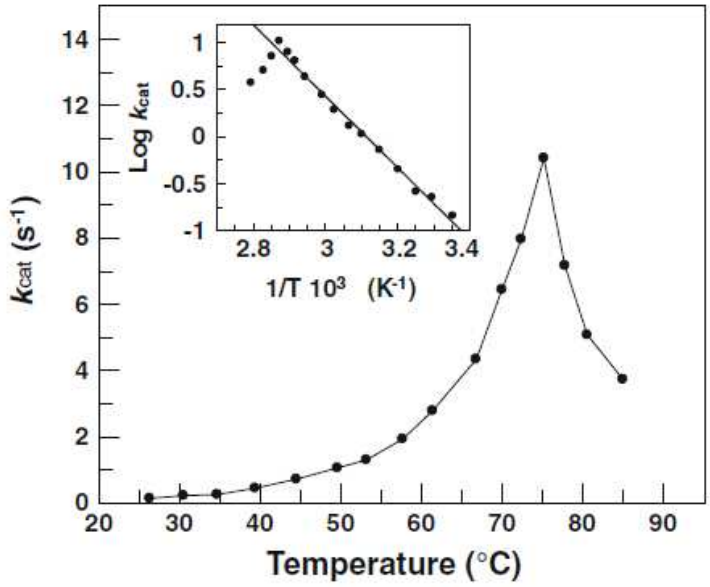

Figure 12. Temperature dependence of the SaADH activity. The assay was carried out as described in Materials and Methods, using cycloheptanol as the substrate. The inset shows the Arrhenius plot from the same data. The value of the activation energy was 72.8 ± 2.0 kJ mol^{-1}.

The reaction rate increases up to 75°C and then decreases rapidly due to thermal inactivation. This optimal temperature value is similar to that of TtADH (73°C) (Pennacchio et al. 2008), lower than that of thermophilic

medium-chain, zinc-containing ADHs such as SsADH (88°C) (Raia et al. 2001) and TbADH (85°C) (Korkhin et al. 1998), and significantly lower than that of *Pyrococcus furiosus* aldo–keto reductase (100°C) (Machielsen et al. 2006). The activation energy for oxidation is 72.8 ± 2.0 kJ mol^{-1}, which is higher than that determined for TtADH (62.9 ± 2.6 kJ mol^{-1}) (Pennacchio et al. 2008) or SsADH (46.7 kJ mol^{-1}) (Raia et al. 2001), and lower than that reported for TbADH (94.1 kJ mol^{-1}) (Korkhin et al. 1998).

Coenzyme and substrate specificity

The enzyme showed no activity with NADP(H) and full activity with NAD(H). This coenzyme preference further supports the evidence that an aspartate residue at position 37 of an SDR enzyme (numbering of LB-RADH) plays a critical role in discriminating NAD(H) from NADP(H) as discussed above. The specificity of SaADH for various alcohols, aldehydes and ketones was examined (Table 7). The enzyme showed no activity on aliphatic linear and branched alcohols (not shown), except for a poor activity on 2-propyn-1-ol, 3-methyl-1-butanol and 2-pentanol; however, it showed a discrete activity on aliphatic cyclic and bicyclic alcohols. Benzyl alcohol and 4-bromobenzyl alcohol were not found to be substrates. In contrast, in view of the great influence that the strong electron-donating methoxy group exerts on the para position of the benzene

Table 7. Substrate specificity of SaADH in the oxidation and reduction reactions

Substrate	Relative activity (%)	Substrate	Relative activity (%)
Alcohols [a]		Ketones [d]	
2-Propyn-1-ol	6	Cyclohexanone	0
3-Methyl-1-butanol	4	2-Methylcyclohexanone	0
(±)-2-Pentanol	5	3-Methylcyclohexanone	29
(*S*)-2-Pentanol	11	4-Methylcyclohexanone	0
(*R*)-2-Pentanol	0	2,6-Dimethylcyclohexanone	0
Cyclopentanol	5	Cycloheptanone	0
Cyclohexanol	8	1-Decalone	14
Cycloheptanol	37	Acetophenone	0
Cyclohexylmethanol [b]	0	2,2,2-Trifluoroacetophenone	100
2-Cyclohexylethanol	0	1-Indanone	0
3-Methylcyclohexanol[b]	14	α-Tetralone	0
3-Cyclohexyl-1-propanol[b]	0	1-phenyl-1,2-propanedione	70
cis-Decahydro-1-naphthol	11	Isatin [e]	300
Benzyl alcohol	0	2-Acetonaphthone	0
2-Methoxybenzyl alcohol	0		
3-Methoxybenzyl alcohol	0	Keto esters [d]	
4-Methoxybenzyl alcohol	5		
(*R*,*S*)-1-Phenylethanol[b]	6	Ethyl pyruvate	43
(*S*)-(−)-1-Phenylethanol	8	Methyl benzoylformate	100
(*R*)-(+)-1-Phenylethanol	0	Methyl *o*-chlorobenzoylformate	160
(±)-1-Phenyl-1-propanol[b]	8	Ethyl benzoylformate	88
1-(1-Naphthyl)ethanol	5	Ethyl 4-chloroacetoacetate	27
(±)-1-(2-Naphthyl)ethanol	6		
(*R*)-1-(2-Naphthyl)ethanol	5		
(*S*)-1-(2-Naphthyl)ethanol	5		
(*R*)-3-Chloro-1-phenyl-1-propanol	5		
(*R*)-1-Indanol[c]	62		
(*S*)-1-Indanol[c]	100		
(*R*)-α-Tetralol[c]	58		
(*S*)-α-Tetralol[c]	12		

[a] The assays were performed using 1 mL of mixture containing 10 mM alcohol and 5 mM NAD^+ in 25 mM sodium phosphate, pH 8.0, at 65°C for 1 min. Relative rates were calculated by setting the activity to be 100 for (*S*)-1-indanol.

[b] Substrates were dissolved in 100% 2-propanol.

[c] Substrate was dissolved in 100% acetonitrile.

[d] The assays were performed using 1 mL of mixture containing 10 mM carbonyl compound and 0.1 mM NADH in 37.5 mM MES-NaOH, pH 5.5, at 65°C for 1 min. Substrates were dissolved in 2-propanol and added to the reaction mixture (10 mM in 2% [vol/vol] 2-propanol). The percent values refer to 2,2,2-trifluoroacetophenone for ketones, and to methyl benzoylformate for ketoesters.

[e] Substrate concentration, 1 mM; solvent, acetonitrile; the enzyme was present at a seven-fold lower concentration.

ring, only the 4-methoxybenzyl alcohol was found to be an active substrate. (*S*)-1-Phenylethanol was also found to be an active substrate, whereas the *S* and *R* enantiomers of α-(trifluoromethyl) benzyl alcohol and methyl and ethyl mandelates showed no apparent activity with SaADH (data not shown). Moreover, the enzyme showed relatively poor activity on (±)-1-phenyl-1-propanol, 1-(1-naphthyl)ethanol and the two enantiomers of 1-(2-naphthyl)ethanol. However, SaADH showed highest activity with 1-indanol and α-tetralol (Table 7). The enzyme was not active on aliphatic and aromatic aldehydes, and on aliphatic linear, branched and cyclic ketones (data not shown) except for 3-methylcyclohexanone (Table 7). However, the enzyme showed a relatively high reduction rate with isatin, 2,2,2-trifluoroacetophenone, and with an aryl diketone such as 1-phenyl-1,2-propanedione, and a bicyclic ketone such as 1-decalone (Table 7). The electronic factor accounts for the discrete activity measured with (*S*)-1-phenylethanol and 2,2,2-trifluoroacetophenone, as compared to the apparent catalytic inactivity observed with acetophenone and (*S*)-α-(trifluoromethyl)benzyl alcohol. In fact, although the CF_3 group is sterically more demanding than the CH_3 group (van der Waals volume = 42.7 and 24.5 Å^3, respectively) (Zhao et al. 2003), the electron-withdrawing character of fluorine favours hydride transfer, inductively decreasing electron density at the acceptor carbon C1. It is noteworthy that

SaADH proved to be very effective in reducing aliphatic and aryl α-keto esters, halogenated aryl α-keto esters, and halogenated β-keto esters (Table 7). These data show that SaADH is a strictly NAD(H)-dependent oxidoreductase that has discrete substrate specificity. As such, SaADH is more similar to the thermophilic TtADH (Pennacchio et al. 2008), than to the three SDR superfamily mesophilic ADHs (i.e., LsADH, LB-RADH, and PED) which are active on a variety of aliphatic as well as aromatic alcohols, ketones, diketones and keto esters.

Kinetic studies

The kinetic parameters of SaADH determined for the most active substrates are shown in Table 8. Based on the specificity constant (k_{cat}/K_m), this enzyme shows a fivefold greater preference for (*R*)- than (*S*)-α-tetralol, but a similar preference for the enantiomers of 1-indanol. (*R*)- and (*S*)-1-(2-naphthyl)ethanol are very poor substrates and display similar specificity constants. Alicyclic alcohols such as 3-methylcyclohexanol, cycloheptanol and cis-decahydro-1-naphthol were oxidized with relatively low efficiency. In the reduction reaction, isatin was preferred more than methyl and ethyl benzoylformate, and the halogenated acetophenones as well as the aryl diketone 1-phenyl-1,2-propanedione. It is noteworthy that a chlorine substituent at position 2 of the phenyl ring of methyl benzoylformate

Table 8 Steady-state kinetic constants of SaADH [a]

Substrate	k_{cat} (s^{-1})	K_m (mM)	k_{cat}/K_m (s^{-1} mM^{-1})
3-Methylcylohexanol	3.4 ± 0.2	9.9 ± 0.5	0.34
Cycloheptanol	4.4 ± 0.1	9.3 ± 0.3	0.47
(±)-1-Indanol	6.6 ± 0.2	2.30 ± 0.02	2.86
(*R*)-Indanol	7.1 ± 0.2	2.39 ± 0.01	2.98
(*S*)-Indanol	13.7 ± 0.4	6.4 ± 0.3	2.14
cis-Decahydro-1-naphthol	0.98 ± 0.04	4.2 ± 0.3	0.23
α-Tetralol	1.2 ± 0.1	0.48 ± 0.09	2.5
(*R*)-α-Tetralol	13.5 ± 0.5	1.28 ± 0.03	10.5
(*S*)-α-Tetralol	2.1 ± 0.2	1.05 ± 0.08	2.0
(±)-1-(2-naphthyl)ethanol	0.43 ± 0.01	3.7 ± 0.4	0.11
(*R*)-(+)-1-(2-naphthyl)ethanol	0.54 ± 0.06	5.3 ± 0.7	0.10
(*S*)- (−)-1-(2-naphthyl)ethanol	0.48 ± 0.01	5.4 ± 0.5	0.09
NAD^+	3.7 ± 0.1	0.44 ± 0.04	8.4
3-Methylcyclohexanone	3.8 ± 0.03	66.0 ± 3.1	0.06
2,2,2-Trifluoroacetophenone	10.0 ± 0.6	23.5 ± 1.3	0.42
1-Phenyl-1,2-propanedione	3.1 ± 0.3	12.1 ± 2.2	0.25
Methyl benzoylformate	6.2 ± 0.21	6.5 ± 0.4	0.95
Methyl *o*-chlorobenzoylformate	9.2 ± 0.9	2.8 ± 0.2	3.3
Ethyl benzoylformate	2.35 ± 0.07	5.3 ± 0.4	0.44
Isatin	22.0 ± 2.5	0.71 ± 0.11	31
NADH	28.0 ± 2.5	0.16 ± 0.02	175

[a] The activity was measured at 65°C as described in Materials and Methods. Kinetic constants for NAD^+ and NADH were determined with 25 mM cycloheptanol and 5 mM isatin, respectively. The k_{cat} and K_m data are the means ± standard deviations.

enhances the reaction rate to 150%, due to the electronwithdrawing character of halogen; it also increases the affinity of the substrate, reflecting the hydrophobic character of the environment surrounding the phenyl group. Moreover, the specificity constant value is 21-fold higher for NADH than NAD^+. These results suggest that the physiological direction of the catalytic reaction is reduction rather than oxidation. However, the natural substrate and function of SaADH are unknown. As far as the

substrate stereospecificity of SaADH is concerned the enzyme does not seem discriminate between the enantiomer *S* and *R* of 1-indanol, α-tetralol and 1-(2-naphthyl)ethanol, based on the similarity in the K_m values.

Coenzyme stereospecificity

The ^{1}H NMR spectrum of the deuterium-labelled NADD obtained by the reaction of SaADH with 1-phenylethanol-d_9 and NAD^+ shows a single peak at 2.68 ppm corresponding to the *pro-R* hydrogen at the C-4 position of NADD in place of a double doublet centered at 2.62 ppm present in the NADH spectrum (data not shown). The presence of a *pro-S* deuterium atom at C-4 of the pyridine ring of the NADD produced indicates that SaADH transfers the deuteride to the *Si*-face of NAD^+, as illustrated in Fig. 13.

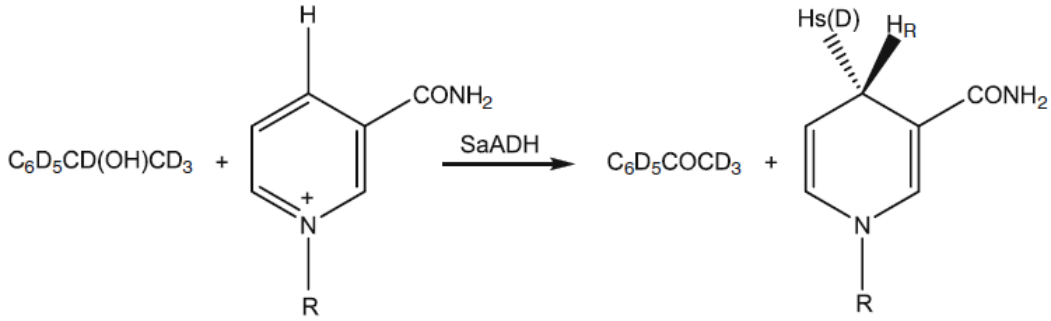

Figure 13. Stereospecificity of hydrogen transfer catalysed by SaADH. R adenosine diphosphate ribose

Therefore, SaADH is a B-type (*pro-S* specific) dehydrogenase in agreement with the classification proposed by Schneider-Bernlöhr et al. (1986) that the SDRs enzymes are *pro-S*, whereas the medium-chain ADHs are *pro-R*, recently substantiated by the structural studies of Kwiecien et al. (2009). SaADH shares the same coenzyme stereospecificity with few other short-chain ADHs such as the thermophilic *T. thermophilus* ADH and the mesophilic enzymes *Leifsonia* sp. strain S749 ADH, 1-phenylethanol dehydrogenase from the denitrifying bacterium strain EbN1, and *Mucor javanicus* and *Drosophila* ADH (Pennacchio et al. 2010b and references therein).

Thermal stability

The thermal stability of SaADH was determined by measuring the residual enzymatic activity after 30 min of incubation over a temperature range from 25 to 95°C (Fig. 14). SaADH was shown to be quite stable up to a temperature of 80°C, above which its activity decreased abruptly, resulting in a $T_{1/2}$ value (the temperature of 50% inactivation) of ~88°C. The residual activity measured after 24 h incubation in 50 mM Tris–HCl, pH 9.0, at 50 and 70°C was 109 and 76%, respectively. In 50 mM Tris–H_3PO_4, pH 7.0, i.e., the buffer used for the bioconversion studies, the residual activity

measured after 6 and 24 h incubation at 50°C was 105 and 107%, respectively.

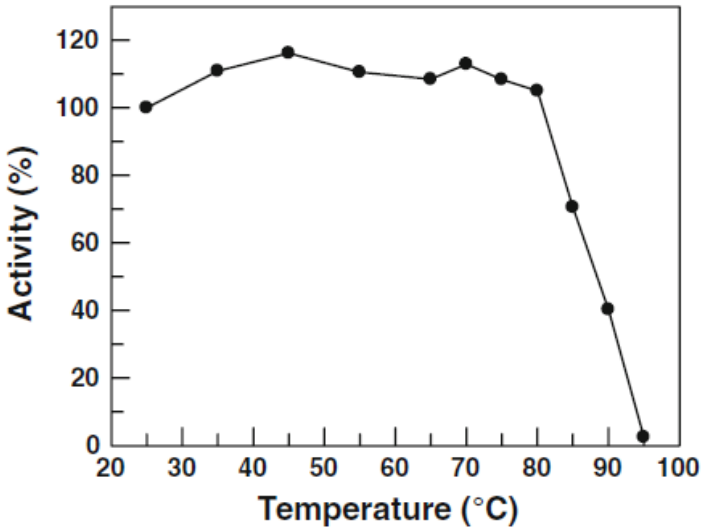

Figure 14. Thermal denaturation of SaADH monitored by dehydrogenase activity. The stability was studied by incubating 0.2 mg mL^{-1} protein samples in 50 mM Tris–HCl, pH 9.0 for 30 min at the indicated temperatures. Activity measurements were carried out under the conditions of the standard assay using cycloheptanol as the substrate. The assay temperature was 65°C.

Effects of various compounds

The effects of salts, ions and reagents on SaADH activity were studied by adding each compound to the standard assay mixture (Table 9). The chlorides of Li^{+}, Na^{+}, K^{+}, Ca^{2+}, Mg^{2+}, and Mn^{2+} did not affect the enzyme's activity, whereas the sulphate of heavy metal ions such as Fe^{2+}, Co^{2+}, and Cu^{2+} caused a slight inactivation. Iodoacetate and Hg^{2+} did, to some extent, affect the activity, indicating that the only Cys residue per monomer, C67,

Table 9. Effect of various compounds on SaADH [a]

Compound	Concn (mM)	Relative activity (%)
None		100
LiCl	1	110
NaCl	1	88
	10	95
KCl	1	99
	10	97
$MgCl_2$	1	94
	10	98
$CaCl_2$	1	100
	10	99
$MnCl_2$	1	95
$FeSO_4$	1	80
$CoSO_4$	1	89
$NiSO_4$	1	106
$CuSO_4$	1	89
$ZnSO_4$	1	91
$Hg(CH_3COO)_2$	1	63
2-Mercaptoethanol	5	112
Iodoacetate	4	88
o-Phenanthroline	1	110
EDTA	1	93
	10	107

[a] Each compounds was added to the reaction mixture at the indicated concentration. The enzyme activity was measured at 65°C using cycloheptanol as substrate.

may have a functional role. The presence of metal-chelating agents did not affect enzyme activity, suggesting that either the protein does not require metals for its activity or the chelating molecule was not able to remove the metal under the assay conditions. Furthermore, the enzyme showed no loss in activity following exhaustive dialysis against EDTA. The EDTA dialysed enzyme turned out to be quite stable at 70°C for 6 h, both in the absence and the presence of EDTA or *o*-phenanthroline (data not shown).

These results suggest that SaADH does not require metals for its activity or structural stabilization. This is usual for the typically non-metal SDRs enzymes, although the well-known LB-RADH shows strong Mg^{2+} dependency (Niefind et al. 2003).

Stability in organic solvents

The effects of common organic solvents, such as 2-propanol, ethyl acetate, acetonitrile, *n*-hexane, *n*-heptane, tert-butylmethyl ether (TBME), methanol, and 1,4-dioxane, on SaADH were investigated at 50°C and at two different time points (Fig. 15). SaADH was activated up to 115% after incubation for 6 h in aqueous buffer and up to 120–125% after incubation for 25 h in the presence of 17% 2-propanol or 17% acetonitrile. Significant increases in enzyme activity occurred after 25 h incubation when ethyl acetate, n-hexane, n-heptane, TBME, and 1,4-dioxane were present at 30% concentration. Activity values ranged from 170 to 210% of the values determined prior to incubation. However, the presence of 2-propanol, acetonitrile, and 1,4-dioxane at a high concentration (30%) resulted in enzyme inactivation to 5–30% of the initial values following 5 h incubation at 50°C. Standard assays performed in the presence of 0.1–0.5% 2-propanol and 0.15% TBME did not affect enzyme activity, suggesting that the enhancement in activity was not due to an immediate effect of solvent on

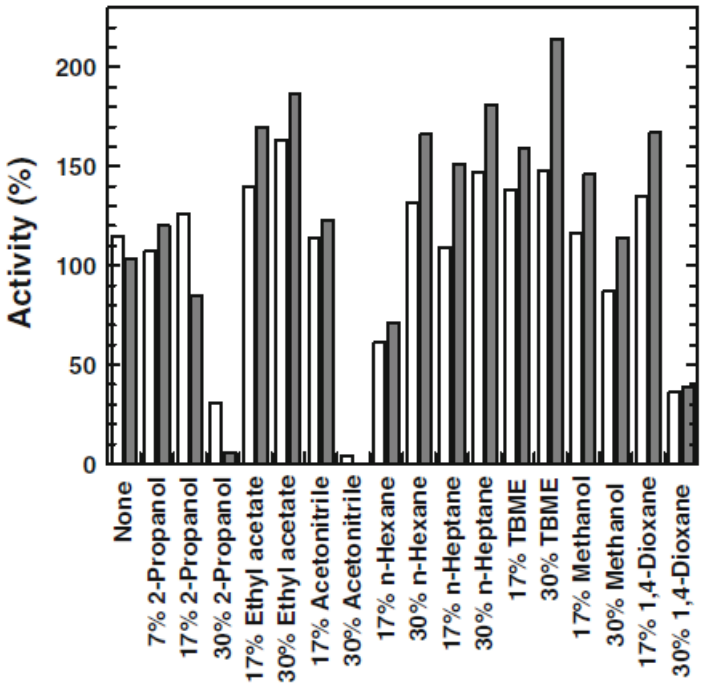

Figure 15. Effect of organic solvents on SaADH. Samples of enzyme (0.5 mg mL^{-1}) were incubated at 50°C in the absence and presence of the organic solvents at the concentrations indicated, and assays were performed after 6 h (white bars) and 25 h (grey bars). The activity assays were performed as described in Materials and Methods using (*R*)-α-tetralol as the substrate. The data obtained in the absence and presence of organic solvents are expressed as percentage of activity relative to the value determined prior to incubation.

the protein structure. A considerable body of literature exists which describes the activation of thermophilic enzymes by loosening of their rigid structure in the presence of protein perturbants (Fontana et al. 1998; Liang et al. 2004). To account for the observed enhancements of SaADH activity, the organic solvent is proposed to induce a conformational change in the protein molecule to a more relaxed and flexible conformation that is optimal for activity. Analogously, the activating effect following heating of SaADH in aqueous buffer at 50°C over a short period (Fig. 15) may be due

to partial loosening of the overall structure, inducing an increased flexibility at the active site, and consequently an increased turnover.

Enantioselectivity

The enantioselectivity of SaADH was tested using α-methyl and α-ethyl benzoylformate, methyl *o*-chlorobenzoylformate, and 1-indanone as substrates, and an NADH regeneration system consisting of glucose and glucose dehydrogenase from *Thermoplasma acidophilum* (TaGDH), a thermophilic enzyme with dual coenzyme specificity, but with a marked preference for NADP(H) over NAD(H) (John et al. 1994). Tris–phosphate buffer pH 7.0 and 50°C was chosen as the pH and temperature conditions suitable for catalysis by the two archaeal enzymes. Thermal stability studies indicated that TaGDH activity dropped to ~70 and 35% following 24 h incubation at 50°C in Tris–phosphate buffer, pH 7.0, in the absence and presence of 10% acetonitrile, respectively (data not shown). Bioconversions of EBF were carried out allowing the reactions to proceed for 1, 3, 6 and 24 h at 50°C. Fig. 16 shows that conversion of EFB was completed in 6 h. However, reaction times as long as 24 h did not improve the enantiomeric excess (*ee*) of the biotransformation. SaADH preferably reduced this keto ester to ethyl (*R*)-mandelate with an *ee* of 50%, after 6 h of reaction.

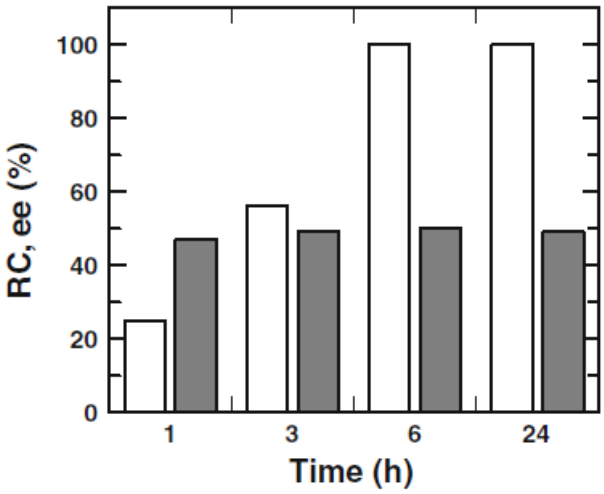

Figure 16. Reduction of ethyl benzoylformate catalysed by SaADH. Biotransformations were carried out at 50°C at different reaction times as described in Materials and Methods. The reactions were stopped by addition of ethyl acetate at the times indicated. The dried extracts were analysed by chiral HPLC to determine the relative conversion (RC, open bars) and the enantiomeric excess (*ee*, grey bars).

Methyl benzoylformate was reduced by SaADH to methyl (*S*)-mandelate with 100% conversion after 6 h of reaction and an *ee* of 17%, and methyl *o*-chlorobenzoylformate was reduced to methyl (*R*)-*o*-chloromandelate with 99% conversion and an *ee* of 72% (Table 10). These results show that enantioselectivity of SaADH is dependent upon the structure of both the phenyl group and alkyl substituent of the ester group of the substrate.

1-indanone was reduced to the corresponding (*S*)-alcohol following a 6-h reaction at 50°C, with a conversion of 6% and an *ee* of 25%, reflecting the apparent inactivity under different assay conditions (see Table 7). It is noteworthy that the optically active alcohols produced are used as chiral building blocks in organic synthesis. Methyl (*R*)-*o*-chloromandelate is an

Table 10. Asymmetric reduction of carbonyl compounds by SaADH

Substrate	Product	Conversion (%) [a]	*ee* (%) [a]	*R*/*S*
Methyl benzoylformate	Methyl mandelate	100 (100)	36 (17)	*S*
Ethyl benzoylformate	Ethyl mandelate	100 (100)	34 (50)	*R*
Methyl *o*-chlorobenzoylformate	Methyl *o*-chloromandelate	100 (99)	72 (71)	*R*

[a] Reactions were performed at 50°C for 6 h in the presence of 10% acetonitrile as described in Materials and Methods. Values in parentheses were obtained with bioconversions performed in the absence of acetonitrile. Conversion yields and enantiomeric excesses were determined by chiral HPLC analysis. Configuration of product alcohol was determined by comparing the retention time with that of standard samples as described in Material and Methods.

intermediate for the platelet aggregation inhibitor clopidogrel (Ema et al. 2008), and (*R*)-ethyl mandelate is precursor for the synthesis of cryptophycins (Gardinier and Leahy 1997).

Conclusion

Although the efficiency of conversion was more than satisfactory, the low purity of the preferred enantiomer precludes SaADH from use in utility-scale applications. However, the work represents the first biochemical characterization of an NAD(H)-dependent archaeal short-chain ADH, and moreover. Moreover, the study adds further support for the critical role of the above-mentioned D37 in SDRs in discriminating NAD(H) from NADP(H) (Pennacchio et al. 2010a).

Biochemical and structural characterization of recombinant short-chain NAD(H)-dependent dehydrogenase/reductase from *Sulfolobus acidocaldarius* highly enantioselective on diaryl diketone benzil

The second gene, *saadh2*, encoding a putative NAD(H)-dependent oxidoreductase has been heterologously overexpressed in *Escherichia coli*, and the resulting protein (SaADH2) purified to homogeneity and characterized in terms of substrate specificity, kinetics and stability. SaADH2 was found to be highly efficient and enantioselective in reducing the diaryl diketone benzil to (*R*)-benzoin, an useful building block. Detailed studies on 3D structure, performed in collaboration with Dr. L Esposito, have provided detailed insights into the enzyme enantioselectivity.

Identification of the putative SDR oxidoreductase gene

Analysis of the *S. acidocaldarius* genome (Chen et al. 2005) for genes encoding short-chain ADHs resulted in identification of a putative oxidoreductase gene. The sequence of the 27,024-Da protein, named SaADH2, showed the highest level of identity to four typical SDRs, LB-RADH (29% identity), LsADH (34 %), TtADH (35%) and SaADH (30%; Fig. 17).

Figure 17. Multiple-sequence alignment of the *S. acidocaldarius* ADH (SaADH2) and ADHs belonging to the SDR family, including *S. acidocaldarius* ADH (SaADH; NCBI accession no. YP_256716.1), *L. brevis* ADH (LB-RADH; PDB code 1ZK4), *Leifsonia* sp. strain S749 ADH (LsADH; NCBI accession no. BAD99642) and *T. thermophilus* ADH (TtADH; PDB code 2D1Y). The sequences were aligned using the ClustalW2 program. Grey shading indicates residues highly conserved in the SDR family. The four members of the catalytic tetrad are indicated by a black background. The following positions are indicated by bold type: the glycine-rich consensus sequence and the sequence motif Dhx[cp] that (in all SDRs) have a structural role in coenzyme binding (Kallberg et al. 2002). The star indicates the major determinant of the coenzyme specificity. The LB-RADH G37D mutant shows preference for NAD^+ over $NADP^+$ (Schlieben et al. 2005)

Expression and protein purification

The saadh2 gene successfully expressed in *E. coli* cells, yielded an active enzyme accounting for about 9% of the total protein content of the cell extract (Table 11).

Table 11. Purification of recombinant *Sulfolobus acidocaldarius* ADH [a]

Step	Total protein (mg)	Total activity (U)	Specific activity (U/mg)	Yield (%)	Purification (fold)
Crude extract	500	3,554	7.1	100	1
Thermal step	174	2,843	16.3	80	2.3
DEAE FF	63	2,170	34.4	61	4.8
Gel filtration	44	1,704	38.7	48	5.4

[a] The data are for a 2-liter culture. The substrate was cycloheptanol, and the assay temperature was 65°C.

Host protein precipitation at 70°C was found to be the most effective purification step. An overall purification of 5.4-fold was achieved from crude-cell-free extracts with an overall yield of 48%. SDS-PAGE of the purified protein showed a single band corresponding to a molecular mass of 29 kDa (data not shown).

The quaternary structure of SaADH2

The quaternary structure of the enzyme was investigated by sucrose density gradient centrifugation. SaADH2 sedimented as one peak nearly overlapping that of TtADH (Fig. 18). The plot of molecular mass of the markers vs fraction number (inset Fig. 18) allowed to determine an apparent molecular mass of 109±10 kDa for SaADH2. The molecular mass of the subunit determined by ESI-MS analysis proved to be 27,024.0 Da (average mass), in agreement with the theoretical value of the sequence.

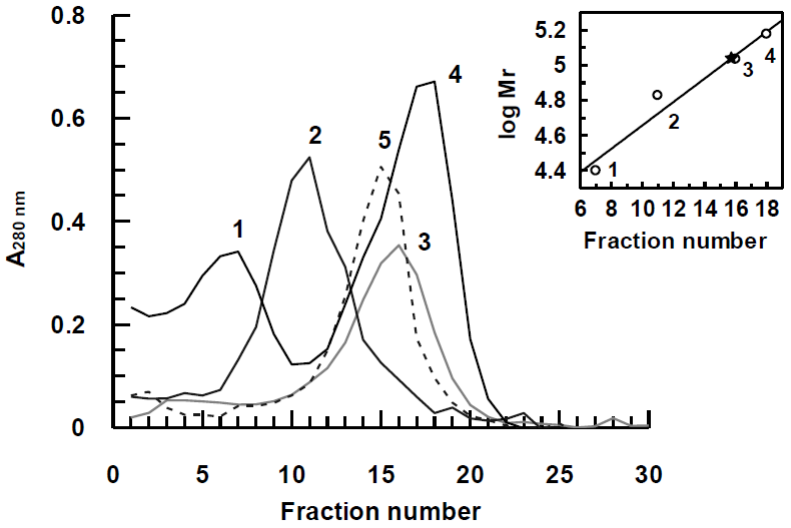

Figure 18. Sucrose gradient centrifugation analysis of SaADH2. 5–25% sucrose gradient was used as described in Material and Methods. Positions of the standards and that of SaADH2 are shown: (1) Chymotrypsinogen; (2) BSA; (3) *T. thermophilus* ADH; (4) *S. solfataricus* ADH; (5) SaADH2. Absorbance values were corrected for the blank i.e. from a blank gradient. The inset shows the semiplot of the molecular masse of the standards 1 to 4 vs fraction numbers. The star indicates the position of SaADH2.

Optimal pH

The pH dependence of SaADH2 in the reduction and oxidation reaction was analysed (Fig. 19). The SaADH2 activity was found to be closely dependent on pH in the reduction reaction, displaying a peak of maximum activity at around pH 5.0. The oxidation reaction showed a less marked dependence on pH, displaying a peak with a maximum at around pH 10.0.

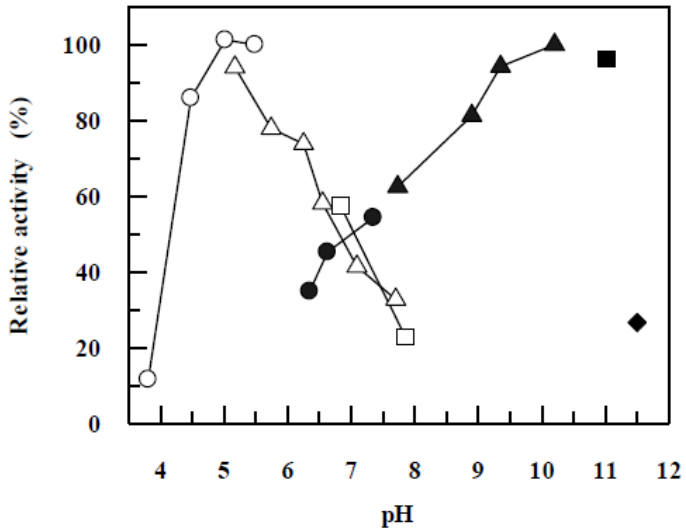

Figure 19. SaADH2 activity as a function of pH in the reduction and oxidation reactions. The following buffer solutions at concentrations ranging from 25 to 55 mM were used: sodium citrate (○), sodium phosphate (Δ), and Tris-HCl (□) in the reduction reaction, and sodium phosphate (●), glycine-NaOH (▲), sodium citrate (■), and sodium phosphate (♦) in the oxidation reaction. The mixture for the reduction reaction contained 20 mM EMO and 0.2 mM NADH, and the mixture for the oxidation reaction contained 18 mM cycloheptanol and 3 mM NAD^+. The assays were performed at 65°C under the conditions described in Materials and Methods.

Thermophilicity and thermal stability

The effect of temperature on SaADH2 activity is shown in Fig. 20. The reaction rate increases up to 78°C and then decreases rapidly due to thermal inactivation. This optimal temperature value is similar to that of TtADH (73°C) and SaADH (75°C) (Pennacchio et al. 2008; 2010a, b), and lower than that of *P. furiosus* aldo-keto reductase (100°C) (Machielsen et al. 2006). The thermal stability of SaADH2 was determined by measuring the residual enzymatic activity after 30 min of incubation over a temperature range from 25 to 95°C (Fig. 20). SaADH2 was shown to be quite stable up

to a temperature of ~75°C, above which its activity decreased abruptly, resulting in a $T_{1/2}$ value (the temperature of 50% inactivation) of ~88°C.

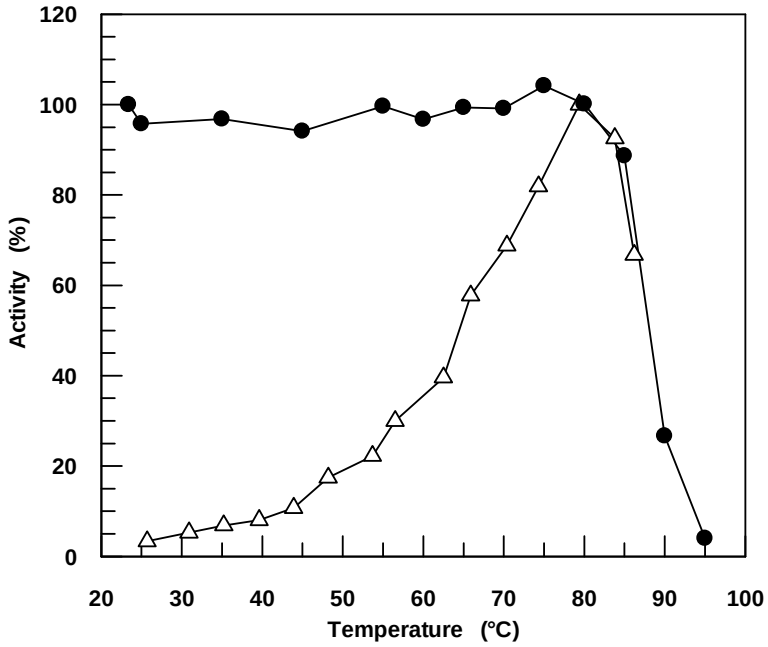

Figure 20. Effect of temperature on activity and stability of SaADH2 monitored by dehydrogenase activity. The assays at the increasing temperature values (triangles) were carried out as described in Materials and Methods, using cycloheptanol as the substrate. The thermal stability (circles) was studied by incubating 0.2 mg mL^{-1} protein samples in 50 mM Tris–HCl, pH 9.0 for 30 min at the indicated temperatures. Activity measurements were carried out under the conditions of the standard assay using cycloheptanol as the substrate. The assay temperature was 65°C. The percentage of residual activity was obtained by the ratio to the activity without heating.

Coenzyme and substrate specificity

The enzyme showed no activity with NADP(H) and full activity with NAD(H). The specificity of SaADH2 for various alcohols, aldehydes and ketones was examined (Table 12). SaADH2 is more similar to the archaeal thermophilic TtADH and SaADH (Pennacchio et al. 2008; 2010a, b), than

to the two representative SDR mesophilic ADHs, i.e. LB-RADH (Schlieben et al. 2005) and LsADH (Inoue et al. 2006), which are active on a variety of aliphatic as well as aromatic alcohols, ketones, diketones and keto esters.

The enzyme showed a poor activity on a discrete number of aliphatic linear and branched alcohols, such as 2-propyn-1-ol, 4-methyl-1- pentanol, the *S* enantiomers of 2-butanol and 2-pentanol as well as on aliphatic cyclic and bicyclic alcohols, except for isoborneol and cycloheptanol which rank first and second, respectively, among the tested alcohols. Benzyl alcohol and substituted benzyl alcohols were found to be poor substrates. Among the aromatic secondary alcohols tested SaADH2 showed a low activity on (*S*)-1-phenylethanol and no activity with the *R* enantiomer, whereas displayed similar poor activities towards the (*S*)- and (*R*)- forms of α-(trifluoromethyl)-benzyl alcohol, 1-(2-naphthyl)ethanol and methyl and ethyl mandelates. Moreover, the enzyme showed poor activity on (±)-1-phenyl-1-propanol and its ortho-chloro derivative, and para-halogenated 1-phenylethanols. However, SaADH2 showed a relatively high activity with 1-indanol and α-tetralol, but a poor activity on the β-hydroxy ester ethyl (*R*)-4-chloro-3-hydroxybutyrate. The enzyme was not active on aliphatic and aromatic aldehydes, and on aliphatic linear, and branched ketones (data

Table 12. Substrate specificity of SaADH2 in the oxidation and reduction reactions[a]

Substrate	Relative activity (%) [c]	Substrate	Relative activity (%) [c]
Alcohols			
2-Propyn-1-ol	5	1-(2-Chlorophenyl)-1-propanol[b]	2
4-Methyl-1-pentanol	2	(±)-1-Indanol[d]	26
(*S*)-2-Butanol	3	(±)-α-Tetralol[b]	51
(*R*)-2-Butanol	0	(±)-1-(2-Naphthyl)ethanol	2
2,3-Butanediol	2	(*S*)-1-(2-Naphthyl)ethanol	3
(±)-2-Pentanol	2	(*R*)-1-(2-Naphthyl)ethanol	2
(*S*)-2-Pentanol	7	Benzoin	0
(*R*)-2-Pentanol	0	*trans*-1,3-Diphenyl-2-propen-1-ol	5
3-Pentanol	1	Ethyl (*R*)-4-chloro-3-hydroxybutyrate	2
2-Hexanol[b]	2	Methyl (*S*)-(−)-mandelate	4
2-Heptanol[b]	2	Methyl (*R*)-(+)-mandelate	3
6-Methyl-5-hepten-2-ol[b]	3	Ethyl (*S*)-(−)-mandelate	2
1-Octanol	1	Ethyl (*R*)-(+)-mandelate	2
Geraniol	2	Ketones[b]	
Cyclopentanol	2	Cyclohexanone	13
Cyclohexanol	6	2-Methylcyclohexanone	33
3-Methylcyclohexanol[b]	10	3-Methylcyclohexanone	60
Cycloheptanol	55	4-Methylcyclohexanone	41
Cyclohexylmethanol[b]	2	Cycloheptanone	0
2-Cyclohexylethanol	1	1-Decalone	85
Chrysanthemyl alcohol	1	(±)-Camphor	0
cis-Decahydro-1-naphthol	3	Acetophenone	0
Isoborneol	100	2,2-Dichloroacetophenone	30
Benzyl alcohol	7	2,2,2-Trifluoroacetophenone	35
2-Methoxybenzyl alcohol	5	2',3',4',5',6'-Pentafluoroacetophenone	45
3-Methoxybenzyl alcohol	6	1-Phenyl-1,2-propanedione	100
4-Methoxybenzyl alcohol	3	1-Indanone[d]	0
4-Bromobenzyl alcohol[b]	9	α-Tetralone	0
(*R*,*S*)-1-Phenylethanol[b]	2	Benzil	62
(*S*)-(−)-1-Phenylethanol	6	2,2'-Dichlorobenzil	0
(*R*)-(+)-1-Phenylethanol	0	Chalcone	0
(*R*,*S*)-α-(Trifluoromethyl)benzyl alcohol	2	Keto esters[b]	
(*S*)-α-(Trifluoromethyl)benzyl alcohol	2	Ethyl pyruvate	16
(*R*)-α-(Trifluoromethyl)benzyl alcohol	2	Ethyl 3-methyl-2-oxobutyrate	100
1-(4-Fluorophenyl)ethanol[b]	5	Ethyl 4-chloroacetoacetate	0
1-(4-Chlorophenyl)ethanol[b]	2	Methyl benzoylformate	8
(±)-1-Phenyl-1-propanol[b]	2	Methyl *o*-chlorobenzoylformate	5
trans-Cinnamyl alcohol[b]	2	Ethyl benzoylformate	23

not shown). However, it was active on aliphatic cyclic and bicyclic ketones such as cyclohexanone, methyl-substituted cyclohexanones and decalone

[a] The activity was measured at 65°C as described in Materials and Methods. The concentration of each substrate was 5 mM.
[b] The substrates were dissolved in 100% 2-propanol.
[c] The percent values refer to cycloheptanol for alcohols, benzyl for ketones and to ethyl 3-methyl-2-oxobutyrate for keto esters.
[d] The substrate was dissolved in 100% acetonitrile.

(Table 12). Two aryl diketones, 1-phenyl-1,2-propanedione and benzyl were good substrates of SaADH2 which also showed a relatively high reduction rate with 2,2-dichloro- and 2,2,2-trifluoroacetophenone and penta-substituted fluoroacetophenone (Table 12).

The electronic factor accounts for the relatively high activity measured with the halogenated acetophenones, as compared to the apparent zero activity observed with acetophenone. The electron withdrawing character of fluorine (or chlorine) favours hydride transfer, inductively decreasing electron density at the acceptor carbon C1. On the other hand, the corresponding ketones of cycloheptanol and isoborneol, cycloheptanone and camphor did not show any apparent activity due to the deactivating effect exerted by the electron donating alkyl groups on the acceptor carbon C1. SaADH2 was also active on aliphatic and aryl α-keto esters but not on β-ketoesters (Table 12).

Kinetic studies

The kinetic parameters of SaADH2 determined for the most active substrates are shown in Table 13. Based on the specificity constant (k_{cat}/K_m), isoborneol is the best substrate in the oxidation reaction; compared to the alicyclic cycloheptanol and aromatic bicyclic alcohols, it displays a higher affinity to the active site probably due to its alicyclic

bridged structure. However, the enzyme shows a 6-fold greater preference for (*S*)- than (*R*)-1-indanol and a 23-fold greater preference for (*S*)- than

Table 13. Steady-state kinetic constants of SaADH2 [a]

Substrate	k_{cat} (s^{-1})	K_m (mM)	k_{cat}/K_m (s^{-1} mM^{-1})
Cycloheptanol	7.0	5.1	1.37
Isoborneol	16.6	0.81	20.5
(±)-1-Indanol	6.2	8.7	0.71
(*R*)-Indanol	2.7	15.3	0.18
(*S*)-Indanol	10.6	10.0	1.06
α-Tetralol	9.6	8.5	1.13
(*R*)-α-Tetralol	1.15	9.2	0.13
(*S*)-α-Tetralol	6.0	2.0	3.0
NAD^+	19.3	0.18	107
Benzil	1.6	0.43	3.72
1-Phenyl-1,2-propanedione	5.3	5.0	1.06
2,2-Dichloroacetophenone	0.65	0.11	5.91
2,2,2-Trifluoroacetophenone	1.7	6.3	0.27
2',3',4',5',6'-Pentafluoroacetophenone	3.2	11.9	0.27
Ethyl 3-methyl-2-oxobutyrate	26	16.6	1.57
Ethyl benzoylformate	1.9	4.2	0.45
NADH	26.2	0.04	655

[a] The activity was measured at 65°C as described in Materials and Methods. Kinetic constants for NAD^+ and NADH were determined with 15 mM isoborneol and 30 mM ethyl 3-methyl-2-oxobutyrate, respectively.

(*R*)-α-tetralol. In the reduction reaction, 2,2-dichloroacetophenone was preferred 22-fold more than 2,2,2-trifluoroacetophenone and 2′,3′,4′,5′,6′-pentafluoroacetophenone, and 1.6- and 6-fold more than the two diketones, benzil and 1-phenyl-1,2-propanedione, respectively, due to its higher affinity. Ethyl 3-methyl-2-oxobutyrate shows the highest turnover among

the carbonyl compound tested, although it binds to the catalytic site with relatively low affinity. Moreover, the specificity constant value is 6-fold higher for NADH than NAD^+. The kinetic data show that for most of chiral substrates SaADH2 is (*S*)-stereospecific and that the physiological direction of the catalytic reaction is reduction rather than oxidation (Table 13).

Effects of various compounds

The effects of salts, ions and reagents on SaADH2 activity were studied by adding each compound to the standard assay mixture. The enzyme activity in the presence of 1 mM of the Li^+, Na^+, K^+, Ca^{2+}, Mg^{2+} and Mn^{2+} chlorides was 115, 113, 102,101, 101 and 110%, respectively, and in the presence of 1 mM of the sulphate of heavy metal ions such as Fe^{2+}, Co^{2+}, Ni^{2+},Cu^{2+} and Zn^{2+} was 93, 108, 104, 102 and 107%, correspondingly, when compared to the enzyme activity measured in the absence of additional metal ions. The presence of 5% ionic liquid (BMIMBF4) inactivated by 50% the enzyme presumably due to a competition of the $BF4^-$ ion with the coenzyme phosphate moiety for the anion-binding site of the enzyme. The addition of 4 mM iodoacetate and 1 mM Hg^{2+} had no significant influence on the enzyme activity, which resulted in 101 and 113% of the control activity, respectively, suggesting that the only Cys residue per monomer, C90, has

no functional role. Even the metal-chelating agents did not affect enzyme activity. The enzyme activity in the presence of either 1mM *o*-phenanthroline, or 10 mM EDTA was 98 and 87%, respectively, suggesting that either the protein does not require metals for its activity or the chelating molecule was not able to remove the metal under the assay conditions. Furthermore, the enzyme showed no loss in activity following exhaustive dialysis against EDTA. The EDTA-dialysed enzyme turned out to be quite stable at 70°C for 5 h, both in the absence and the presence of EDTA (data not shown). The analysis of the effects of ions reveals that SaADH2 does not require metals for its activity or structural stabilization; this is typical of non-metal SDR enzymes, although the well-known LB-RADH shows strong Mg^{2+} dependency (Niefind et al. 2003).

Stability in organic solvents

The effects of common organic solvents, such as acetonitrile, DMSO, 1,4-dioxane and ethyl acetate on SaADH2 were investigated at 50°C, at two different time points and 18% concentration (Fig. 21). SaADH2 activated after 6 and 24 h incubation in aqueous buffer (120 and 105% the initial values, respectively), and inactivated by 15 and 30% in the presence of 18% acetonitrile following incubation for 6 and 24 h, respectively. A slightly reduced activity (95%) remained after 6 and 24 h incubation in

aqueous solution containing 18% ethyl acetate. Interestingly, significant increases in enzyme activity occurred after 6 h incubation in the presence

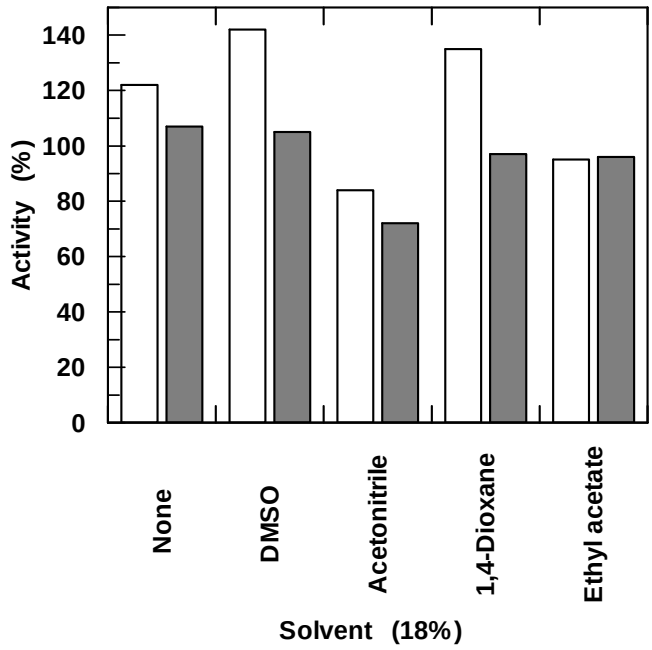

Figure 21. Effects of various solvents on SaADH2. Samples of enzyme (0.20 mg mL^{-1}) were incubated at 50°C in the absence and presence of the organic solvents at 18% concentrations, and the assays were performed after 6 h (white bars) and 24 h (grey bars). The activity assays were performed at 50°C as described in Materials and Methods using cycloheptanol as the substrate. The data obtained in the absence and presence of organic solvents are expressed as percentage of activity relative to the value determined prior to incubation.

of 18% DMSO (>140%) and 1,4-dioxane (135%). After 24 h incubation in the presence of these two solvents, the enzyme activity remained nearly unchanged with respect to the initial value. The activation of thermophilic enzymes by loosening of their rigid structure in the presence of protein perturbants is a well documented phenomenon (Fontana et al. 1998; Liang et al. 2004). The two organic solvents discussed above (Fig. 21) may

induce a conformational change in the protein molecule to a more relaxed and flexible state that is optimal for activity.

Enantioselectivity

The enantioselectivity of SaADH2 was tested on benzil using an NADH recycling system consisting of thermophilic NAD(H)-dependent BsADH (Fig. 22).

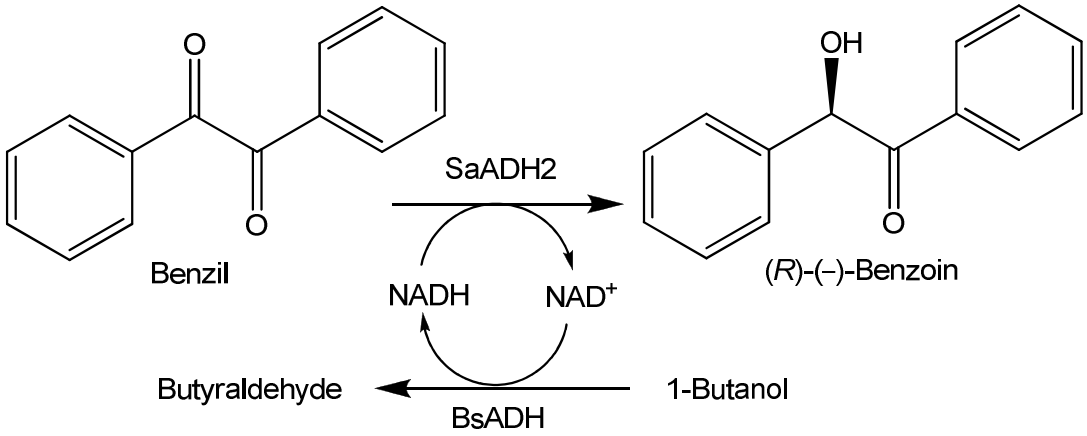

Figure 22. Coenzyme recycling in the production of chiral diaryl alcohol with SaADH2 utilizing BsADH and 1-butanol.

As previously mentioned, BsADH is mainly active on aliphatic and aromatic primary and secondary alcohols and aldehydes, but not on aliphatic and aromatic ketones, nor on the carbonyl substrates of SaADH2 and corresponding alcohols (data not shown). Since 2-propanol is not a substrate of SaADH2, it may be a suitable substrate for BsADH in NADH recycling, as well as being used as a co-solvent. Bioconversions were

carried out for 24 h using 5 mM benzil as substrate and 2-propanol at three different concentrations. Sodium phosphate buffer, pH 7.0 and 50°C was chosen as a compromise between cofactor stability and catalytic activity of the two ADHs at suboptimal pH (Pennacchio et al. 2008.). Chiral HPLC analysis of the extracts obtained from the bioconversions showed that benzyl was reduced by the archaeal enzyme to the (*R*)-enantiomer of benzoin with a level of conversion of 35, 100 and 99% and an enantiomeric excess (*ee*) of 85, 82 and 80% using 4, 14 and 18% (v/v) 2-propanol as ancillary substrate, respectively.

In addition to 2-propanol (k_{cat}/K_m = 9 s^{-1} mM^{-1}), BsADH oxidizes other alcohols with even greater efficiency such as ethanol (k_{cat}/K_m = 64 s^{-1} mM^{-1}), 1-propanol (286 s^{-1} mM^{-1}), 1-butanol (437 s^{-1} mM^{-1}), 1-pentanol (64 s^{-1} mM^{-1}) and 1-hexanol (64 s^{-1} mM^{-1}; Raia, unpublished data).We therefore tested these alcohols as alternative hydride source for NADH recycling and also to improve the solubility of the substrate in the aqueous phase. Moreover, these alcohols and the respective aldehydes are not substrates of SaADH2. Thus, only the cofactor is the co-substrate of SaADH2 and BsADH.

Fig. 23 summarizes the results of the bioconversions carried out using different alcohol substrates at 18% concentrations. As for the case of 2-propanol, benzil was reduced to the (*R*)-alcohol with excellent conversion

(>99%) but modest enantioselectivity using ethanol and 1-propanol. However, in the presence of 1-butanol, 1-pentanol and 1-hexanol excellent optical purity (98–99% *ee*) and levels of conversion decreasing from 98 to

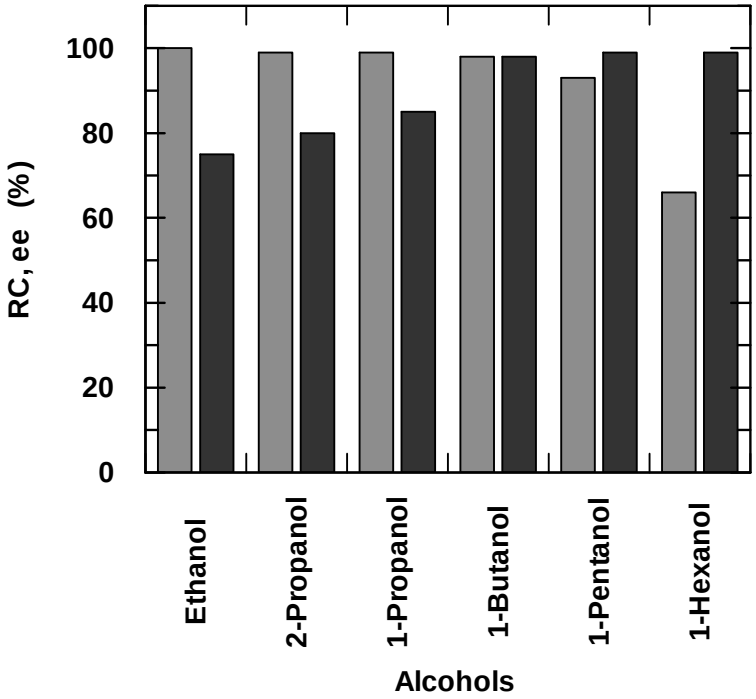

Figure 23. Reduction of benzil catalyzed by SaADH2. Biotransformations were carried out at 50°C with different alcohols at 18% (*v/v*) concentrations. The reactions were stopped after 24 h by addition of ethyl acetate. The dried extracts were analysed by chiral HPLC to determine the relative conversion (*RC, grey bars*) and the enantiomeric excess (*ee, dark grey bars*). Error limit, 2% of the stated values. The alcohols are plotted according to increasing log P (P=partition coefficient) values; from *left to right*: log *P* =−0.24, 0.07, 0.28, 0.8, 1.3 and 1.8. Log *P* values were from Laane et al. (1987).

93% and 66%, respectively, were obtained. This suggests that ethanol and linear/branched propanol acted as good substrates and solvents for the bioconversion system, but negatively affected the prochiral selectivity of SaADH2 that was instead enhanced by longer chain-linear alcohols (four to six carbons). The decrease in conversion rate with 1-pentanol and 1-

hexanol could be due to different effects: (1) substrate excess inhibition, (2) BsADH deactivation and (3) reduced substrate solubility. The finely tuned solvent dependence of the prochiral selectivity shown by SaADH2 is remarkable and agrees with the general observation that enzyme selectivity (enantiomeric, prochiral and regiomeric) can change, or even reverse, from one solvent to another (Carrea and Riva 20050; Klibanov 2001). Overall, the solvent enantioselectivity study emphasizes the versatility and high efficiency of the BsADH/ alcohol substrate system in recycling the reduced cofactor. α-Hydroxy ketones are highly valuable building blocks for many applications for the fine chemistry sector as well as pharmaceuticals (Hoyos et al. 2010). It is noteworthy that optically pure (*R*)-benzoin is useful as urease inhibitor (Tanaka et al. 2004), and to prepare amino alcohols used as important chiral synthons (Aoyagi et al. 2000), or to synthesize different heterocycles (Wildemann et al. 2003). Many examples of stereoselective reduction of several benzyls to the corresponding benzoins using whole microbial cells have been recently reviewed (Hoyos et al. 2010). The microorganisms *Bacillus cereus*, *Pichia glucozyma*, *Aspergillus oryzae*, *Fusarium roseum*, *Rhizopus oryzae* (at pH 4.5–5.0) and *B. cereus* Tm-r01 were reported to give (*S*)-benzoin while the microorganisms *R. oryzae* (at pH 6.8–8.5) and *Xanthomonas oryzae* were reported to transform benzil to (*R*)-benzoin with different yields and optical

purity (Hoyos et al. 2010 and references therein). However, recombinant B. cereus NADPH-dependent benzil reductase belonging to SDR superfamily which reduces benzil to 97% optically pure (*S*)-benzoin in vitro was characterized (Maruyama et al. 2002).

The SaADH2 enantioselectivity was further examined with other aromatic ketones using the system BsADH/1-butanol.

Table 14 shows that SaADH2 preferably reduced benzil to (*R*)-benzoin with an *ee* of 98% and 98% conversion after 24 h of reaction, and that the selectivity was reduced when 2-propanol instead of 1-butanol was used.

Table 14. Asymmetric reduction of carbonyl compounds by SaADH2 [a]

Substrate	Product	Conversion (%)	*ee* (%)	*R*/*S*
Benzil	Benzoin	98(99)	98(80)	*R*
2,2'-Dichlorobenzil	1,2-Bis(2-chlorophenyl)-2-hydroxyethanone	33	91	*R*
Acetophenone	1-Phenylethanol	4	92	*S*

[a] Reactions were performed at 50°C for 24 h as described in Materials and Methods, using 18% 1-butanol as ancillary substrate. Conversion and enantiomeric excess were determined by chiral HPLC analysis. Configuration of product alcohol was determined by comparing the retention time with that of standard samples as described in Material and Methods. Values in parentheses refer to data obtained with 18% 2-propanol as ancillary substrate.

However, 2,2′-dichlorobenzil was reduced to (*R*)-1,2-bis(2-chlorophenyl)-2-hydroxyethanone with lower conversion (33%) and *ee* of 91%, despite the apparent inactivity under different assay conditions (Table 12). Presumably, the presence of chlorine, a bulky atom with electron-withdrawing properties, disturbs the fitting of the diketone molecule in the substrate-binding pocket as well as the interactions that stabilize the transition state. Acetophenone was reduced to (*S*)-1-phenylethanol with a 4% conversion and an *ee* of 92%, while no conversion was observed for camphor, the ketone corresponding to the highly preferred alcohol isoborneol (see Table 13). Kinetic tests showed that neither racemic benzoin nor (*R*)-benzoin was oxidized in the presence of NAD^+ as well as both were not reduced in the presence of NADH. Accordingly, the HPLC analysis indicated that no further reduction of benzoin occurred since no trace of hydrobenzoin could be found within the detection limits (data not shown).

Structural characterization

The functional characterization of SaADH2 was complemented by the determination of the crystal structure of SaADH2–NADH complex at 1.75 Å resolution. The determined crystal structure reveals a tetrameric organization similar to other members of the short chain

dehydrogenase/reductase (SDR) family that corroborates the results obtained by sucrose density gradient centrifugation. Although SaADH2 has low sequence similarities with other SDR proteins, it shares common structural features with them (Kallberg et al. 2002; Kavanagh et al 2008). The overall structure is typical of SDRs that is an α/β fold with characteristic Rossmann-fold motifs for the binding of the dinucleotide cofactor at the N-terminal region of the chain. Indeed, the structure confirmed that SaADH2 is a NAD-dependent enzyme with a cofactor-binding domain composed of a seven-stranded parallel sheet flanked by helices on each side.

Overall tertiary and quaternary structure

The structural comparison of SaADH2 with other SDRs demonstrated that SaADH2 exhibits a high degree of overall structural homology despite the low sequence similarities. Indeed, when aligning the monomeric structures by the DALI server the first 100 best superimpositions showed RMS deviations on Cα atoms ranging from 1.5 to 2.5 Å (with a minimum of 222/255 aligned residues). Some structural neighbours are superimposed onto a single chain of SaADH2 in Fig. 24. Major conformational differences are found on the molecular surface and at the C terminal region of the polypeptide chain which contributes to the shaping of the active site.

Analysis of the crystal packing (using PISA server: http://www.ebi.ac.uk/pdbe/prot_int/pistart.html), indicates that the tetramer is the biologically active form.

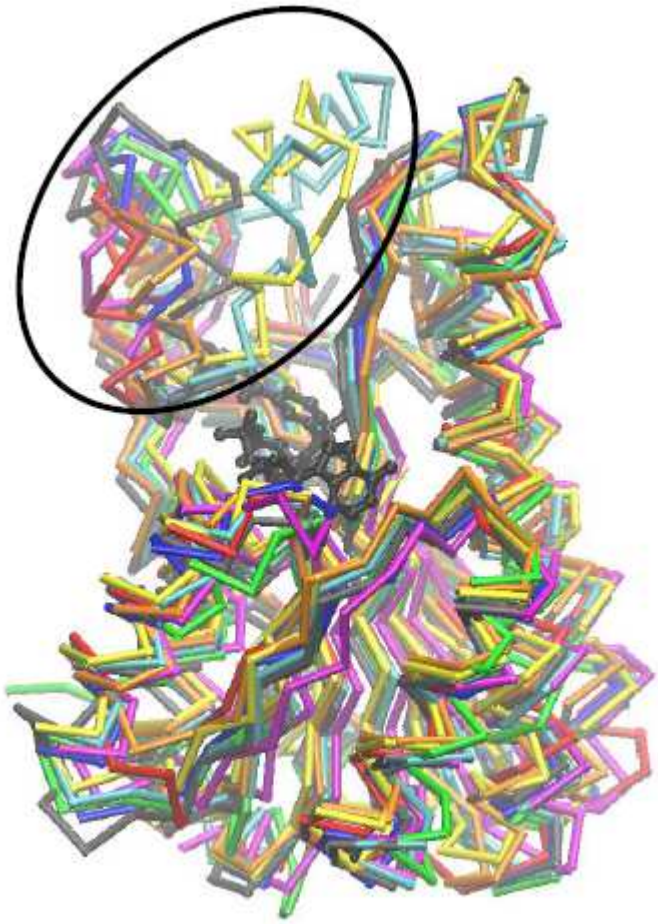

Figure 24. Superimposed Cα traces of SaADH2 single chain (cyan) and some of its structural neighbours, as derived from the DALI server (http://ekhidna.biocenter.helsinki.fi/dali_server). The NADH molecule of SaADH2 structure is highlighted in dark grey as ball-and-stick representation. The black ellipse includes the substrate binding loop region (SaADH2 residues 193-211).
The structural alignment includes: SaADH2 (cyan); *T. thermophilus* ADH (PDB code 2D1Y) (orange); 3-oxoacyl-(acyl carrier protein) reductase from *B. anthracis* (PDB code 2UVD) (blue); *L. brevis* ADH (PDB code 1ZK4) (red); *C. acquaticum* levodione reductase (PDB code 1IY8) (grey); *P. falciparum* Oxoacyl-acp reductase (PDB code 2c07) (green); *S. Clavuligerus* clavulanic acid dehydrogenase (PDB code 2JAP) (yellow); putative glucose/ribitol dehydrogenase from *C. thermocellum* (PDB code 2HQ1) (magenta).

The tetramer shows 222 point group symmetry and approximate dimensions of 80×70×55 Å (Fig. 25).

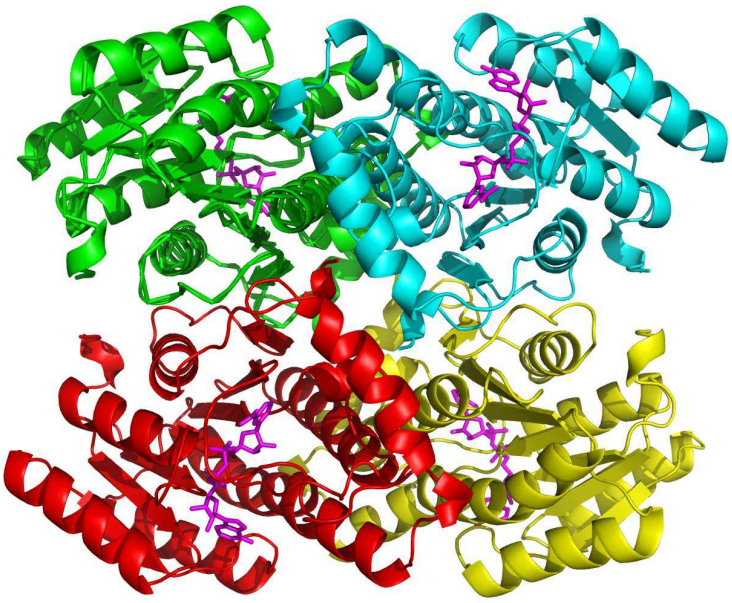

Figure 25. Ribbon diagram of the overall structure of tetrameric SaADH2 in complex with NADH (magenta). The chains are shown in cyan (A), green (B), yellow (C), and red (D).

The largest dimeric interface is the one involving AB or CD assemblies (~1,630 $Å^2$). The central elements in this interface are the long α6 helices (residues 156–179, Fig. 26) facing each other from adjacent subunits. Other segments involved in this interface are α4 and α5 helices (Fig. 26).

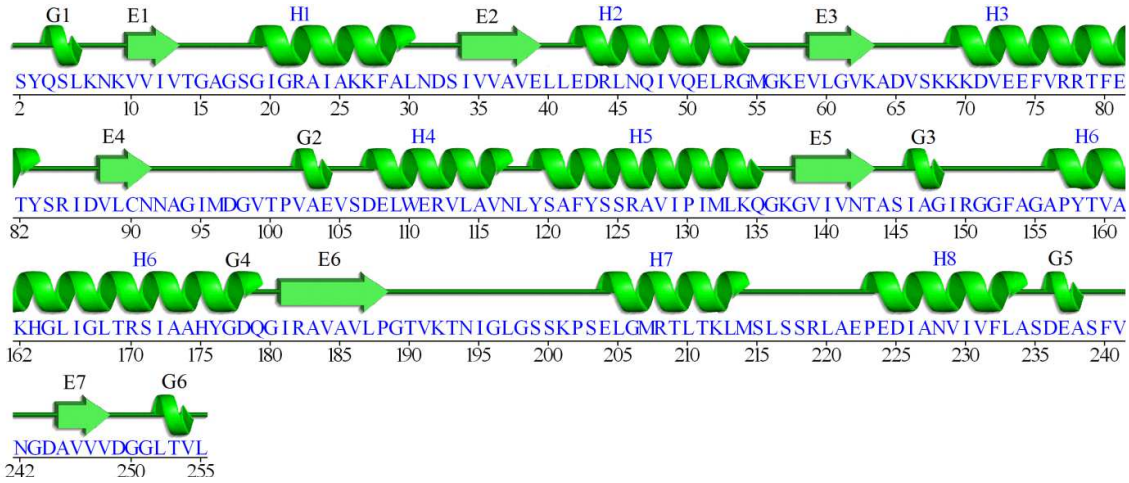

Figure 26. Sequence and secondary structure of SaADH2. The α-helices and β-strands are indicated with H and E, respectively, and numbered sequentially. Small 310 helical segments are indicated with G.

The second large interface involving AC or BD assemblies (~1,250 $Å^2$) mainly comprises the Cterminal regions (residues 216–255) of the two subunits. The very terminal segment (residue 253–255) also contributes to the smallest interface involving AD or BC assemblies (~445 $Å^2$); indeed, this segment forms inter-subunit interactions with residues belonging to 150–153 segment. It is worth noting that residues from the 209–218 region of the structure also mediate intersubunit interactions in this interface.

Cofactor-binding site

The reductase activity measurements showed that the protein is not active with NADP(H), having a definite preference for NAD(H) cofactor. This cofactor specificity is consistent with structural results.

A highly defined electron density was observed for the whole NAD(H) molecule thus allowing unambiguous identification of the positions of the cofactor in all the four molecules of the asymmetric unit (Fig. 27).

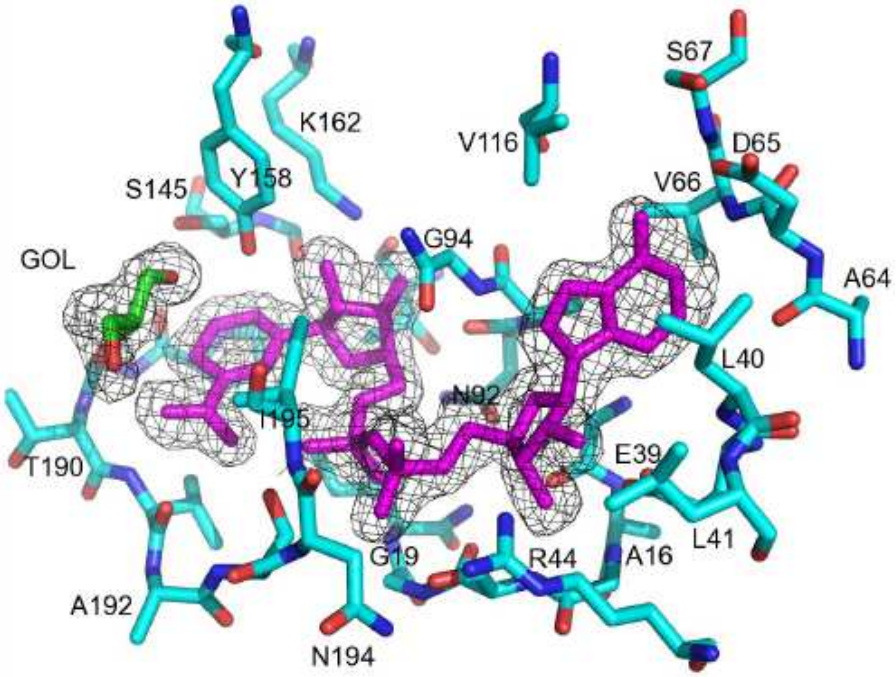

Figure 27. Electron density for NAD(H) (magenta) and glycerol molecules (GOL, green) of chain C. The Fo-Fc omit map is contoured at 2.5σ. All the residues having at least one atom within 5.0 Å from NADH molecule are represented in stick. Some residue labels are omitted for clarity.

The cofactor binding site is located at the C-terminal end of the central parallel β-sheet. The NAD(H) cofactor specificity is explained by the presence of Glu39 whose side chain oxygen atoms form hydrogen bonds with two oxygen atoms of the adenosine ribose of NAD(H) hampering the binding of NADP(H). The adenine ring of NAD binds in a hydrophobic pocket on the enzyme surface formed by the side chains of Val116, Leu40,

Val66, Ala93 and Gly15. Hydrogen bonds are formed by N6 of adenine and the Asp65 side chain and by N1 and the peptide nitrogen of Val66.

The segment 14-TGAGSGIG-21 corresponds to the glycine-rich sequence (TGxxx[AG]xG) present in NAD-binding site of "classical" SDR (Kavanagh et al 2008). This region interacts with the adenine ribose and the diphosphate moiety of NAD(H).

The phosphate groups also interact with Thr193-Ala194. The 2′- and 3′-hydroxyls of the second ribose, attached to the nicotinamide ring, form a bifurcated hydrogen bond with Lys162. The 3′-hydroxyl is also hydrogen bonded to the active site Tyr158. The syn face of the nicotinamide ring displays vdW contacts with the hydrophobic side-chains of Ile20, Pro188 and Val191. The amide part of the nicotinamide portion is anchored to the protein by hydrogen bonds to Thr193 and Val19.

Substrate-binding site

The SaADH2 contains the conserved catalytic residues, Ser145, Tyr158 and Lys162, located in the active-site cleft with position and orientation similar to those found in other SDRs (Schlieben et al. 2005). Besides the catalytic triad, also Asn117 is structurally conserved; this residue has been suggested as a key residue in a catalytic mechanism based on a tetrad instead of a triad (Filling et al. 2002) and it plays a role in maintaining the

active-site architecture and the building up of a proton-relay system in SDR structures (Filling et al. 2002; Schlieben et al. 2005). Moreover, its side chain atoms form hydrogen bonds with main chain atoms of Ile95. In many SDRs the substrate-binding site is a deep cleft with a floor created by the NADH molecule and the rightside and left-side walls formed by the substrate-binding region (residues 193-221 in SaADH2 numbering) and the loop between β5 and β6 strands (Fig. 28).

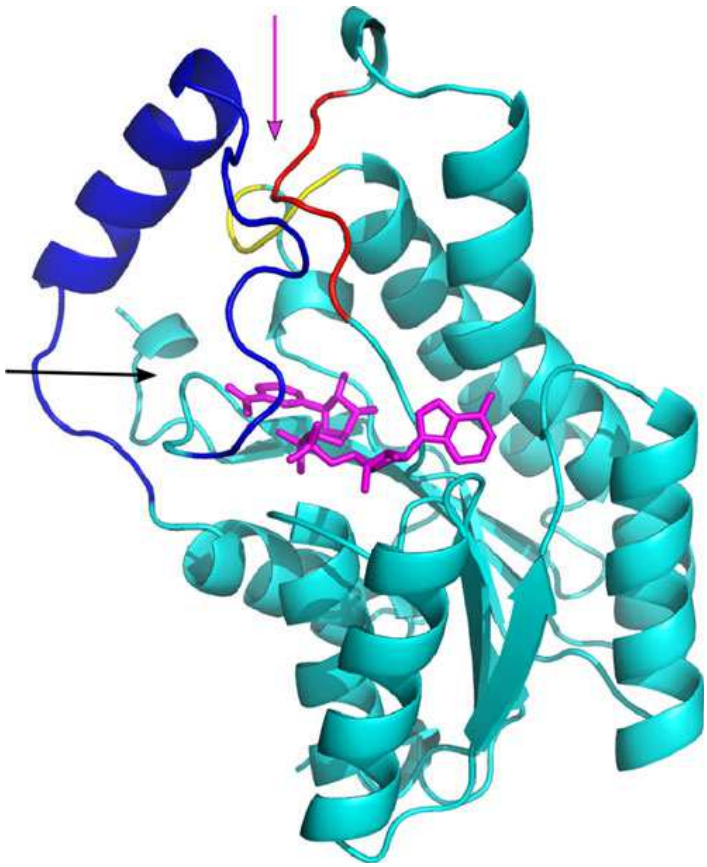

Figure 28. Overall tertiary structure of one of the subunits of SaADH2. Bound NADH is shown in stick representation (magenta). The substrate-binding loop, the stretches 152–155 and 96–101 are highlighted in blue, yellow and red, respectively. The arrows point toward the substrate-binding cleft; the directions of approach are shown in magenta and black (see the text for details).

In three out of four subunits of the asymmetric unit there is a glycerol molecule occupying the position that is approximately suited for the binding of substrate. Indeed, the glycerol O2 and O3 oxygen atoms are hydrogen bonded to the oxygen of the NAD carboxamide and to the oxygen of Tyr158 side chain, respectively. Glycerol was used as cryoprotectant agent and therefore diffused through the water channels of the crystals up to the binding site. The lacking of glycerol binding in one of the subunits (chain B) of the tetramer is due to crystal packing which restricts the access to NADH in subunit B. Indeed, a nearby symmetric molecule (#B) inserts its 50–57 region into the substrate-binding region (residues 193–221) that covers the access to the NADH site. On the other hand, the other subunits of the tetramer do not show direct interactions with adjacent symmetric molecules through the substrate-binding loop. It is worth noting that, despite the different crystal environments experienced by the four molecules of the asymmetric unit, the substrate-binding loops adopt similar conformations in the four subunits of the tetramer with 0.36–0.68 Å. Furthermore, the structure of the loop (residues 193–221, in blue in Fig. 24) represents the most significant difference between SaADH2 and the other SDR structures aligned with it. Indeed, as can be seen in Fig. 24, this loop (in cyan) is remarkably different from the other structures. This is not unexpected since the conformation, the length and the composition of

the substrate-binding loop are rather variable in SDR proteins thus conferring different substrate specificity. In most of SDR structures the substrate binding loop contains two segments of α-helix on opposite sides of the loop. In addition, part of the loop is often disordered thus revealing a considerable mobility. In SaADH2 the loop shows the following features: (1) it is well defined in the electron density; (2) it contains only one stretch of α-helix lacking the one usually present at the Cterminal end and (3) it partially obstructs the access to the substrate-binding cleft indicated with a magenta arrow in Fig. 24. Indeed, a detailed comparison with other SDR aligned structures reveals that three stretches (193–221, 96–101 and 152–155) of SaADH2 structure adopt a different conformation by getting closer to the NADH nicotinamide ring which becomes inaccessible to solvent/substrate from the top of the molecule (magenta arrow in Fig. 24). Interestingly, the segment 152.155 contains a Phe residue (Phe153) which points deep into the active site and can play a relevant role for substrate specificity (Fig. 28). The region 96–101 is also closer to the nicotinamide ring thus contributing to the reduced accessibility of the site where hydride transfer has to occur (Fig. 28). The cofactor ring is, however, still accessible to ligands through a side cavity (black arrow in Fig. 24) lined by residues Met96, Ser145, Ile146, Ala147, Phe153, Ala154, Tyr158, Gly189, Thr190, Ile195, Gly196, Leu197, Leu210 and Met214 (Fig. 29). As a

consequence, the manual modelling of the bulky benzyl molecule in the active site, guided by the position of glycerol molecule bound and by preliminary results of rigid docking, cannot avoid the presence of unfavourable contacts. However, it can be suggested that minor changes in the three segments of the protein structure discussed above as well as in the conformation of the benzil α-diketone may well accommodate this substrate in the site (Fig. 30).

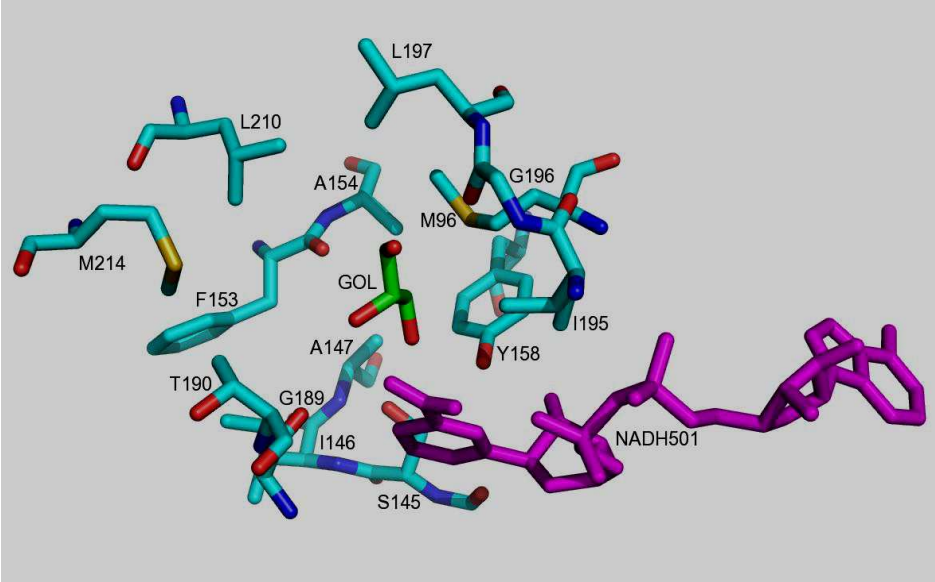

Figure 29. Stick representation of residues from the substrate binding pocket (the subunit C of the tetramer is considered). The NAD(H) molecule is depicted in magenta, whereas the glycerol molecule is in green.

The mouth of the cavity is composed of atoms from residues 190, 195–197, 210 and 214, as confirmed by CastP server (http://sts.bioengr.uic.edu/castp/calculation.php). The benzil molecule is an

interesting substrate of the enzyme that reduces it to (*R*)-benzoin in the presence of NADH with excellent conversion (>99%).

The elucidation of the ternary complex structure will ultimately provide details of the conformational changes in both the enzyme and the substrate necessary to obtain a fully productive state which guarantees high enantioselectivity. Nonetheless, the modelling explains the enantioselectivity of the benzil reduction. Several attempts were performed to crystallize a ternary complex of the enzyme bound to a benzil molecule, but they were unsuccessful. To envision how the enzyme binds the substrate and to probe the stereoselectivity of the hydride transfer we have manually modelled the benzil molecule in the active site. The starting structure for the alpha-diketone modeling was the crystal structure present in the small molecule structure database (Allen 2002). This structure shows a conformation of the molecule with the two aromatic rings forming a dihedral angle of 114° around the diketo bond. A single benzil carbonyl group is bonded to two substituents: a smaller phenyl group and a larger carbophenyl group. In order to obtain a (*R*)-alcohol, the hydride has to be added to the *Si*-face of the carbonyl ketone and this means that the smaller group is located in deep pocket in the active site opposite to the bulky carboxamide group of NADH (Fig. 30).

A rigid docking of the benzil compound performed by the patchdock server identifies an orientation in the substrate site which is consistent with the stereoselectivity of the reduction reaction leading to (*R*)-benzoin. However, it has to be noted that in the best docked conformational ensemble of benzil, the carbonyl C atom, to be attacked by hydride, is still rather far from the hydrogen at the NADH C4 position (>5.5 Å). In addition, the oxygen atom of the carbonyl is not hydrogen bonded to the catalytic Tyr158 side chain (4.7 Å apart) as expected in case of a fully productive state of the enzyme–substrate complex. Due to the steric hindrance of the benzil molecule an efficient accommodation in the substrate site would require a structural rearrangement of residues from the three segments (193–221, 96–101, and 152–155) which line the site and/or a change in the conformation of the diketone. A better packing of benzil in the site can be indeed obtained when the torsional angle around the carbon–carbon bond linking the two carbonyl moieties is reduced to values around 80–90°. Although approximate, this manually docked substrate position identifies a small pocket deep into the active site (Fig. 30) which is lined by Ser145, Leu146, Ala147, Tyr158, Phe153, Ala154 and Gly189.

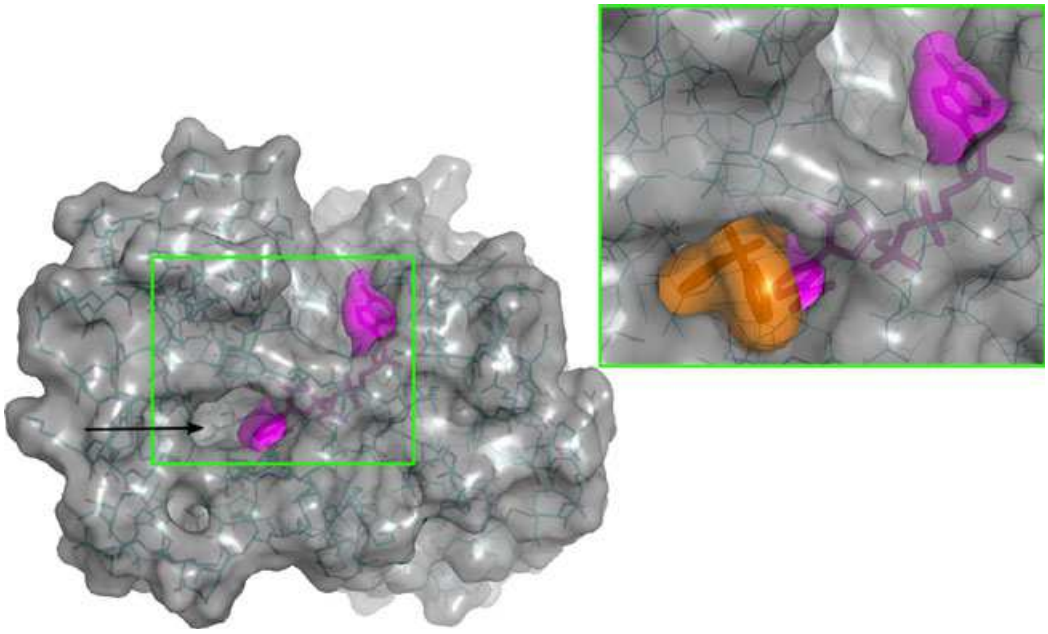

Figure 30. Surface representation of a single chain of SaADH2. The NADH molecule is highlighted in magenta, as both stick and surface representations. The black arrow indicates the channel by which the nicotinamide ring is accessible. The green box is a close-up view of the binding site with the benzil molecule (in orange) manually docked into it. The figure was prepared using the PyMOL software (www.pymol.org).

This pocket can accommodate the small phenyl group of benzil. Indeed, this phenyl ring would display mostly favourable contacts with Phe153, Ile146 and Ala147; the phenyl ring lies with its ring between two main-chain oxygen atoms from residues Phe153 and Glu189. On the other hand, the large carbophenyl group of benzil would point toward the channel opened to the solvent (Fig. 30) and lined by Met96, Thr190, Ile195, Gly196, Leu197, Leu210 and Met214 (Fig. 29). However, this bulky carbophenyl group would display steric clashes with the NADH and Thr190 when the intercarbonyl dihedral angle is about 80°. Some bad contacts can be relieved by a deviation of the phenyl group from the plane

defined by the carbonyl moiety as well as by small rearrangements of the carboxyamide group of the nicotinamide ring (Fig. 30). Conformational rearrangements with respect to the crystal structure of benzil can be accessible at a reasonable energetic cost since both experimental and theoretical studies have indicated a significant flexibility of the molecular structure even depending on the environmental conditions (Pawelka et al. 2001; Lopes et al. 2004). The presence of the deep pocket in the active site, well suited for an aromatic ring, also explains why, in the case of acetophenone and its derivatives, the alcohol obtained by the reduction reaction is the (*S*)-enantiomer. Indeed, the deep pocket in the active site, well suited for an aromatic ring, can efficiently accommodate the phenyl group of the acetophenone whereas the methyl group can point toward the channel; this orientation of the substrate in the site leads to the (*S*)-1-phenylethanol product (Table 14).

Conclusion

A new short-chain dehydrogenase from *S. acidocaldarius* was identified and overexpressed. The purified enzyme was shown to possess remarkable thermal resistance as well as high enantioselectivity on the aryl diketone benzil molecule. It shows many advantages with regard to its preparative application: ease of purification, preservability of the biocatalyst and absolute preference for NAD(H). It is also amenable for coupling with a thermophilic bacillar ADH (BsADH) in an efficient and sustainable bioconversion process based on coenzyme recycling, where both enzymes have only the coenzyme as cosubstrate.

The remarkable resistance of SaADH2 to organic solvents proves the sturdiness of this biocatalyst and suggests exploratory investigations on conversions of poorly water-soluble prochiral substrates. In addition, the availability of the crystal structure of the enzyme provides the opportunity to rationalize the stereospecificity and stereoselectivity of the enzyme and to design proper mutations to broaden the scope of possible substrates.

Synthesis of cinnamyl alcohol from cinnamaldehyde with *Bacillus stearothermophilus* alcohol dehydrogenase as the isolated enzyme and in recombinant *E. coli* cells

Cinnamyl alcohol

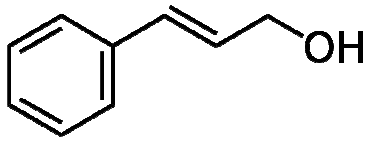

Cinnamyl alcohol (CMO) is a versatile chemical due to its aroma and its fixative properties; it is used in the fragrance and flavouring industries for cinnamon notes and the rounding off of fruit aromas. It may be found in fragrances used in decorative cosmetics, fine fragrances, shampoos, toilet soaps and other toiletries as well as in non-cosmetic products such as household cleaners and detergents.

It is also a valuable intermediate for the production of aroma-relevant esters (Fahlbusch et al. 2008) the syntheses of the Taxol's C13 side chain (Bonini and Righi 1994), the antibiotic Chloromycetin (Eilerman 1992) and the antidepressant reboxetine mesylate (Henegar et al. 2007).

Production of cinnamyl alcohol

CMO can be prepared by chemical reduction of cynnamaldehyde (CMA) under different heterogeneous catalysis conditions (Gallezot and Richard 1998; Machado 2008) (Fig. 31).

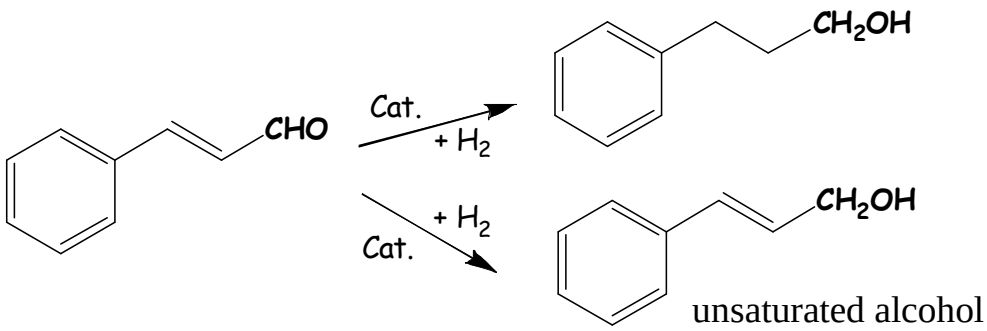

Figure 31. Chemical reduction of cynnamaldehyde.

However, selective hydrogenation of C=O over C=C is still an important issue since, besides the desired unsaturated alcohol, the process can lead to non-desirable saturated aldehyde and alcohol as side-products that may result in odour performance issues. Moreover, the use of extreme operational conditions and hazardous chemicals lead to serious operational and economic concerns. Noteworthy, the perception of smell is an enantioselective process; so, it frequently occurs that the different stereoisomers of an odorant induce quite different sensorial reactions, i.e., they have a different scent. In fact, the opposite enantiomers of an odorant

may show odor profiles that are different in both quality and intensity (Ciappa et al. 2008).

Biocatalysis provides a valuable alternative to achieve improvements addressing the above mentioned issues.

Biocatalytic production of cinnamyl alcohol

During the third year of my PhD project, the main focus was to study a suitable synthesis of CMO by means of enzymatic reduction of CMA under smooth and environmentally friendly conditions using the alcohol dehydrogenase from *Bacillus stearothermophilus* both as an isolated enzyme, and in recombinant *E. coli* whole cells.

Alcohol dehydrogenases from *Bacillus stearothermophilus* (BsADH)

BsADH is a Zn-containing, homotetrameric, NAD(H)-dependent, and medium chain ADH identified in the moderate thermophilic bacterium *Bacillus stearothermophilus LLD-R strain* (BsADH, Fig. 32), cloned and expressed in *E. coli* (Cannio et al. 1994; Guagliardi et al. 1996).

This ADH has been successfully applied to hydrogen tunnelling effect studies across a broad temperature range (Kohen et al. 1999), as well as in structural and molecular dynamic studies (Ceccarelli et al. 2004; Zhang and Bruice 2007). BsADH is NAD(H)-dependent and is mainly active on

aliphatic and aromatic primary and secondary alcohols and aldehydes, but not on aliphatic and aromatic ketones (Guagliardi et al 1996). These requisites make BsADH a versatile auxiliary enzyme suitable for NADH regeneration in the well-established enzyme-coupled approach for redox bioconversion processes, which utilize isolated enzymes or whole cells (De Wildeman et al. 2006; Berenguer-Murcia and Fernandez-Lafuente 2007; Hall and Bommarius 2011). In fact, BsADH was recently proved to efficiently regenerate NADH *in situ* for the enantioselective reduction catalysed by *Thermus thermophilus* ADH of different aromatic ketones in the presence of 2-propanol, methyl benzoylformate and *o*-chlorobenzoyl formate in the presence of ethanol, and for the benzil to (*R*)-benzoin reduction catalysed by *Sulfolobus acidocaldarius* ADH (see previous Sections). A feasible protocol for the synthesis of [4*R*-^{2}H]NADH with high yield was also set up by enzymatic oxidation of 2-propanol-d_8 catalyzed by BsADH (Pennacchio et al. 2010b).

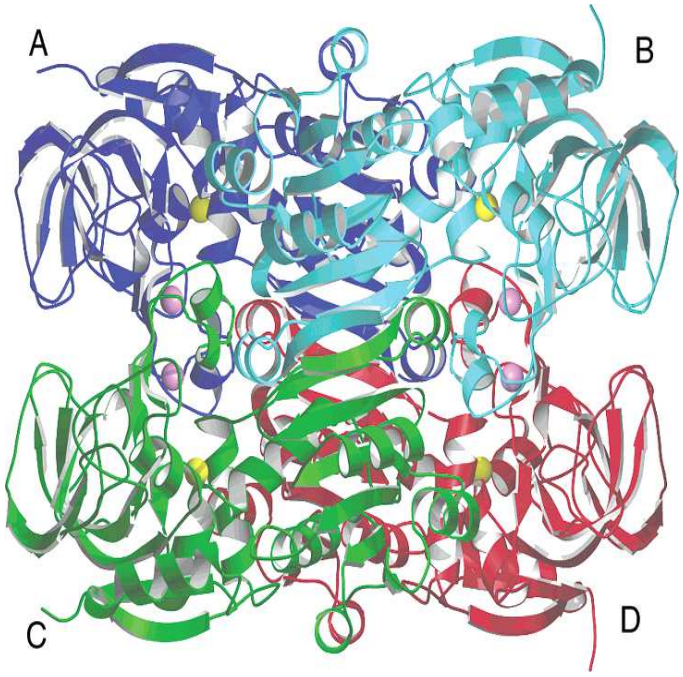

Ceccarelli et al. (2004)
Biochemistry 43:5266–5277

Figure 32. Overall structure of tetrameric BsADH**.**

Biocatalytic synthesis of cinnamyl alcohol employing recombinant BsADH

The *E. coli* expression system developed for BsADH in our laboratory is quite efficient, producing ~30 mg homogeneous enzyme per litre of culture with a specific activity of 250 U/mg. This easy availability and very high efficiency has allowed to exploit the high potential of the enzyme for application in bioconversion as auxiliary ADH for NADH regeneration as mentioned above. In the present work, BsADH plays the dual role as the production enzyme and as the NADH regeneration enzyme as shown in Scheme 3.

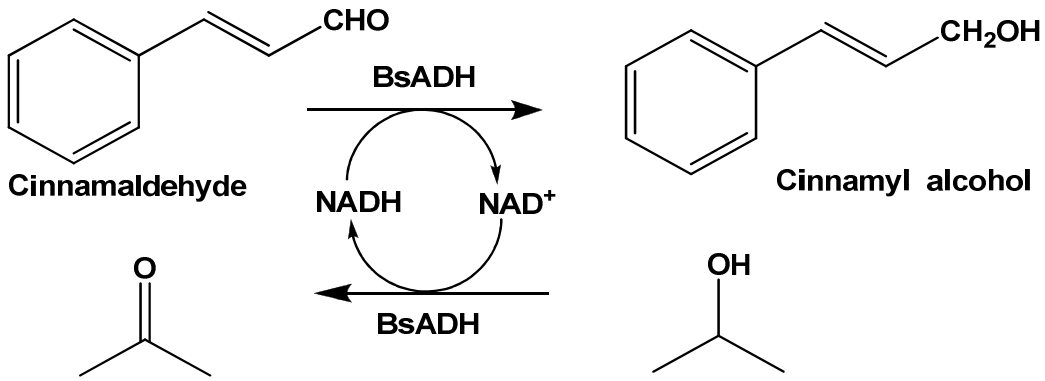

Scheme 3. Enzymatic reduction of CMA and recycling of cofactor utilizing BsADH and 2-propanol.

The kinetic parameters for each substrate and product involved in the scheme reactions were determined in order to analyse the cofactor regeneration system as a whole (Table 15).

Table 15. Steady-state kinetic constants of BsADH

Substrate	k_{cat} (s^{-1})	K_m (mM)	k_{cat}/K_m (s^{-1} mM^{-1})
CMA	55	0.03	1,835
CMO	43	0.11	391
2-Propanol	287	57.8	5
Acetone	NA [a]		
NADH	43	0.016	2,687
NAD^+	33	0.45	73

[a] NA, no measurable activity.

BsADH displays higher catalytic efficiency with CMA and NADH than with CMO and NAD^+ and a relatively very low catalytic efficiency in 2-propanol oxidation, but shows no activity on the corresponding co-product

acetone. This suggests that the preferred reaction catalyzed by BsADH is the CMA reduction compared to the reverse reaction, and that the reduction of NAD^+ could be favourably driven to NADH formation in the presence of a relatively high excess of the co-substrate 2-propanol. Thus the regeneration reaction is practically irreversible and relatively straight forward. The experimental conditions, including buffer, pH, and temperature were chosen to optimize the productivity of the bioconversion process. Previous studies indicated that the optimal pH for the reduction reaction is 6.0, and 8.0–8.5 for the oxidation reaction, and that the optimal temperature is around 63°C (Guagliardi et al. 1996). Due to instability of the reduced cofactor under acidic conditions, neutral pH was chosen as a compromise between cofactor stability and BsADH activity at suboptimal pH. Moreover a reaction temperature of 50°C was chosen, since BsADH is highly active and retains full activity over 24 h at this temperature. Table 16 summarizes the results of a study carried out to optimize the production of CMO in analytical scale by changing several parameters, time and enzyme, 2-propanol and cofactor concentrations. The results of entries 1–3 suggest that the 2-propanol concentration plays a critical role in the enzyme efficiency in the CMA bioconversion.

Table 16. Analytical-scale bioreduction of CMA by isolated BsADH

Entry	2-Propanol (%)	CMA (mg mL^{-1})	BsADH (mg mL^{-1})	NAD^+ (mM)	Time [a] (h)	Conversion [a] (%)
1	5	0.125	0.12	1	3 (6)	95 (97)
2	10	0.125	0.12	1	3 (6)	99 (99)
3	15	0.125	0.12	1	3 (6)	83 (85)
4	10	0.125	0.12	2	3 (6)	96 (99)
5	10	1.0	0.12	1	3 (6)	98 (98)
6	10	1.0	0.05	1	3 (6)	98 (98)
7	10	1.0	0.005	1	3 (24) [b]	54 (60) [b]

[a] Values in parentheses refer to reactions carried out for 6 h.
[b] Reaction time, 24 h

The reduction of 0.125 mg of CMA in the presence of 5% 2-propanol was 95 and 97% after 3 and 6 h, respectively, and 99% in the presence of 10% 2-propanol after both 3 and 6 h. However, the reaction performed in the presence of 15% 2-propanol yielded CMO with a conversion of 83 and 85% after 3 and 6 h, respectively, presumably due to excess-substrate inhibition or low stability of NAD^+ in the presence of relatively elevated concentrations of 2-propanol (Schroer et al. 2009), or both. By doubling the cofactor concentration, the conversion decreased slightly in 3 h (96%), but reached 99% in 6 h reaction (entry 4). Bioconversions were then carried out in the presence of 1 mM NAD^+ at 8-fold higher substrate concentration (entry 5). The level of conversion was 98% following 3 and 6 h of reaction and remained the same using lower amounts of enzyme (entry 6). However, a further 10-fold decrease in enzyme concentration resulted in nearly 50%

conversion in 3 h and only slightly higher at reaction times as long as 24 h (entry 7). Therefore, based on data of entry 6, 0.05 mg mL^{-1} enzyme and 1 mg mL^{-1} substrate were chosen as tentative concentration values to scale the bioreduction process up to one hundred fold the amount of CMA.

Table 17 (entry 1) shows that the bioreduction of 100 mg CMA occurred with 94% conversion in 3 h, at a temperature of 50°C, using 10% 2-propanol and 1 mM NAD^+ in aqueous buffer, pH 7.0.

Table 17. Lab-scale bioreduction of CMA by isolated BsADH

Entry	Volume (mL)	CMA (gL^{-1})	CMA (mg)	BsADH (mg mL^{-1})	Time (h)	Conversion (%)	Yield (%)
1	100	1	100	0.05	3	94	ND [a]
2	200	0.5	100	0.05	3	99	75
3	200	0.5	100	0.01	3	99	77
4	400	0.5	200	0.01	3	97	88

[a] ND, not determined

However, when the same reaction was carried out in double the reaction volume, a conversion nearing 100% was achieved (entry 2). Diluting the substrate by half was successfully applied to the reduction of 100 mg substrate performed in the presence of five-fold lower enzyme concentration (entry 3). A 99% conversion and 77% yield was obtained. Analogously, 97% conversion was achieved from reduction of twice the amount of substrate (entry 4); in this case, extractive downstream-processing yielded the desired product CMO to high purity (≥98% by NMR

spectral data) with a yield of 88%, which corresponds to the productivity of 0.44 g L^{-1} (weight of isolated product per liter of initial reaction volume) and 50 g/g_{enzyme}.

Since scaling up the bioconversion of over 200 mg of CMA (4 mM) would have required a work up of very significant volumes and large amounts of homogeneous enzyme, we further explored the applicative potential of BsADH by incorporating it directly into recombinant *E. coli* cells.

Biocatalytic synthesis of cinnamyl alcohol employing recombinant *E. coli*/BsADH

E. coli RB791 cells harboring BsADH showed an activity of 43 U/mg, which was about 6-fold less than that of homogeneous enzyme. Control experiments using non-transformed cells and non-induced transformed cells were carried out to ascertain whether any dehydrogenases/reductase was present in the *E. coli* strain which was active on CMA and CMO. No conversion was observed suggesting that no NAD(H) dependent ADH, if any, was active on CMA and CMO under the experimental conditions used (data not shown).

Table 18 summarizes the results of a study on CMA microbial reduction with recombinant *E. coli*/BsADH cells by keeping constant the substrate concentration and increasing the reaction volumes.

Table 18. Lab-scale bioreduction of CMA by recombinant *E. coli*/BsADH cells

Entry	Volume (mL)	CMA ($g\ L^{-1}$)	CMA (mg)	Cells ($mg\ mL^{-1}$)	Time (h)	Conversion (%)	Yield (%)
1	10	12.5	125	200	3	97	79
2	20	12.5	250	200	3	98	78
3	40	12.5	500	200	3	69	ND [a]
4	40	12.5	500	200	6	95	81
5	40	12.5	500	300	3	95	73
6	80	12.5	1000	300	6	97	82

[a] ND, not determined

The bioreduction of 125 mg of CMA at 37°C for 3 h resulted in 97% conversion, as determined by HPLC analysis. The subsequent work-up gave 98.7 mg of highly pure product (≥98% by NMR, data not shown). A similar result was obtained with twice the amount of substrate (entry 2). However, by further doubling of the CMA amount, the conversion decreased from 98% to 69% (entry 3), most likely due to catalyst deficiency or short reaction time; the same reaction carried out doubling the reaction time (entry 4) or increasing by 1.5-fold the cell concentration (entry 5) significantly improved the system efficiency, resulting in 95% conversion in both cases. This combination of reaction time and cell concentration turned out to be suitable for converting 1 g (94 mM) of substrate. An excellent conversion and a more than satisfactory yield of 82% was obtained (entry 6), which corresponds to the productivity of 34

$g/g_{wet\ cell\ weight}$ and 10.25 g L^{-1}, i.e. 23-fold higher with respect to that obtained by the isolated enzyme (Table 17).

Due to the high conversion levels, additional amounts of cofactor were not necessary. Presumably, the levels of oxidized and reduced cofactor in the recombinant *E. coli* are high enough to saturate the substrate-coupled system (Scheme 3). This may be explained by the fact that the total intracellular cofactor concentration in *E. coli*, which is around 2.6 mM NAD^+ and 0.083 mM NADH (Bennett et al. 2009) and the K_m values of BsADH for NAD^+ and NADH, which are 0.45 mM and 0.016 mM respectively (Table 15).

Permeabilization of *E. coli cell* was not pursued due to the high yield of the microbial reductions described above. Presumably, the exposure to a large amount of aromatic substrate and 2-propanol at relatively long reaction times and high temperatures partially permeabilizes the cell wall (as reported for example in (Cánovas et al. 2005)), to a sufficient degree to facilitate mass transfer. Furthermore, it is worthy of note the remarkable stability of the microbial catalyst under the experimental conditions used in the presence of relatively high substrate/product concentrations. A widely held notion is that the synthetic reductase is oftentimes more stable within the cellular environment as compared to the isolated enzyme (Goldberg et al. 2007; Kratzer et al. 2008).

Conclusion

In this study, the enzymatic synthesis of cinnamyl alcohol, a versatile fine chemical, has been developed in a one phase-system, using a whole-cell biocatalyst that is based on an *E. coli* strain expressing a thermophilic NAD(H)-dependent ADH from *Bacillus stearothermophilus* to a high level of activity. The enzyme regenerates by itself the endogenous reductase cofactor NADH without requiring expensive additional cofactor, in the presence of cheap sacrificial substrate 2-propanol as hydrogen donor. The method is characterized by favourable thermodynamics since alcohol/ketone does not interfere with the synthesis reaction, and gives CMO with high yield and purity. Taken together, our study points out the advantage of whole cell biocatalyst in comparison to isolated enzyme thanks to its ease of preparation, cofactor cost, simplified work-up, and good productivity; it also demonstrates that the optimized microbial process can be implemented on a larger preparative scale using suitable reaction times and cell concentrations. These features, in addition to effective *in-vivo* cofactor regeneration system, are valuable prerequisites for the commercial viability of a biotechnological process.

MATERIALS and METHODS

Chemicals

$NAD(P)^+$ and NAD(P)H were obtained from AppliChem. (Darmstadt, Germany). Alcohols, aldehydes, ketones and keto esters were obtained from Sigma-Aldrich. MES {2-(N-morpholino) ethanesulfonic acid} was obtained from Sigma Chemical Co. (St. Louis, MO). Aldolase was obtained from Amersham Biosciences. Dimethylsuberimidate (DMS) and dimethyladipimate (DMA) chemical cross-linkers were from Pierce. Methyl *o*-chlorobenzoylformate and 1-Phenylethanol-d_9 [$C_6D_5CD(OH)CD_3$] were obtained from Ricci Chimica (Perugia, Italy). 1-Butyl-3-methylimidazolium tetrafluoroborate (BMIMBF4) was a kind gift from Professor S. Cacchi. Other chemicals were A grade substances from Applichem. Solutions of NAD(P)H and $NAD(P)^+$ were prepared as previously reported (Pennacchio et al. 2008). All solutions were made up with MilliQ water.

TtADH Material and Methods

Enzymes and kinetic assays

Recombinant *Thermus thermophilus* ADH (TtADH) and recombinant *Bacillus stearothermophilus LLD-R strain* (BsADH) were prepared as described previously (Pennacchio et al. 2008). Glucose dehydrogenase from *Thermoplasma acidophilum* (TaGDH) was from Sigma, St. Luis, MO. TtADH activity was assayed spectrophotometrically at 65°C by measuring the change in absorbance of NADH at 340 nm using a Cary 1E spectrophotometer equipped with a Peltier effect-controlled temperature cuvette holder. The kinetic parameters of TtADH for α-keto esters were determined as described previously (Pennacchio et al. 2008). TaGDH was assayed at 50°C by measuring the change in absorbance of NADPH at 340 nm. The standard assay was performed by adding 0.25 μg of enzyme to 1 mL of preheated assay mixture containing 50 mM glucose and 0.4 mM $NADP^+$ in 50 mM sodium phosphate, pH 7.0.

The effect of organic solvents on TaGDH was investigated by incubating 0.025 mg mL^{-1} protein in 50 mM sodium phosphate, pH 7.0, at 50°C, in the absence and presence of organic solvents. At specific time intervals, the samples were centrifuged and small aliquots were withdrawn and assayed.

The volume of solution in the tight capped test tube did not change during incubation.

Procedure for bioreduction

Bioreduction of α-keto esters was performed at 50°C using two NADH regeneration systems. The first consisted of TaGDH and glucose. For analytical biotransformation the reaction mixture contained 6.2 mM carbonyl compound, 1 mM NAD^+, 50 mM glucose, 25 μg TtADH, and 5.5 μg TaGDH in 0.2 mL of 100 mM sodium phosphate, pH 7.0. Semi-preparative reactions were performed on a 0.1 g scale in a reaction volume up to 10 mL, using 0.05 mg mL^{-1} TtADH, and 0.01 mg mL^{-1} TaGDH. During the reaction the pH was maintained at pH 6.5–7.0 with the addition of a 2 M NaOH solution.

The second NADH regeneration system consisted of BsADH and 2-propanol or different linear alcohols as described previously (Pennacchio et al. 2008) with some modifications. The reaction mixture contained 6.2 mM carbonyl compound, 1 mM NAD^+, 15 μg of BsADH, 0.6 to 4% v/v alcohol substrate, and 125 μg TtADH in 1 mL of 100 mM sodium phosphate, pH 7.0, 0,5 mM 2-mercaptoethanol and 100 mM KCl. Semi-preparative reactions were performed on a 0.1 g scale in a reaction volume up to 10 mL, using 0.05 mg mL^{-1} TtADH, and 0.01 mg mL^{-1} BsADH. In both

systems the mixtures were shaken at 160 rpm for different reaction times in a temperature-controlled water bath. Upon termination of the reaction, the mixtures were extracted twice with ethyl acetate, dried with anhydrous Na_2SO_4 and concentrated under reduced pressure. The samples were prepared in hexane/2-propanol (9:1) for HPLC analysis.

To determine the isolated yield of the semi-preparative reactions carried out using the two NADH regeneration systems, the ethyl acetate extracts were dried with anhydrous Na_2SO_4, filtered, and concentrated under reduced pressure. Purification by silica gel column chromatography (hexane/ethyl acetate, 9:1) gave methyl (*R*)-mandelate or methyl (*R*)-*o*-chloromandelate as colourless oils; yield: 77 mg (77% isolated yield; conversion: 78%) and 81 mg (81%; 99%) of methyl (*R*)-mandelate produced by the TtADH/TaGDH and TtADH/BsADH system, respectively; 86 mg (86% isolated yield; conversion: 96%) and 78 mg (78%; 98%) of (*R*)-*o*-chloromandelate produced by TtADH/TaGDH and TtADH/BsADH system, respectively.

The degree of conversion and enantiomeric purity of the products were determined on the basis of the peak areas of ketone substrates and alcohol products separated and visualized by HPLC, on a Chiralcel OD-H column (Daicel Chemical Industries, Ltd., Osaka, Japan). The absolute configuration of product alcohols was determined by comparing the HPLC

data with standard samples. Products were analyzed with isocratic elution under the following conditions: hexane/2-propanol (9:1) (mobile phase), flow rate of 1 mL min^{-1}, detection for bioconversions of MBF and ClMBF at 210 nm. At this wavelength, both MBF and methyl (*R*)-mandelato as well as ClMBF and methyl (*R*)-*o*-chloromandelate have the same molar extinction coefficient values, so that areas of substrates and products are equally proportional to concentrations. Retention times were as follows: 6.14, 8.82 and 14.15 min for MBF, methyl (*S*)-mandelate and methyl (*R*)-mandelate, respectively; 6.92, 10.12 and 17.16 min for ClMBF, methyl (*S*)-*o*-chloromandelate and methyl (*R*)-*o*-chloromandelate, respectively. The absolute stereochemistry of the two halogenated alcohol enantiomers were assigned by comparison to the values described in the literature for methyl *o*-chloromandelates (Ema et al. 2008). The log *P* values were obtained from Laane and coworkers (1987).

Optimal reaction time and concentration determination

The reactions were carried out at 50°C in 50 mM sodium phosphate, pH 7.0, 100 mM KCl and NADH regeneration system of TaGDH and glucose. Reaction volume, 0.2 mL; TtADH and TaGDH 25 and 5.5 µg, respectively; NAD^+, 1.0 mM; MBF, 1.0 g L^{-1}; glucose, 50 mM. The reactions were stopped by addition of ethyl acetate at the times indicated. The dried

extracts were analysed by chiral HPLC and the relative conversion calculated as the area of alcohol products divided by the total area.

The reactions were carried out for 24 h under same conditions as above at increasing substrate concentrations in the absence and presence of 5% v/v acetonitrile and 20% v/v hexane.

Effect of the BsADH alcohol substrates on the enantioselectivity and efficiency of the reduction catalysed by TtADH.

The reactions were carried out for 24 h at 50°C in presence of 4% v/v alcohol, in buffer, 100 mM sodium phosphate, pH 7.0, 100 mM KCl, 5 mM 2-mercaptoethanol. Reaction volume, 10 mL; TtADH and BsADH concentrations, 0.05 and 0.01 mg mL^{-1}, respectively; 1 mM NAD^{+}; MBF 10 g L^{-1}. The relative conversion was determined by HPLC {Chiralcel OD-H, hexane/*i*PrOH [(9:1)]}.

SaADH Material and Methods

Amplification and cloning of the *saadh* gene

Chromosomal DNA was extracted by caesium chloride purification as described by Sambrook et al. (1989). Ethidium bromide and caesium chloride were removed by repeated extraction with isoamyl alcohol and extensive dialysis against 10 mM Tris–HCl pH 8.0, 1 mM EDTA, respectively. DNA concentration was determined spectrophotometrically at 260 nm, and the molecular weight was checked by electrophoresis on 0.8% agarose gel in 90 mM Tris–borate pH 8.0, 20 mM EDTA, using DNA molecular size markers. The saadh gene was amplified by polymerase chain reaction (PCR) using oligonucleotide primers based on the saadh sequence of *Sulfolobus acidocaldarius* strain DSM 639 (GenBank accession no. YP_256716.1). The following oligonucleotides were used: 50-GGTTGGCATATGGACATTGATAGGCTCTTTTCAGTA-30 as the forward primer (the NdeI restriction site is underlined in the sequence) and the oligonucleotide 50-GGTTGGGAATTCCTACACCTTTGGGTCATA TCTACCATCTA-3 as the reverse primer. This latter oligonucleotide introduces a translational stop following the last codon of the ADH gene, followed by an EcoRI restriction site, which is underlined in the sequence shown. The PCR product was cloned into the expression vector pET29a (Novagen, Madison, WI, USA) and digested with the appropriate

restriction enzymes to create pET29a-saADH. The insert was sequenced in order to verify that mutations had not been introduced during PCR.

Expression and purification of recombinant SaADH

Recombinant protein was expressed in *E. coli* BL21(DE3) cells (Novagen) transformed with the corresponding expression vector. Cultures were grown at 37°C in 2 L of LB medium containing 30 µg mL^{-1} kanamycin. When the A_{600} of the culture reached 1.4, protein expression was induced by addition of isopropyl β-D-1-thiogalactopyranoside (IPTG) to a concentration of 1.0 mM. The bacterial culture was incubated at 37°C for a further 24 h. Cells were harvested by centrifugation, and the pellet was stored at −20°C until use. The cells obtained from 2 L of culture were suspended in 20 mM Tris–HCl buffer (pH 7.5) containing 0.1 mM phenylmethylsulfonyl fluoride (PMSF) and were lysed using a French pressure cell (Aminco Co., Silver Spring, MD) at 2,000 psi (1 psi = 6.9 kPa). The lysate was centrifuged, and the supernatant was incubated in the presence of DNase I (50 µg per mL of solution) and 5 mM $MgCl_2$ for 30 min at 37°C, followed by protamine sulphate (1 mg per mL of solution) at 4°C for 30 min. The nucleic acid fragments were removed by centrifugation, and the supernatant was incubated at 75°C for 15 min. The

host protein precipitate was removed by centrifugation. The supernatant was dialysed overnight at 4°C against 20 mMTris–HCl, pH 8.4 (buffer A) containing 1 mM PMSF. The dialysed solution was applied to a DEAE-Sepharose Fast Flow (1.6 x 12 cm) column equilibrated in buffer A. After washing with 1 bed volume of the same buffer, elution was performed with a linear gradient of 0–0.06 MNaCl (80 mL of each concentration) in buffer A, at a flow rate of 60 mL h^{-1}. The active pool was dialysed against buffer A, concentrated fivefold with a 30,000 MWCO centrifugal filter device (Millipore), and applied to a Sephadex G-75 (1.6 x 30 cm) column equilibrated in buffer A containing 0.15 MNaCl. The active pool was dialysed against buffer A and concentrated to obtain 2.5 mg protein mL^{-1} as described previously. SaADH was stored at -20°C, without loss of activity following several months of storage. SDS-PAGE and non-denaturing PAGE were carried out according to the Laemmli method (1970), with minor modifications (Raia et al. 2001). The subunit molecular mass value was determined by electrospray ionization mass spectrometry (ESI-MS) with a QSTAR Elite instrument (Applied Biosystems, USA). The protein concentration was determined with a Bio-Rad protein assay kit using BSA as a standard.

Size-exclusion chromatography

Molecular masses were determined by size-exclusion chromatography using a Superdex 200 10/300 GL column (Amersham Biosciences), equilibrated with 50 mM Tris–HCl, pH 9.0, containing 0.15 M NaCl, at a flow rate of 0.5 mL min^{-1}. The following molecular mass standards were used for calibration: vitamin B12 (1,350 Da), horse myoglobin (17.5 kDa), chicken ovalbumin (44 kDa), beef γ-globulin (158 kDa), and thyroglobulin (670 kDa) from Bio-Rad. In order to calculate the distribution coefficient, the void and total volumes of the column were determined with blue dextran and tryptophan, respectively.

Chemical cross-linking

Cross-linking reactions of SaADH with DMA and DMS were conducted for 1 h at 25°C in a 25-µ volume of 0.1 M triethanolamine–HCl, pH 8.5 at 0.20 mg mL^{-1} protein, and 0.1 mg mL^{-1} bifunctional reagent. The molecular mass of cross-linked SaADH species was estimated by SDS-PAGE according to the procedure described by Davies and Stark (1970).

Enzyme assay

SaADH activity was assayed spectrophotometrically at 65°C by measuring the change in absorbance of NADH at 340 nm using a Cary 1E

spectrophotometer equipped with a Peltier effect-controlled temperature cuvette holder. The standard assay for the reduction reaction was performed by adding 5–25 µg of the enzyme to 1 mL of preheated assay mixture containing 25 mM ethyl benzoylformate (EBF) and 0.3 mM NADH in 37.5 mM MES–NaOH, pH 5.5. The standard assay for the oxidation reaction was performed using a mixture containing 25 mM cycloheptanol and 5 mM NAD^+ in 25 mM sodium phosphate, pH 8.0. Screening of the substrates was performed using 1 mL of assay mixture containing either 10 mM alcohol and 5 mM NAD^+ in 25 mM sodium phosphate, pH 8.0, or 10 mM carbonyl compound and 0.1 mM NADH in 37.5 mM MES–NaOH, pH 5.5. One unit of SaADH represented 1 µmol of NADH produced or utilized per min at 65°C, on the basis of an absorption coefficient of 6.22 mM^{-1} cm^{-1} for NADH at 340 nm.

Effect of pH on activity

The optimum pH values for the reduction and oxidation reactions were determined at 65°C under the conditions used for EBF and cycloheptanol, respectively, except that different buffer systems were used. The pH was controlled in each assay mixture at 65°C.

Kinetics

The SaADH kinetic parameters were calculated from measurements determined in duplicate or triplicate and by analysing the kinetic results using the program GraFit (Leatherbarrow 2004). The turnover value (k_{cat}) for SaADH was calculated on the basis of a molecular mass of 29 kDa, assuming that the four subunits are catalytically active.

Thermophilicity and thermal stability

SaADH was assayed in a temperature range of 30–95°C using standard assay conditions and 22 µg of protein mL^{-1} of assay mixture. The stability at various temperatures was studied by incubating 0.2–mg mL^{-1} protein samples in 50 mM Tris–HCl, pH 9.0 at temperatures between 25 and 95°C for 30 min. Each sample was then centrifuged at 5°C, and the residual activity was assayed as described above. Long-term stability was studied by incubating protein samples (0.2 mg mL^{-1}) in 50 mM Tris–HCl, pH 9.0, at 50 and 70°C, or in 50 mM Tris–H_3PO_4, pH 7.0 at 50 and 60°C and the residual activity was assayed after 6 and 24 h as described above. The effect of chelating agents on enzyme stability was studied by measuring the activities before and after exhaustive dialysis of the enzyme against buffer A, containing 1 mM EDTA, and then against buffer A alone. An aliquot of the dialysed enzyme was then incubated at 70°C in the absence and

presence of 1 mM EDTA or *o*-phenanthroline, and the activity was assayed at different times.

Effects of compounds on enzyme activity

The effects of salts, metal ions, and chelating agents on SaADH activity were investigated by assaying the enzyme in the presence of an appropriate amount of each compound in the standard assay mixture used for the oxidation reaction. The effects of organic solvents were investigated by measuring the activity in enzyme samples (0.5 mg mL^{-1} in 100 mM MES, pH 6.0, 5 mM 2-mercaptoethanol) immediately after the addition of organic solvents at different concentrations, and 6 and 24 h of incubation at 50°C. The percentage activity for each sample was calculated by comparison with the value measured prior to incubation. The volume of the solution in a tightly capped test tube did not change during incubation.

Enantioselectivity

The enantioselectivity of SaADH was determined by examining the reduction of bicyclic ketones and α-keto esters using an NADH regeneration system consisting of glucose and glucose dehydrogenase from Thermoplasma acidophilum (TaGDH) (Sigma, St. Louis, MO). The reaction mixture contained 1 mM NAD^+, 5–10 mM carbonyl compound, 50

mM glucose, 125 µg SaADH, and 25 µg of TaGDH in 1 mL of 50 mM Tris–H_3PO_4, pH 7.0. The reactions were carried out at 50°C at different times in a temperature-controlled water bath. Upon termination of the reaction, the reaction mixture was extracted twice with ethyl acetate. The conversion yield and enantiomeric purity of the product were determined on the basis of the peak areas of ketone substrates and alcohol products by HPLC, on a Chiralcel OD-H column (Daicel Chemical Industries Ltd., Osaka, Japan). The absolute configuration of product alcohols was identified by comparing the chiral HPLC data with the standard samples. Products were analysed with isocratic elution, under the following conditions: hexane/2-propanol (9:1) (mobile phase), flow rate of 1 mL min-1, detection at 210 nm for bioconversions of methyl and ethyl benzoylformate and for methyl *o*-chlorobenzoylformate; hexane/2-propanol (95:5), flow rate of 1 mL min^{-1}, detection at 217 nm for 1-indanone. Retention times were the following: 5.7, 8.1 and 13.4 min for methyl benzoylformate, methyl (*S*)-mandelate and methyl (*R*)-mandelate; 5.5, 7.4 and 12.1 min for ethyl benzoylformate, ethyl (*S*)-mandelate and ethyl (*R*)-mandelate; 6.9, 8.8 and 9.7 min for methyl *o*-chlorobenzoylformate, methyl (*R*)-*o*-chloromandelate and methyl (*S*)-*o*-chloromandelate; 8.8, 9.7, 10.8 min for 1-indanone and (*S*)- and (*R*)-1-indanol, respectively.

Coenzyme stereospecificity determination

The SaADH stereospecificity was investigated by NMR analysis of NADD obtained from the reaction of NAD^+ with 1-phenylethanol-d_9. The reaction mixture contained 2.0 mmol 1-phenylethanol-d_9, 30 µmol NAD^+, 26 units of SaADH and 0.25 mmol sodium phosphate buffer (pH 8.0) in a total volume of 5 mL. The reaction proceeded at 50°C while monitoring at 340 nm. When the A_{340} of the mixture reached a maximum (after 4 h), the solution was cooled and then applied to a DEAE-FF Sepharose column (1.6 x 8 cm) previously equilibrated with 10 mM sodium phosphate buffer (pH 8.0). The column was washed enough with the same buffer and then NADD was eluted with 20 mM sodium phosphate buffer (pH 8.0) containing 20 mM NaCl. Fractions with value of A_{260}/A_{340} ratio B2.3 were collected and the pool (8.2 µmol of NADD) was lyophilized for ^{1}H-NMR analysis. ^{1}H-NMR spectra were recorded on a Bruker cryoprobe™ Avance DRX instrument operating at 600 MHz. Samples were dissolved in 0.5 mL of D_2O. Chemical shifts were given in ppm (δ) scale; the HDO signal was used as the internal standard (δ 4.68).

SaADH2 Material and Methods

Amplification and cloning of the *saadh2* gene

Chromosomal DNA was extracted by caesium chloride purification as described by Sambrook et al. (1989). Ethidium bromide and caesium chloride were removed by repeated extraction with isoamyl alcohol and extensive dialysis against 10 mM Tris-HCl pH 8.0, 1 mM EDTA, respectively. DNA concentration was determined spectrophotometrically at 260 nm, and the molecular mass checked by electrophoresis on 0.8% agarose gel in 90 mM Tris-borate pH 8.0, 20 mM EDTA, using DNA molecular size markers. The *saadh2* gene was amplified by polymerase chain reaction (PCR) using oligonucleotide primers based on the *saadh2* sequence of *Sulfolobus acidocaldarius* strain DSM 639 (GenBank accession no. YP_255871.1). The following oligonucleotides were used: (5′-TGCATAGTAGCATATGTCATATCAGAGTTTG-3′) as the forward primer (the *Nde I* restriction site is underlined in the sequence) and the oligonucleotide (5′-AGGAATTCACATTACAGTACAGTTAAACCACC-3′) as the reverse primer. This latter oligonucleotide introduces a translational stop following the last codon of the ADH gene, followed by an *EcoRI* restriction site, which is underlined in the sequence shown. The PCR product was digested with the appropriate restriction enzymes and cloned into the expression vector pET29a (Novagen, Madison, Wisconsin,

USA) to create the recombinant pET29a-saADH plasmid. The insert was sequenced in order to verify that mutations had not been introduced during PCR.

Expression and purification of recombinant SaADH2

Recombinant protein was expressed in *E. coli* BL21(DE3) cells (Novagen) transformed with the corresponding expression vector. Cultures were grown at 37°C in 2 litres of LB medium containing 30 μg mL^{-1} kanamycin. When the A_{600} of the culture reached 1.4, protein expression was induced by addition of isopropyl β-D-1-thiogalactopyranoside (IPTG) to a concentration of 1.0 mM. The bacterial culture was incubated at 37°C for a further 24 h. Cells were harvested by centrifugation, and the pellet stored at –20°C until use. The cells obtained from 2 L of culture were suspended in 20 mM Tris-HCl buffer (pH 7.5) containing 0.1 mM phenylmethylsulfonyl fluoride (PMSF) and were lysed using a French pressure cell (Aminco Co., Silver Spring, MD) at 2,000 p.s.i. (1 p.s.i.= 6.9 kPa). The lysate was centrifuged, and the supernatant incubated in the presence of DNase I (50 μg per mL of solution) and 5 mM $MgCl_2$ for 30 min at 37°C, followed by protamine sulfate (1 mg per mL of solution) at 4°C for 30 min. The nucleic acid fragments were removed by centrifugation, and the supernatant incubated at 70°C for 15 min. The host protein precipitate was removed by

centrifugation. The supernatant was dialysed overnight at 4°C against 20 mM Tris-HCl, pH 8.4 (buffer A) containing 1 mM PMSF. The dialysed solution was applied to a DEAE-Sepharose Fast Flow (1.6 × 12 cm, Pharmacia) column equilibrated in buffer A at 120 mL h^{-1}. The active pool did not bind to the column matrix. The flowthrough fractions were combined and dialysed against buffer A, concentrated 5-fold with a 30,000 MWCO centrifugal filter device (Millipore), and applied to a Sephadex G-75 (1.6 × 30 cm, Pharmacia) column equilibrated in buffer A containing 150 mM NaCl. The active pool was dialysed against buffer A and concentrated to obtain 2.0 mg protein mL^{-1} as described previously. SaADH2 was stored at –20°C in buffer A containing 50% glycerol, without loss of activity following several months of storage. SDS-PAGE was carried out according to the Laemmli method (1970). The subunit molecular mass was determined by electrospray ionization mass spectrometry (ESI-MS) with a QSTAR Elite instrument (Applied Biosystems, Unites States). The protein concentration was determined with a Bio-Rad protein assay kit using BSA as a standard.

Sucrose density gradient centrifugation

One hundred microliters of a 1 mg mL^{-1} purified SaADH2 solution was layered on top of a 10 mL 5–20% preformed sucrose gradient in 50 mM

Tris-HCl, pH 8.4. The standards were also prepared by layering 100 µl of 1 mg mL^{-1} chymotripsinogen (25 kDa), BSA (67 kDa), *T. thermophilus* ADH (a 108-kDa tetramer), and *S. solfataricus* ADH (a 150-kDa tetramer) on top of another identical sucrose gradient. By using a Beckman SW 41 Ti rotor, the tubes containing the samples were spun at 37,000 rpm for 18 h at 4°C in a Beckman LE-80 ultracentrifuge. Immediately after centrifugation, gradients were collected in 250 µl-fractions and assayed for absorption at 280 nm to determine the position of the marker protein. The mass of SaADH2 was estimated from the position of the peak relative to those of the markers.

Enzyme assay

SaADH2 activity was assayed spectrophotometrically at 65°C by measuring the change in absorbance of NADH at 340 nm using a Cary 1E spectrophotometer equipped with a Peltier effectcontrolled temperature cuvette holder. The standard assay for the reduction reaction was performed by adding 5-25 µg of the enzyme to 1 mL of preheated assay mixture containing 20 mM ethyl 3-methyl-2-oxobutyrate (EMO) and 0.2 mM NADH in 37.5 mM sodium phosphate, pH 5.0. The standard assay for the oxidation reaction was performed using a mixture containing 18 mM cycloheptanol and 3 mM NAD^+ in 50 mM glycine/NaOH, pH 10.5.

Screening of the substrates was performed using 1 mL of assay mixture containing either 10 mM alcohol and 3 mM NAD^+ in 50 mM glycine/NaOH, pH 10.5, or 10 mM carbonyl compound and 0.1 mM NADH in 37.5 mM sodium phosphate, pH 5.0. One unit of SaADH2 represented 1 μmol of NADH produced or utilized per min at 65°C, on the basis of an absorption coefficient of 6.22 mM^{-1} cm^{-1} for NADH at 340 nm.

Effect of pH on activity

The optimum pH values for the reduction and oxidation reactions was determined at 65°C under the conditions used for EMO and cycloheptanol, respectively, except that different buffer were used. The concentration of each buffer solution was diluted to get the similar conductivity (~1.1 mS). The pH was controlled in each assay mixture at 65°C.

Kinetics

The SaADH2 kinetic parameters were calculated from measurements determined in duplicate or triplicate and by analysing the kinetic results using the program GraFit (Leatherbarrow 2004). The turnover value (k_{cat}) for SaADH2 was calculated on the basis of a molecular mass of 27 kDa, assuming that the four subunits are catalytically active.

Thermophilicity and thermal stability

SaADH2 was assayed in a temperature range of 25–90°C using standard assay conditions and 22 μg of protein mL^{-1} of assay mixture. The stability at various temperatures was studied by incubating 0.2-mg mL^{-1} protein samples in 50 mM Tris-HCl, pH 9.0 at temperatures between 25°C and 95°C for 30 min. Each sample was then centrifuged at 5°C, and the residual activity assayed as described above. The effect of chelating agents on enzyme stability was studied by measuring the activities before and after exhaustive dialysis of the enzyme against buffer A, containing 1 mM EDTA, and then against buffer A alone. An aliquot of the dialysed enzyme was then incubated at 70°C in the absence and presence of 1 mM EDTA, and the activity assayed at different times.

Effects of compounds on enzyme activity

The effects of salts, metal ions, and chelating agents on SaADH2 activity were investigated by assaying the enzyme in the presence of an appropriate amount of each compound in the standard assay mixture used for the oxidation reaction. The effects of organic solvents were investigated by measuring the activity in enzyme samples (0.2 mg mL^{-1} in 100 mM sodium phosphate, pH 7.0) immediately after the addition of organic solvents at different concentrations and after incubation for 6 and 24 h at 50°C. The

percentage activity for each sample was calculated by comparison with the value measured prior to incubation. The volume of the solution in a tightly capped test tube did not change during incubation.

Enantioselectivity

The enantioselectivity of SaADH2 was determined by examining the reduction of acetophenone, the bicyclic ketones benzyl, and 2,2'-dichlorobenzil using an NADH regeneration system consisting of BsADH and a substrate alcohol (see below). The reaction mixture contained 2 mM NAD^+, 5 mM carbonyl compound, 4 to 18% v/v alcohol, 250 μg SaADH2, and 50 μg of BsADH in 1 mL of 100 mM sodium phosphate, pH 7.0. The reactions were carried out at 50°C for 24 h in a temperaturecontrolled water bath. Upon termination of the reaction, the reaction mixture was extracted twice with ethyl acetate. The percentage of conversion and enantiomeric purity of the product were determined on the basis of the peak areas of ketone substrates and alcohol products by HPLC, on a Chiralcel OD-H column (Daicel Chemical Industries, Ltd., Osaka, Japan). The absolute configuration of product alcohols was identified by comparing the chiral HPLC data with the standard samples. Products were analyzed with isocratic elution, under the following conditions: hexane/2-propanol (9:1) (mobile phase), flow rate of 1 mL min^{-1}, detection at 210 nm. Retention

times were the following: 5.6, 11.9 and 16.7 for benzil, (*S*)- and (*R*)-benzoin, respectively; 6.98, 12.73 and 15.13, for 2,2'-dichlorobenzil, (*S*)- and (*R*)-1,2-bis(2-chlorophenyl)-2-hydroxyethanone, respectively; 5.27, 6.2, and 7.5 for acetophenone, (*R*)- and (*S*)-1-phenylethanol, respectively. The absolute stereochemistry of 1,2-bis(2-chlorophenyl)-2-hydroxyethanone enantiomers was assigned by analogy to the values of (*S*)- and (*R*)-benzoin.

Structural characterization

The purified protein was concentrated to 8–10 mg mL^{-1} in 20 mM Tris/HCl buffer at pH 8.4. The protein solution was added with NADH to obtain a 8.5 mg mL^{-1} protein solution containing 2.2 mM NADH in the above buffer. Crystallization was performed by hanging-drop vapor diffusion method at 296 K. The best crystals were grown by mixing 1 μl of protein solution with the same volume of a solution containing 2.0 M ammonium sulfate in 100 mM HEPES buffer (pH 7.5). The crystals belong to P21 space group with unit cell parameters a=83.80 Å, b=60.48 Å, c=107.1 Å, β=99.8°. Crystals were transferred to a stabilizing solution containing 20% glycerol as cryoprotectant and Xray data were then collected in-house at 100 K using a Rigaku Micromax 007 HF generator producing Cu Kα radiation and equipped with a Saturn944 CCD detector. Intensity data up to

1.75 Å resolution were processed and scaled using program HKL2000 (HKL Research). Data collection statistics are shown in Table 19. The crystal structure was solved by MR methods by using as a search model the coordinates of a putative glucose/ribitol dehydrogenase from *Clostridium thermocellum* (PDB code 2HQ1), which showed the best sequence-alignment with SaADH2 (39% sequence identity). Model building was first performed with ARP/WARP package using the warpNtrace automated procedure. Later model building and refinement was performed by the program CNS version 1.1. The final structure shows R and R-free factors of 17.4% and 19.5% respectively. Refinement statistics are summarized in Table 19. Fold similarities searches were performed with the DALI server (http://ekhidna.biocenter.helsinki.fi/dali_server).

Table 19. Data collection and refinement statistics

Data collection	
Space group	P21
Cell dimensions (Å;°)	a=83.80, b=60.48, c=107.1; β=99.78
Resolution range (Å)	40.0–1.75 (1.81–1.75)
No. of unique reflections	106,431 (10,388)
Average redundancy	4.2 (2.8)
Completeness	99.7 (98.0)
$<I/\sigma(I)>$	19.8 (3.6)
Rmerge	0.065 (0.36)
Refinement	
No. of reflections used (with $\|F\| > 0$)	101,786
No. of reflections working/test set	96,639/5,147
Resolution range (Å)	40.0–1.75
R-factor/R-free (%)	16.8/19.1
No. of protein atoms	7,512
No. of water/glycerol/sulphate/NADH	687/5/1/4
RMS deviation on bond distances (Å)	0.007
RMS deviation on bond angles (°)	1.4

BsADH Material and Methods

Enzyme assay

BsADH activity was assayed spectrophotometrically at 50°C by measuring the change in absorbance at 340 nm of NADH using a Cary 1E spectrophotometer equipped with a Peltier effect-controlled temperature cuvette holder. Measurement was carried out in 1 mL of assay mixture containing either 8 mM alcohol, and 18 mM NAD^+ in 200 mM glycine-NaOH, pH 8.5, or 8 mM aldehyde and 0.3 mM NADH in 100 mM Tris-HCl, pH 7.7. Aliquots of 0.5 and 1.0 µg of BsADH were used for the forward and reverse reactions, respectively. One unit of BsADH represented 1 µmol of NADH produced or utilized per min at 50°C, on the basis of an absorption coefficient of 6.22 $mM^{-1}\times cm^{-1}$ for NADH at 340 nm.

Kinetics

The BsADH kinetic parameters were calculated from measurements carried out in duplicate or triplicate, and analysing the kinetic results using the program GraFit (Leatherbarrow 2004). Coefficients of variation were around 5% for V_{max} and 16% for K_m estimates. The turnover value (k_{cat}, s^{-1}) for BsADH was calculated on the basis of a molecular mass of 36 kDa, assuming that the four subunits are catalytically active.

Determination of protein concentration

The protein concentration was determined with a Bio-Rad protein assay kit using bovine serum albumin as a standard (A_{280} of 1% bovine serum albumin in 50 mM sodium phosphate [pH7.0]–0.9% NaCl, 6.6).

Biocatalytic synthesis of cinnamyl alcohol by isolated BsADH

Reaction mixture for analytical biotransformation typically contained 0.125 g L^{-1} (1 mM) CMA, 5 to 15% 2-propanol, 1 mM NAD^+, 5 mM 2-mercaptoethanol, 0.12 mg mL^{-1} BsADH in 1 mL of 50 mM sodium phosphate, pH 7.0. Each reaction mixture was shaken at 200 rpm for specific reaction times at 50°C in a temperature-controlled water bath. Upon termination, the reaction mixture was extracted three times with ethyl acetate (1:1 vol/vol). Products were analyzed by HPLC (Ultimate 3000, Dionex) using a Jupiter® 5 µm C18 300 Å LC column (250 × 4.6 mm Phenomenex, CA, USA). The degree of conversion was determined on the basis of the peak areas of aldehyde substrate and alcohol product eluted under the following conditions: 0.085% v/v H_3PO_4 in water (solvent A) and 95% v/v acetonitrile in 0.085% v/v H_3PO_4 (solvent B) as mobile phases. Choromatographic conditions: initial isocratic elution, 10% B for 4 min, followed by a gradient phase, 10 to 90% B for 5 min, then isocratic elution with 90% B for 6 min, followed by a descending gradient, 90 to 10% B for

1 min, and isocratic elution, 10% B for 4 min at a 1 mL min^{-1} flow rate. The detector was set at 268 nm. Retention times were the following: 11.4 and 11.9 min for CMO and CMA respectively. Semi-preparative biotransformations were performed on a 0.1 to 0.2 g scale in a reaction volume from 100 mL to 400 mL, using 0.01 to 0.05 mg mL^{-1} BsADH, 1 mM NAD, in 50 mM sodium phosphate, pH 7.0, 5 mM 2-mercaptoethanol. The reactions were carried out at 50°C for 3 h as described above. Upon termination of the reaction, the mixtures were extracted three times with ethyl acetate (1:1 vol/vol). The combined organic layers of the ethyl acetate extracts were dried with anhydrous sodium sulphate, filtered, and concentrated under reduced pressure. Purification by silica gel column chromatography (hexane/ethyl acetate 9:1, the first two column volumes, followed by hexane/ethyl acetate 7:3) yielded CMO as colourless oils. ^{1}H-NMR spectra were recorded on a Bruker Biospin instrument operating at 400 MHz. Samples were dissolved in 0.5 mL $CDCl_3$. Chemical shifts were given in ppm (δ) scale; the $CHCl_3$ signal was used as the internal standard (δ 7.26). ^{13}C-NMR spectra were recorded on a Bruker Biospin instrument operating at 75 MHz. Samples were dissolved in 0.5 mL of $CDCl_3$. Chemical shifts were given in ppm (δ) scale; the $CDCl_3$ signal was used as the internal standard (δ 77.0).

Preparation of the whole cell catalyst

The preparation of active cells was performed as described previously (Fiorentino et al. 1998). Briefly, cultures of *E. coli* RB791 harbouring BsADH were grown at 37°C in 2 L of LB medium containing 30 μg mL^{-1} ampicillin. When the A_{600} of a culture reached 1.6, protein expression was induced by addition of isopropyl β-D-1-thiogalactopyranoside to 1.0 mM. The bacterial culture was incubated at 37°C for a further 24 h. The cell pellets harvested by centrifugation were stored as a 0.38 gmL^{-1} cell suspension in 50 mM sodium phosphate buffer (pH 7.0) at –20°C and used for biotransformation in 7 days. To determine the BsADH activity in the cells, an aliquot of pellet was suspended in 50 mM sodium phosphate buffer (pH 7.0) and lysed using a French pressure cell (Aminco Co., Silver Spring, MD) at 2,000 p.s.i.(1 p.s.i.= 6.9 kPa). The supernatant obtained by centrifugation was assayed for protein concentration and BsADH activity as described above, using benzyl alcohol as substrate.

Biocatalytic synthesis of cinnamyl alcohol by whole-cells

The stored wet cells of recombinant *E. coli* RB791 were suspended to a concentration of 200 to 300 mg mL^{-1} in 10 to 80 mL of 50 mM sodium phosphate buffer (pH 7.0) containing 12.5 mg mL^{-1} (100 mM) CMA, 10% 2-propanol, 5 mM 2-mercaptoethanol in a 50 to 250 mL glass flask. The

mixture was incubated at 37°C with continuous shaking at 180 rpm. After 3 to 6 h reaction, the work-up was carried out by lowering the pH to 3 with ~6 M hydrochloric acid and addition of 0.75 to 6.0 g of the filter aid material Celite Hyflo Supercel (Macherey-Nagel) to the reaction mixture (0.075 g mL^{-1}). After 30 min stirring and subsequent filtration, the filter cake was washed with ethyl acetate and the aqueous phase extracted three times with ethyl acetate (1:1 vol/vol). The resulting organic fractions were then combined and dried over sodium sulphate; the organic phase was concentrated to dryness, and the oily crude product was purified by flash chromatography as described above. Each sample was analysed by HPLC before the work-up, while NMR spectra was performed on a representative sample obtained from flash chromatography.

References

Allen FH (2002) The Cambridge Structural Database: a quarter of a million crystal structures and rising. *Acta Crystallogr* B 58:380–388

Aoyagi Y, Agata N, Shibata N, Horiguchi M, Williams RM (2000) Lipase TL-mediated kinetic resolution of benzoin: facile synthesis of (1*R*,2*S*)-erythro-2-amino-1,2-diphenylethanol. *Tetrahedron Lett* 41:10159–10162

Asada Y, Endo S, Inoue Y, Mamiya H, Hara A, Kunishima N, Matsunaga T (2009) Biochemical and structural characterization of a short-chain dehydrogenase/reductase of *Thermus thermophilus* HB8: a hyperthermostable aldose-1-dehydrogenase with broad substrate specificity. *Chem Biol Interact* 178:117–126

Bennett BD, Kimball EH, Gao M, Osterhout R, Van Dien SJ and Rabinowitz JD (2009) Absolute metabolite concentrations and implied enzyme active site occupancy in *Escherichia coli*. *Nat. Chem. Biol*. 5, 593–599.

Berenguer-Murcia A and Fernandez-Lafuente R (2010) New Trends in the Recycling of NAD(P)H for the Design of Sustainable Asymmetric Reductions Catalyzed by Dehydrogenases. *Current Organic Chemistry*, 14, 1000–1021.

Bonini C and Righi G (*1994)* Enantio-and stereo-selective route to the taxol side chain *via*asymmetric epoxidation of *trans*-cinnamyl alcohol and subsequent expoxide ring opening. *J. Chem. Soc. Chem. Commun*. 24, 2767–2768

Bousquet A, Musolino A (1999) PCT Int. Appl., WO9918110 A1. *Chem. Abstr.130*, 296510e

Breuer M, Ditrich K, Habicher T, Hauer B, Kesseler M, Stuermer R, Zelinski T (2004) Industrial methods for the production of optically active intermediates. *Angew Chem Int Ed Engl* 43, 788-824.

Broussy S, RW Cheloha, DB Berkowitz (2009) Enantioselective, ketoreductase-based entry into pharmaceutical building blocks: ethanol as tunable nicotinamide reductant. *Org. Lett. 11*, 305–308

Cannio R, Rossi M and Bartolucci S (1994) A few amino acid substitutions are responsible for the higher thermostability of a novel NAD-dependent bacillar alcohol dehydrogenase. *Eur. J. Biochem.* 222, 345–352

Cánovas M, Torroglosa T and Iborra JL (2005) Permeabilization of *Escherichia coli* cells in the biotransformation of trimethylammonium compounds into L-carnitine. *Enzyme Microb. Technol*. 37, 300–308

Carrea G and Riva S (2000) Properties and Synthetic Applications of Enzymes in Organic Solvents. *Angew*. *Chem. 39*, 2226–2254

Ceccarelli C, ZX Liang, M Strickler, G Prehna, BM Goldstein, JP Klinman and BJ Bahnson (2004) Crystal structure and amide H/D exchange of binary complexes of alcohol dehydrogenase from *Bacillus stearothermophilus*: insight into thermostability and cofactor binding. *Biochemistry* 43:5266–5277

Chen L, Brügger K, Skovgaard M, Redder P, She Q, Torarinsson E, Greve B, Awayez M, Zibat A, Klenk HP, Garrett RA (2005) The genome of *Sulfolobus acidocaldarius*, a model organism of the Crenarchaeota. *J Bacteriol* 187:4992–4999

Ciappa A, Bovo S, Bertoldini M, Scrivanti A, and Matteoli U (2008) Homogeneous Asymmetric Catalysis in Fragrance Chemistry. *Chemistry & Biodiversity*, 5, 1058–1069

Davies GE, Stark GR (1970) Use of dimethyl suberimidate, a crosslinking reagent, in studying the subunit structure of oligomeric proteins. *Proc Natl Acad Sci USA* 66:651–656

De Wildeman SMA, Sonke T, Schoemaker HE and May O (2007*).* Biocatalytic reductions: from lab curiosity to "first choice". *Acc. Chem. Res*., 40*,* 1260–1266.

Duester G (1996) Involvement of alcohol dehydrogenase, short-chain dehydrogenase/reductase, aldehyde dehydrogenase, and cytochrome P450 in the control of retinoid signaling by activation of retinoic acid synthesis. *Biochemistry* 35(38), 12221-7

Eilerman RE (1992) in Kirk-Othmer Encyclopedia of Chemical Technology. (Kroschwitz, J.I. ed.), Wiley, NY, p. 349

Ema T, Ide S, Okita N, Sakai T (2008) Highly efficient chemoenzymatic synthesis of methyl (*R*)-*o*-chloromandelate, a key intermediate for clopidogrel, via asymmetric reduction with recombinant *Escherichia coli*. *Adv Synth Catal* 350:2039–2044

Faber K (2000) Reduction reactions. In: Faber K, editor. *Biotransformations in organic chemistry.* Berlin: Springer, pp. 177-219

Faber K (2004) Biotransformations in organic chemistry, 5th edn. Springer, Berlin

Fahlbusch KG, Hammerschmidt FJ, Panten J, Pickenhagen W and Schatkowski D (2008) in Flavors and Fragrances: *Ullmann's Encyclopedia of Industrial Chemistry*, Wiley-*VCH* Verlag, Weinheim

Filling C, KD Berndt, J Benach, S Knapp, T Prozorovski, E Nordling, R Ladenstein, H Jörnvall and U Oppermann (2002) Critical residues for structure and catalysis in short-chain dehydrogenases/reductases. *J. Biol. Chem.* 277:25677–25684

Fiorentino G, Cannio R, Rossi M and Bartolucci S (1998) Decreasing the stability and changing the substrate specificity of the *Bacillus stearothermophilus* alcohol dehydrogenase by single amino acid replacements. *Protein. Eng.* 11, 925–930

Fontana A, De Filippis V, Polverino de Laureto P, Scaramella E and Zambonin M (1998) Stability and Stabilization of Biocatalists. Ballesteros A, Plou FJ, Iborra J L,Halling PJ Editori

Friest JA, Y Maezato, S Broussy, P Blum, DB Berkowitz (2010) Use of a robust dehydrogenase from an archael hyperthermophile in asymmetric catalysis-dynamic reductive kinetic resolution entry into (*S*)-profens. *J. Am. Chem. Soc. 132*, 5930–5931

Galletti P, E Emer, G Gucciardo, A Quintavalla, M Pori, D Giacomini (2010) Chemoenzymatic synthesis of (2*S*)-2-arylpropanols through a dynamic kinetic resolution of 2-arylpropanals with alcohol dehydrogenases. *Org. Biomol. Chem. 8*, 4117–4123

Gallezot P and Richard D (1998) Catalysis Reviews – *Science and Engineering*, 40, 81–126

Gardinier KM, Leahy JW (1997) Enantiospecific total synthesis of the potent antitumor macrolides cryptophycins 1 and 8. *J Org Chem* 62:7098–7099

Giordano A, F Febbraio, C Russo, M Rossi, and CA Raia (2005) Evidence for co-operativity in coenzyme binding to tetrameric *Sulfolobus solfataricus* alcohol dehydrogenase and its structural basis: fluorescence, kinetic and structural studies of the wild-type enzyme and non-co-operative N249Y mutant. *Biochem. J.* 388:657–667

Goldberg K, Schroer K, Lütz S and Liese A (2007) Biocatalytic ketone reduction—a powerful tool for the production of chiral alcohols—part II: whole-cell reductions. *Appl. Microbiol. Biotechnol.* 76, 249–255.

Guagliardi A, Martino M, Iaccarino I, De Rosa M, Rossi M and Bartolucci S. (1996) Purification and characterization of the alcohol dehydrogenase from a novel strain of *Bacillus stearothermophilus* growing at 70 degrees C. Int. *J. Biochem. Cell Biol.* 28, 239–246

Guy JE, MN Isupov and JA Littlechild (2003) The structure of an alcohol dehydrogenase from the hyperthermophilic archaeon *Aeropyrum pernix*. *J. Mol. Biol.* 331:1041–1051

Hall M and Bommarius AS (2011). Enantioenriched compounds via enzyme-catalyzed redox reactions. Chem. Rev., 111, 4088–5110

Henegar KE, Ball CT, Horvath CM, Maisto KD and Mancini SE (2007) *Org.* Process Res. Dev. 11, 346–353

Henne A, H Bruggemann, C Raasch, A Wiezer, T Hartsch, H Liesegang, A Johann, T Lienard, O Gohl, R Martinez-Arias, C Jacobi, V Starkuviene, S Schlenczeck, S Dencker, R Huber, HP Klenk, W Kramer, R Merkl, G Gottschalk and HJ Fritz (2004) The genome sequence of the extreme thermophile *Thermus thermophilus*. *Nat. Biotechnol.* 22:547–553

Höffken HW, M Duong, T Friedrich, M Breuer, B Hauer, R Reinhardt, R Rabus and J Heider (2006) Crystal structure and enzyme kinetics of the (*S*)-specific 1-phenylethanol dehydrogenase of the denitrifying bacterium strain EbN1. *Biochemistry* 45:82–93

Hoyos P, Sinisterra JV, Molinari F, Alcántara AR, Domínguez de María P (2010) Biocatalytic strategies for the asymmetric synthesis of alpha-hydroxy ketones. *Acc Chem Res* 43:288–299

Hu J and Xu Y (2006) Anti-prelog reduction of prochiral carbonyl compounds by *Oenococcus oeni* in a biphasic system. *Biotechnol. Lett. 28*, 1115–1119

Hummel W (1999) Large-scale applications of NAD(P)-dependent oxidoreductases: recent developments. *Trends Biotechnol.* 17:487–492

Inoue K, Y Makino, T Dairi and N Itoh (2006) Gene cloning and expression of *Leifsonia* alcohol dehydrogenase (LsADH) involved in asymmetric hydrogen-transfer bioreduction to produce (*R*)-form chiral alcohols. *Biosci. Biotechnol. Biochem.* 70:418–426

Jamali F, Mehvar R and Pasutto FM (1989) Enantioselective aspects of drug action and disposition: therapeutic pitfalls. *J Pharm Sci* 78:95–715

Johanson T, Katz M, Gorwa-Grauslund MF (2005) Strain engineering for stereoselective bioreduction of dicarbonyl compounds by yeast reductases. *FEMS Yeast Res. 5*, 513-525

John J, SJ Crennell, DW Hough, MJ Danson, GL Taylor (1994) The crystal structure of glucose dehydrogenase from *Thermoplasma acidophilum. Structure 2*, 385–393

Jones JB and JF Beck (1976) Applications of biochemical systems in organic chemistry, p. 248–401. *In* J. B. Jones, C. J. Sih, and D. Perlman (ed.), *Techniques of chemistry series*, part I, vol. 10. John Wiley & Sons, New York, NY

Jönsson Å, E Wehtje, P Adlercreutz, B Mattiasson (1999) Thermodynamic and kinetic aspects on water vs. organic solvent as reaction media in the enzyme-catalysed reduction of ketones. *Biochim. Biophys. Acta 1430*, 313–322

Kallberg Y, U Oppermann, H Jörnvall and B Persson (2002) Short-chain dehydrogenases/reductases (SDRs). *Eur. J. Biochem.* 269:4409–4417

Kaluzna IA, Matsuda T, Sewell AK, Stewart JD (2004) Systematic investigation of *Saccharomyces cerevisiae* enzymes catalyzing carbonyl reductions. *J. Am. Chem. Soc. 126*, 12827-12832

Kavanagh KL, Jörnvall H, Persson B, Oppermann U (2008) The SDR superfamily: functional and structural diversity within a family of metabolic and regulatory enzymes. *Cell Mol Life Sci* 65:3895–3906

Keinan E, EK Hafely, KK Seth and R Lamed (1986) Thermostable enzymes in organic synthesis. Asymmetric reduction of ketones with alcohol dehydrogenase from *Thermoanaerobium brockii*. *J. Am. Chem. Soc.* 108:162–169

Klibanov AM (2001) Improving enzymes by using them in organic solvents. *Nature 409*, 241–246

Kobayashi Y, Y Takemoto, Y Ito, S Terashima (1990) *Tetrahedron Lett. 31*, 3031–3034

Kohen A, Cannio R, Bartolucci S and Klinman JP (1999) Enzyme dynamics and hydrogen tunnelling in a thermophilic alcohol dehydrogenase. *Nature* 399, 496–499.

Korkhin Y, AJ Kalb (Gilboa), M Peretz, O Bogin, Y Burstein and F Frolow (1998) NADP-dependent bacterial alcohol dehydrogenases: crystal structure, cofactor-binding and cofactor specificity of the ADHs of *Clostridium beijerinckii* and *Thermoanaerobacter brockii*. *J. Mol. Biol*. 278:967–981

Kratzer R, Pukl M, Egger S and Nidetzky B (2008) Whole-cell bioreduction of aromatic alpha-keto esters using *Candida tenuis* xylose reductase and *Candida boidinii* formate dehydrogenase co-expressed in *Escherichia coli. Microb. Cell Fact*., 7, 37

Kroutil W, Mang H, Edegger K, Faber K (2004) Recent advances in the biocatalytic reduction of ketones and oxidation of secalcohols. *Curr Opin Chem Biol* 8:120–126

Kwiecien RA, Ayadi F, Nemmaoui Y, Silvestre V, Zhang BL, Robins RJ (2009) Probing stereoselectivity and pro-chirality of hydride transfer during short-chain alcohol dehydrogenase activity: a combined quantitative ^{2}H NMR and computational approach. *Arch Biochem Biophys* 482:42–51

Laane C, Boeren S, Hilhorst R, Veeger C (1987) Optimization of biocatalysis in organic media. In: Laane C, Tramper J, Lilly MD (eds) Biocatalysis in organic media, vol 29. *Elsevier,* Amsterdam, pp 65–84

Laemmli UK (1970) Cleavage of structural proteins during the assembly of the head of bacteriophage T4. *Nature* 227:680–685

Leatherbarrow RJ (2004) GraFit Version 5.0.11. Erithacus Software Ltd., Horley, UK

Liang ZX, Lee T, Resing KA, Ahn NG, Klinman JP (2004) Thermalactivated protein mobility and its correlation with catalysis in thermophilic alcohol dehydrogenase. *Proc Natl Acad Sci USA 101*:9556–9561

Liese, A., Seelbach, K. & Wandrey, C. (2000). Industrial Biotransformations, Wiley-VCH, Weinheim.

Lopes S, Gòmez-Zavaglia A, Lapinski L, Chattopadhyay N, Fausto R (2004) Matrix-isolation FTIR spectroscopy of benzil: probing the flexibility of the C–C torsional coordinate. *J Phys Chem A* 108:8256–8263

Machado B.A.F.R. (2008) Ph. D. Dissertation, University of Porto, Portugal.

Machielsen R, Uria AR, Kengen SW, van der Oost J (2006) Production and characterization of a thermostable alcohol dehydrogenase that belongs to the aldo–keto reductase superfamily. *Appl Environ Microbiol* 72:233–238

Maruyama R, Nishizawa M, Itoi Y, Ito S, Inoue M (2002) The enzymes with benzil reductase activity conserved from bacteria to mammals. *J Biotechnol* 94:157–169

Nakamura K, Matsuda T (2002) Reduction of ketones. In: Drauz K, Waldmann H (eds) *Enzyme catalysis in organic synthesis*, vol. III, 2nd edn. Wiley–VCH Verlag GmbH, Weinheim, pp 991–1047

Niefind K, Müller J, Riebel B, Hummel W, Schomburg D (2003) The crystal structure of *R*-specific alcohol dehydrogenase from *Lactobacillus brevis* suggests the structural basis of its metal dependency. *Journal of Molecular Biology* 327(2):317-328

Pawelka Z, Koll A, Zeegers-Huyskens Th (2001) Solvent effect on conformation of benzil. *J Mol Struct* 597:57–66

Pennacchio A, Pucci B, Secundo F, La Cara F, Rossi M and Raia CA (2008) Purification and characterization of a novel recombinant highly enantioselective short-chain NAD(H)-dependent alcohol dehydrogenase from *Thermus thermophilus*. *Appl. Environ. Microbiol.* 74, 3949–3958

Pennacchio A, Giordano A, Pucci B, Rossi M, Raia CA. (2010a) Biochemical charaterization of a recombinant short-chain NAD(H)-dependent dehydrogenase/reductase from *Sulfolobus acidocaldarius. Extremophiles* 14:193-204.

Pennacchio A, A Giordano, L Esposito, E Langella, M Rossi, CA Raia (2010b) Insight into the stereospecificity of short-chain *Thermus thermophilus* alcohol dehydrogenase showing *pro-S* hydride transfer and prelog enantioselectivity. *Protein Pept. Lett. 17*, 437–444

Pousset C, M Haddad, M Larchevêque (2001) *Tetrahedron 57*, 7163–7167

Radianingtyas H, Wright PC (2003) Alcohol dehydrogenases from thermophilic and hyperthermophilic archaea and bacteria. *FEMS Microbiol Rev* 27:593–616

Raia CA, A Giordano and M Rossi (2001) Alcohol dehydrogenase from *Sulfolobus solfataricus*. *Methods Enzymol.* 331:176–195

Sambrook J, Fritsch EF, Maniatis T (1989) Molecular cloning: a laboratory manual, 2nd edn. Cold Spring Harbor Laboratory Press, Cold Spring Harbor, NY

Schlieben NH, K Niefind, J Muller, B Riebel, W Hummel and D Schomburg (2005) Atomic resolution structures of *R*-specific alcohol dehydrogenase from *Lactobacillus brevis* provide the structural bases of its substrate and cosubstrate specificity. *J. Mol. Biol.* 349:801–813

Schneider-Bernlöhr H, Adolph H-W, Zeppezauer M (1986) Coenzyme stereospecificity of alcohol/polyol dehydrogenases: conservation of protein types vs. functional constraints. *J Am Chem Soc* 108:5573–5576

Schroer K, Zelic B, Oldiges M and Lütz S (2009) Metabolomics for biotransformations: Intracellular redox cofactor analysis and enzyme kinetics offer insight into whole cell processes. *Biotechnol. Bioeng.* 104, 251–260

Smith LD, N Budgen, SJ Bungard, MJ Danson, DW Hough (1989) Purification and characterization of glucose dehydrogenase from the thermoacidophilic archaebacterium *Thermoplasma acidophilum*. *Biochem. J. 261,* 973–977

Sundby E. (2003) Biological reductions and esterifications for the production of enantiopure secondary alcohols. A thesis submitted in the partial fulfillment for the academic degree Doctor Scientarium NTNU, Norwegian University of Science and Technology Department of Chemistry

Tanaka T, Kawase M, Tani S (2004) Alpha-hydroxyketones as inhibitors of urease. *Bioorg Med Chem* 12:501–505

van der Donk WA, Zhao H. (2003) Recent developments in pyridine nucleotide regeneration. *Curr Opin Biotechnol.* 14(4):421-6

Villela Filho M, T Stilliger, M Müller, A Liese, C Wandrey (2003) Is logP a convenient criterion to guide the choice of solvents for biphasic enzymatic reactions? *Angew. Chem. Int. Ed. 4*, 2993–2996

Wildemann H, Dünkelmann P, Müller M, Schmidt B (2003) A short olefin metathesis-based route to enantiomerically pure arylated dihydropyrans and alpha, beta-unsaturated delta-valero lactones. *J Org Chem* 68:799–804

Woodward J, KA Cordray, RJ Edmonston, M Blanco-Rivera, SM Mattingly, BR Evans (2000) Enzymatic Hydrogen Production: Conversion of Renewable Resources for Energy Production. *Energy Fuels 14*, 197–201

Zhang X and Bruice TC (2007) Temperature-dependent structure of the E x S complex of *Bacillus stearothermophilus* alcohol dehydrogenase. *Biochemistry*, 46, 837−843

Zhang R, Zhu G, Zhang W, Cao S, Ou X, Li X, Bartlam M, Xu Y, Zhang XC, Rao Z. (2008) Crystal structure of a carbonyl reductase from *Candida parapsilosis* with anti-Prelog stereospecificity.*Protein Sci.* 17(8):1412-23

Zhao YH, Abraham MH, Zissimos AM (2003) Fast calculation of van der Waals volume as a sum of atomic and bond contributions and its application to drug compounds. *J Org Chem* 68:7368–7373

Zhu D, Malik HT, Hua L (2006) Asymmetric ketone reduction by a hyperthermophilic alcohol dehydrogenase. The substrate specificity, enantioselectivity and tolerance of organic solvents. *Tetrahedron: Asymmetry* 17:3010–3014

List of publications

Angela Pennacchio, Mosè Rossi and Carlo A.Raia Synthesis of cinnamyl alcohol from cinnamaldehyde with *Bacillus stearothermophilus* alcohol dehydrogenase as the isolated enzyme and in recombinant *E. coli* cells. (*2013, under reviewing*).

Angela Pennacchio, Vincenzo Sannino, Giosuè Sorrentino, Mosè Rossi , Carlo A. Raia, and Luciana Esposito
Biochemical and structural characterization of recombinant short-chain NAD(H)-dependent dehydrogenase/reductase from *Sulfolobus acidocaldarius* highly enantioselectiv e on diaryl diketone benzyl (2012). *Appl. Microbiol. Biotechnol.* DOI 10.1007/s00253-012-4273-z

Angela Pennacchio, Assunta Giordano, Mosè Rossi and Carlo A.Raia
Asymmetric Reduction of α-Keto Esters with *Thermus thermophilus* NADH-Dependent Carbonyl Reductase using Glucose Dehydrogenase and Alcohol Dehydrogenase for Cofactor Regeneration (2011). *Eur. J. Org. Chem.* 23, 4361-4366

Pennacchio A., Giordano A, Pucci B, Rossi M, Raia CA.
Biochemical charaterization of a recombinant short-chain NAD(H)-dependent dehydrogenase/reductase from *Sulfolobus Acidocaldarius* (2010).
Extremophiles 14:193-204.

Angela Pennacchio, Mosè Rossi and Carlo A. Raia

Synthesis of cinnamyl alcohol from cinnamaldehyde with *Bacillus stearothermophilus* alcohol dehydrogenase as the isolated enzyme and in recombinant *E. coli* cells *(Under reviewing)*

Abstract The synthesis of the aroma chemical cinnamyl alcohol (CMO) by means of enzymatic reduction of cinnamaldehyde (CMA) was investigated using NADH-dependent alcohol dehydrogenase from *Bacillus stearothermophilus* both as an isolated enzyme, and in recombinant *E. coli* whole cells. The influence of parameters such as reaction time and cofactor, substrate, co-substrate 2-propanol and biocatalyst concentrations on the bioreduction reaction was investigated and an efficient and sustainable one phase-system developed. The reduction of CMA (0.5 g/L, 3.8 mmol/L) by the isolated enzyme occurred in 3 h at 50 °C with 97% conversion, and yielded high purity CMO (≥98%) with a yield of 88% and a productivity of 50g/g $_{enzyme}$. The reduction of 12.5 g/L (94 mmol/L) CMA by whole cells in 6 h, at 37 °C and no requirement of external cofactor occurred with 97% conversion, 82% yield of 98% pure alcohol and a productivity of 34 g/g $_{wet\ cell\ weight}$. The results demonstrate the microbial system as a practical and efficient method for larger scale synthesis of CMO.

Appl Microbiol Biotechnol
DOI 10.1007/s00253-012-4273-z

BIOTECHNOLOGICALLY RELEVANT ENZYMES AND PROTEINS

Biochemical and structural characterization of recombinant short-chain NAD(H)-dependent dehydrogenase/reductase from *Sulfolobus acidocaldarius* highly enantioselective on diaryl diketone benzil

Angela Pennacchio · Vincenzo Sannino · Giosuè Sorrentino · Mosè Rossi · Carlo A. Raia · Luciana Esposito

Received: 16 May 2012 / Revised: 27 June 2012 / Accepted: 28 June 2012

Abstract The gene encoding a novel alcohol dehydrogenase that belongs to the short-chain dehydrogenases/reductases superfamily was identified in the aerobic thermoacidophilic crenarchaeon *Sulfolobus acidocaldarius* strain DSM 639. The *saadh2* gene was heterologously overexpressed in *Escherichia coli*, and the resulting protein (SaADH2) was purified to homogeneity and both biochemically and structurally characterized. The crystal structure of the SaADH2 NADH-bound form reveals that the enzyme is a tetramer consisting of identical 27,024-Da subunits, each composed of 255 amino acids. The enzyme has remarkable thermophilicity and thermal stability, displaying activity at temperatures up to 80 °C and a 30-min half-inactivation temperature of ~88 °C. It also shows good tolerance to common organic solvents and a strict requirement for NAD(H) as the coenzyme. SaADH2 displays a preference for the reduction of alicyclic, bicyclic and aromatic ketones and α-ketoesters, but is poorly active on aliphatic, cyclic and aromatic alcohols, showing no activity on aldehydes. Interestingly, the enzyme catalyses the asymmetric reduction of benzil to (*R*)-benzoin with both excellent conversion (98 %) and optical purity (98 %) by way of an efficient in situ NADH-recycling system involving a second thermophilic ADH. The crystal structure of the binary complex SaADH2–NADH, determined at 1.75 Å resolution, reveals details of the active site providing hints on the structural basis of the enzyme enantioselectivity.

Keywords Archaea · *Sulfolobus acidocaldarius* · Short-chain dehydrogenases/reductases · Crystal structure · Bioreduction · Benzil

Electronic supplementary material The online version of this article (doi:10.1007/s00253-012-4273-z) contains supplementary material, which is available to authorized users.

A. Pennacchio (✉) · V. Sannino · M. Rossi · C. A. Raia
Istituto di Biochimica delle Proteine, CNR,
Via P. Castellino 111,
80131 Naples, Italy
e-mail: a.pennacchio@ibp.cnr.it

G. Sorrentino · L. Esposito (✉)
Istituto di Biostrutture e Bioimmagini, CNR,
Via Mezzocannone 16,
80134 Naples, Italy
e-mail: luciana.esposito@unina.it

Published online: 18 July 2012

Introduction

Dehydrogenases/reductases are found throughout across a wide range of organisms where they are involved in a broad spectrum of metabolic functions (Jörnvall 2008), and a system of short-, medium- and long-chain dehydrogenase/reductases has been recently identified based on molecular size, sequence motifs, mechanistic features and structural comparisons (Kavanagh et al. 2008; Persson et al. 2009). Many studies have been addressed to characterize alcohol dehydrogenases (ADHs) from thermophiles and hyperthermophiles, mainly to understand their evolution and structure/function/stability relationship (Radianingtyas and Wright 2003) and develop their biotechnological potential in the synthesis of chiral alcohols (Jones and Beck 1976; Keinan et al. 1986; Hummel 1999; Kroutil et al. 2004; Müller et al. 2005; Goldberg et al. 2007). Recently, ADHs displaying distinct substrate specificity, good efficiency and high enantioselectivity have been described, such as the NADP-dependent (*R*)-specific ADH from *Lactobacillus brevis* (LB-RADH) (Schlieben et al. 2005), the NAD-

dependent ADH from *Leifsonia* sp. strain S749 (LSADH) (Inoue et al. 2006), and the NADP-dependent carbonyl reductase from *Candida parapsilosis* (Nie et al. 2007). These enzymes originate from mesophilic microorganisms and belong to the short-chain dehydrogenases/reductases (SDRs) superfamily (Kavanagh et al. 2008) which is characterized by ~250 residue subunits, a Gly-motif in the coenzyme-binding regions, and a catalytic tetrad formed by the highly conserved residues Asn, Ser, Tyr and Lys (Filling et al. 2002; Schlieben et al. 2005; Persson et al. 2009). Representative examples of ADHs from thermophilic microorganisms are medium-chain enzymes, including *Thermoanaerobacter brockii* ADH (Korkhin et al. 1998), the ADH from *Bacillus stearothermophilus* strain LLD-R (BsADH) (Ceccarelli et al. 2004) and two archaeal enzymes, the ADH from *Aeropyrum pernix* (Guy et al. 2003) and *Sulfolobus solfataricus* (Giordano et al. 2005; Friest et al. 2010). However, two archaeal short-chain ADHs have been identified in *Pyrococcus furiosus*, an NADP(H)-dependent SDR (van der Oost et al. 2001; Machielsen et al. 2008), and an NAD(H)-preferring ADH, that belongs to the aldo-keto reductase superfamily (Machielsen et al. 2006; Zhu et al. 2006, 2009). Furthermore, two short-chain NAD(H)-dependent ADHs, TtADH and SaADH, identified in *Thermus thermophilus* HB27 and *Sulfolobus acidocaldarius*, respectively, have been recently purified and characterized in our laboratory (Pennacchio et al. 2008, 2010a, 2010b, 2011).

With the aim to find novel dehydrogenase/reductases that are both stable and NAD^+ dependent, we focused our attention on the genomes of thermophilic organisms containing genes encoding putative ADHs belonging to the SDR superfamily and applied the criteria used for TtADH and SaADH to select enzymes with a high probability of being NAD^+ dependent (Pennacchio et al. 2008). An open reading frame coding for a protein belonging to the SDR superfamily with relatively high sequence identity to that of most representative ADHs (LB-RADH, LSADH, TtADH and SaADH) was found in the genome of *S. acidocaldarius*, an aerobic thermoacidophilic crenarcheon which grows optimally at 80 °C and pH 2 (Chen et al. 2005). The amino acid sequence revealed the presence of a glutamic acid residue at position 39. Noteworthy, an aspartate residue at the homologous position plays a critical role in determining the preference of SDRs for NAD(H) as shown for the LB-RADH mutant G37D (Schlieben et al. 2005) and by the evidence that the SDRs LSADH (Inoue et al. 2006), TtADH and SaADH (Pennacchio et al. 2008, 2010a, b) are strictly NAD(H)-dependent and have an aspartate residue at the same position within the sequence (Fig. 1). Due to Glu and Asp chemical similarity, the putative dehydrogenase/reductase identified in *S. acidocaldarius* (SaADH2) was expected to display a preference for NAD(H) rather than NADP(H). This preference as well as an intrinsic thermostability are the features that make an oxidoreductase more attractive from an application perspective (Kroutil et al. 2004; Zhu et al. 2006; Huisman et al. 2010).

This report describes cloning, heterologous expression and structural characterization of the *S. acidocaldarius saadh2* gene, which encodes the SDR SaADH2. The purified enzyme was characterized in terms of substrate specificity, kinetics and stability as well as enantioselectivity. SaADH2 was found to be highly efficient and enantioselective in reducing the diaryl diketone benzil to (*R*)-benzoin.

Materials and methods

Chemicals

$NAD(P)^+$ and NAD(P)H were obtained from AppliChem (Darmstadt, Germany). Alcohols, aldehydes, ketones and keto esters were obtained from Sigma-Aldrich. 1-Butyl-3-methylimidazolium tetrafluoroborate (BMIMBF4) was a kind gift from Professor S. Cacchi. Recombinant BsADH was prepared as previously described (Fiorentino et al. 1998). Other chemicals were A grade substances from Applichem. Solutions of NADH and NAD^+ were prepared as previously reported (Raia et al. 2001). All solutions were made up with MilliQ water.

Amplification and cloning of the *saadh2* gene

Chromosomal DNA was extracted by caesium chloride purification as described by Sambrook et al. (1989). Ethidium bromide and caesium chloride were removed by repeated extraction with isoamyl alcohol and extensive dialysis against 10 mM Tris–HCl pH 8.0 and 1 mM EDTA, respectively. DNA concentration was determined spectrophotometrically at 260 nm, and the molecular mass checked by electrophoresis on 0.8 % agarose gel in 90 mM Tris–borate pH 8.0 and 20 mM EDTA, using DNA molecular size markers. The *saadh2* gene was amplified by polymerase chain reaction (PCR) using oligonucleotide primers based on the *saadh2* sequence of *S. acidocaldarius* strain DSM 639 (GenBank accession no. YP_255871.1). The following oligonucleotides were used: (5′-TGCATAGTAGCATATG TCATATCAGAGTTTG-3′) as the forward primer (the *Nde I* restriction site is underlined in the sequence) and the oligonucleotide (5′-AGGAATTCACATTACAGTACAG TTAAACCACC-3′) as the reverse primer. This latter oligonucleotide introduces a translational stop following the last codon of the ADH gene, followed by an *EcoRI* restriction site, which is underlined in the sequence shown. The PCR product was digested with the appropriate restriction enzymes and cloned into the expression vector pET29a (Novagen, Madison, Wisconsin, USA) to create the

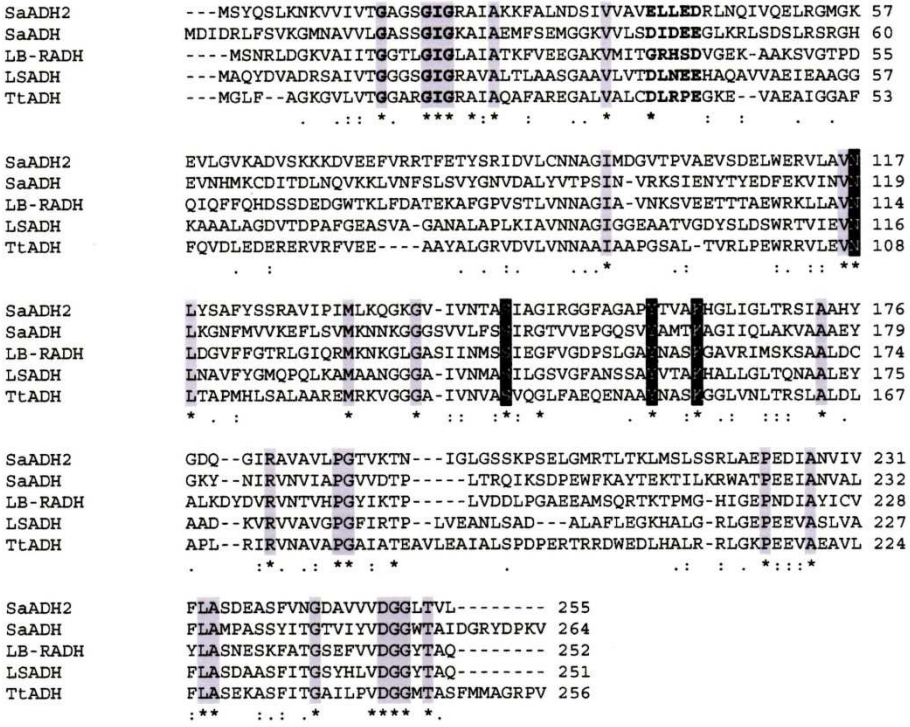

Fig. 1 Multiple-sequence alignment of the *S. acidocaldarius* ADH (SaADH2) and ADHs belonging to the SDR family, including *S. acidocaldarius* ADH (SaADH; NCBI accession no. YP_256716.1), *L. brevis* ADH (LB-RADH; PDB code 1ZK4), *Leifsonia* sp. strain S749 ADH (LSADH; NCBI accession no. BAD99642) and *T. thermophilus* ADH (TtADH; PDB code 2D1Y). The sequences were aligned using the ClustalW2 program. *Grey shading* indicates residues highly conserved in the SDR family. The four members of the catalytic tetrad are indicated by a *black background*. The following positions are indicated by *bold type*: the glycine-rich consensus sequence and the sequence motif Dhx[cp] that (in all SDRs) have a structural role in coenzyme binding (Kallberg et al. 2002). The *star* indicates the major determinant of the coenzyme specificity. The LB-RADH G37D mutant shows preference for NAD^+ over $NADP^+$ (Schlieben et al. 2005)

recombinant pET29a–saADH plasmid. The insert was sequenced in order to verify that mutations had not been introduced during PCR.

Expression and purification of recombinant SaADH2

Recombinant protein was expressed in *Escherichia coli* BL21(DE3) cells (Novagen) transformed with the corresponding expression vector. Cultures were grown at 37 °C in 2 L of LB medium containing 30 μg ml^{-1} kanamycin. When the A_{600} of the culture reached 1.4, protein expression was induced by addition of isopropyl β-D-1-thiogalactopyranoside to a concentration of 1.0 mM. The bacterial culture was incubated at 37 °C for a further 24 h. Cells were harvested by centrifugation, and the pellet stored at −20 °C until use. The cells obtained from 2 L of culture were suspended in 20 mM Tris–HCl buffer (pH 7.5) containing 0.1 mM phenylmethylsulfonyl fluoride (PMSF) and were lysed using a French pressure cell (Aminco Co., Silver Spring, MD) at 2,000 psi (1 psi=6.9 kPa). The lysate was centrifuged, and the supernatant incubated in the presence of DNase I (50 μg/ml of solution) and 5 mM $MgCl_2$ for 30 min at 37 °C, followed by protamine sulphate (1 mg/ml of solution) at 4 °C for 30 min. The nucleic acid fragments were removed by centrifugation, and the supernatant incubated at 70 °C for 15 min. The host protein precipitate was removed by centrifugation. The supernatant was dialysed overnight at 4 °C against 20 mM Tris–HCl, pH 8.4 (buffer

A) containing 1 mM PMSF. The dialysed solution was applied to a DEAE-Sepharose Fast Flow (1.6×12 cm) column equilibrated in buffer A at 120 ml h^{-1}. The active pool did not bind to the column matrix. The flowthrough fractions were combined and dialysed against buffer A, concentrated 5-fold with a 30,000 MWCO centrifugal filter device (Millipore), and applied to a Sephadex G-75 (1.6×30 cm) column equilibrated in buffer A containing 0.15 M NaCl. The active pool was dialysed against buffer A and concentrated to obtain 2.0 mg protein·ml^{-1} as described previously. SaADH2 was stored at −20 °C in buffer A containing 50 % glycerol, without loss of activity following several months of storage. SDS-PAGE was carried out according to the Laemmli method (1970). The subunit molecular mass was determined by electrospray ionization mass spectrometry (ESI-MS) with a QSTAR Elite instrument (Applied Biosystems, USA). The protein concentration was determined with a Bio-Rad protein assay kit using BSA as a standard.

Sucrose density gradient centrifugation

One hundred microlitres of a 1 mg/ml purified SaADH2 solution was layered on top of a 10-ml 5–20 % preformed sucrose gradient in 50 mM Tris–HCl, pH 8.4. The standards were also prepared by layering 100 µl of 1 mg/ml chymotripsinogen (25 kDa), BSA (67 kDa), *T. thermophilus* ADH (a 108-kDa tetramer) and *S. solfataricus* ADH (a 150-kDa tetramer) on top of another identical sucrose gradient. By using a Beckman SW 41 Ti rotor, the tubes containing the samples were spun at 37,000 rpm for 18 h at 4 °C in a Beckman LE-80 ultracentrifuge. Immediately after centrifugation, gradients were collected in 250-µl fractions and assayed for absorption at 280 nm to determine the position of the marker protein. The mass of SaADH2 was estimated from the position of the peak relative to those of the markers.

Enzyme assay

SaADH2 activity was assayed spectrophotometrically at 65 °C by measuring the change in absorbance of NADH at 340 nm using a Cary 1E spectrophotometer equipped with a Peltier effect-controlled temperature cuvette holder. The standard assay for the reduction reaction was performed by adding 5–25 µg of the enzyme to 1 ml of preheated assay mixture containing 20 mM ethyl 3-methyl-2-oxobutyrate (EMO) and 0.2 mM NADH in 37.5 mM sodium phosphate, pH 5.0. The standard assay for the oxidation reaction was performed using a mixture containing 18 mM cycloheptanol and 3 mM NAD^+ in 50 mM glycine/NaOH, pH 10.5. Screening of the substrates was performed using 1 ml of assay mixture containing either 10 mM alcohol and 3 mM NAD^+ in 50 mM glycine/NaOH, pH 10.5, or 10 mM carbonyl compound and 0.1 mM NADH in 37.5 mM sodium phosphate, pH 5.0. One unit of SaADH2 represented 1 µmol of NADH produced or utilized per minute at 65 °C, on the basis of an absorption coefficient of 6.22 mM^{-1} cm^{-1} for NADH at 340 nm.

Effect of pH on activity

The optimum pH value for the reduction and oxidation reactions was determined at 65 °C under the conditions used for EMO and cycloheptanol, respectively, except that different buffer were used. The concentration of each buffer solution was diluted to get the similar conductivity (~1.1 mS). The pH was controlled in each assay mixture at 65 °C.

Kinetics

The SaADH2 kinetic parameters were calculated from measurements determined in duplicate or triplicate and by analysing the kinetic results using the program GraFit (Leatherbarrow 2004). The turnover value (k_{cat}) for SaADH2 was calculated on the basis of a molecular mass of 27 kDa, assuming that the four subunits are catalytically active.

Thermophilicity and thermal stability

SaADH2 was assayed in a temperature range of 25–90 °C using standard assay conditions and 22 µg protein·ml^{-1} of assay mixture. The stability at various temperatures was studied by incubating 0.2 mg ml^{-1} protein samples in 50 mM Tris–HCl, pH 9.0, at temperatures between 25 and 95 °C for 30 min. Each sample was then centrifuged at 5 °C, and the residual activity assayed as described above.

The effect of chelating agents on enzyme stability was studied by measuring the activities before and after exhaustive dialysis of the enzyme against buffer A, containing 1 mM EDTA, and then against buffer A alone. An aliquot of the dialysed enzyme was then incubated at 70 °C in the absence and presence of 1 mM EDTA, and the activity assayed at different times.

Effects of compounds on enzyme activity

The effects of salts, metal ions and chelating agents on SaADH2 activity were investigated by assaying the enzyme in the presence of an appropriate amount of each compound in the standard assay mixture used for the oxidation reaction.

The effects of organic solvents were investigated by measuring the activity in enzyme samples (0.2 mg ml^{-1} in 100 mM sodium phosphate, pH 7.0) immediately after the addition of organic solvents at different concentrations and

after incubation for 6 and 24 h at 50 °C. The percentage activity for each sample was calculated by comparison with the value measured prior to incubation. The volume of the solution in a tightly capped test tube did not change during incubation.

Enantioselectivity

The enantioselectivity of SaADH2 was determined by examining the reduction of acetophenone, the bicyclic ketones benzyl and 2,2'-dichlorobenzil using an NADH regeneration system consisting of BsADH and a substrate alcohol (see below). The reaction mixture contained 2 mM NAD^+, 5 mM carbonyl compound, 4 to 18 %*v*/*v* alcohol, 250 μg SaADH2 and 50 μg of BsADH in 1 ml of 100 mM sodium phosphate, pH 7.0. The reactions were carried out at 50 °C for 24 h in a temperature-controlled water bath. Upon termination of the reaction, the reaction mixture was extracted twice with ethyl acetate. The percentage of conversion and enantiomeric purity of the product were determined on the basis of the peak areas of ketone substrates and alcohol products by HPLC, on a Chiralcel OD-H column (Daicel Chemical Industries, Ltd., Osaka, Japan). The absolute configuration of product alcohols was identified by comparing the chiral HPLC data with the standard samples. Products were analyzed with isocratic elution, under the following conditions: hexane/2-propanol (9:1) (mobile phase), flow rate of 1 ml min^{-1}, detection at 210 nm. Retention times were the following: 5.6, 11.9 and 16.7 for benzil, (*S*)- and (*R*)-benzoin, respectively; 6.98, 12.73 and 15.13, for 2,2'-dichlorobenzil, (*S*)- and (*R*)-1,2-bis(2-chlorophenyl)-2-hydroxyethanone, respectively and 5.27, 6.2 and 7.5 for acetophenone, (*R*)- and (*S*)-1-phenylethanol, respectively. The absolute stereochemistry of 1,2-bis(2-chlorophenyl)-2-hydroxyethanone enantiomers was assigned by analogy to the values of (*S*)- and (*R*)-benzoin.

Structural characterization

The purified protein was concentrated to 8–10 mg ml^{-1} in 20 mM Tris/HCl buffer at pH 8.4. The protein solution was added with NADH to obtain a 8.5-mg ml^{-1} protein solution containing 2.2 mM NADH in the above buffer. Crystallization was performed by hanging-drop vapour diffusion method at 296 K. The best crystals were grown by mixing 1 μl of protein solution with the same volume of a solution containing 2.0 M ammonium sulphate in 0.1 M HEPES buffer (pH 7.5). The crystals belong to P21 space group with unit cell parameters a=83.80 Å, b=60.48 Å, c=107.1 Å and β=99.8°. Crystals were transferred to a stabilizing solution containing 20 % glycerol as cryoprotectant and X-ray data were then collected in-house at 100 K using a Rigaku Micromax 007 HF generator producing Cu Kα radiation and equipped with a Saturn944 CCD detector. Intensity data up to 1.75 Å resolution were processed and scaled using program HKL2000 (HKL Research). Data collection statistics are shown in Table 1.

The crystal structure was solved by MR methods by using as a search model the coordinates of a putative glucose/ribitol dehydrogenase from *Clostridium thermocellum* (PDB code 2HQ1), which showed the best sequence alignment with SaADH2 (39 % sequence identity). Model building was first performed with ARP/WARP package using the warpNtrace automated procedure. Later model building and refinement was performed by the program CNS version 1.1. The final structure shows R and R-free factors of 16.8 and 19.1 %, respectively. Refinement statistics are summarized in Table 1. Fold similarities searches were performed with the DALI server (http://ekhidna.biocenter.helsinki.fi/dali_server).

Results

Expression and protein purification

Analysis of the *S. acidocaldarius* genome (Chen et al. 2005) for genes encoding short-chain ADHs resulted in identification of a putative oxidoreductase gene. The sequence of the 27,024-Da protein, named SaADH2, showed the highest level of identity to four typical SDRs, LB-RADH (29 % identity), LSADH (34 %), TtADH (35 %) and SaADH (30 %; Fig. 1). The *saadh2* gene was successfully expressed in *E. coli* cells, yielding an active enzyme accounting for

Table 1 Data collection and refinement statistics

Data collection	
Space group	P21
Cell dimensions (Å;°)	a=83.80, b=60.48, c=107.1; β=99.78
Resolution range (Å)	40.0–1.75 (1.81–1.75)
No. of unique reflections	106,431 (10,388)
Average redundancy	4.2 (2.8)
Completeness	99.7 (98.0)
$<I/\sigma(I)>$	19.8 (3.6)
Rmerge	0.065 (0.36)
Refinement	
No. of reflections used (with $\|F\| > 0$)	101,786
No. of reflections working/test set	96,639/5,147
Resolution range (Å)	40.0–1.75
R-factor/R-free (%)	16.8/19.1
No. of protein atoms	7,512
No. of water/glycerol/sulphate/NADH	687/5/1/4
RMS deviation on bond distances (Å)	0.007
RMS deviation on bond angles (°)	1.4

about 9 % of the total protein content of the cell extract (Supplementary material Table S1). Host protein precipitation at 70 °C was found to be the most effective purification step. An overall purification of 5.4-fold was achieved from crude-cell-free extracts with an overall yield of 48 %. SDS-PAGE of the purified protein showed a single band corresponding to a molecular mass of ~29 kDa (data not shown).

The quaternary structure of the enzyme was investigated by sucrose density gradient centrifugation. SaADH2 sedimented as one peak nearly overlapping that of TtADH (Supplementary Material Fig. S1). The plot of molecular mass of the markers vs fraction number (inset Fig. S1) allowed to determine an apparent molecular mass of 109± 10 kDa for SaADH2. The molecular mass of the subunit determined by ESI-MS analysis proved to be 27,024.0 Da (average mass), in agreement with the theoretical value of the sequence.

Optimal pH

The pH dependence of SaADH2 in the reduction and oxidation reaction was analysed (Fig. S2). The SaADH2 activity was found to be closely dependent on pH in the reduction reaction, displaying a peak of maximum activity at around pH 5.0. The oxidation reaction showed a less marked dependence on pH, displaying a peak with a maximum at around pH 10.0.

Thermophilicity and thermal stability

The effect of temperature on SaADH2 activity is shown in Fig. 2. The reaction rate increases up to 78 °C and then decreases rapidly due to thermal inactivation. This optimal temperature value is similar to that of TtADH (73 °C) and SaADH (75 °C) (Pennacchio et al. 2008, 2010a, b), and lower than that of *P. furiosus* aldo-keto reductase (100 °C) (Machielsen et al. 2006). The thermal stability of SaADH2 was determined by measuring the residual enzymatic activity after 30 min of incubation over a temperature range from 25 to 95 °C (Fig. 2). SaADH2 was shown to be quite stable up to a temperature of ~75 °C, above which its activity decreased abruptly, resulting in a $T_{1/2}$ value (the temperature of 50 % inactivation) of ~88 °C.

Coenzyme and substrate specificity

The enzyme showed no activity with NADP(H) and full activity with NAD(H).

The specificity of SaADH2 for various alcohols, aldehydes and ketones was examined (Table 2). The enzyme showed a poor activity on a discrete number of aliphatic linear and branched alcohols, such as 2-propyn-1-ol, 4-methyl-1-pentanol, the *S* enantiomers of 2-butanol and 2-pentanol as well as on aliphatic cyclic and bicyclic alcohols, except for isobomeol and cycloheptanol which rank first and second, respectively, among the tested alcohols. Benzyl alcohol and substituted benzyl alcohols were found to be poor substrates. Among the aromatic secondary alcohols tested SaADH2 showed a low activity on (*S*)-1-phenylethanol and no activity with the *R* enantiomer, whereas displayed similar poor activities towards the (*S*)- and (*R*)- forms of α-(trifluoromethyl)-benzyl alcohol, 1-(2-naphthyl)ethanol and methyl and ethyl mandelates. Moreover, the enzyme showed poor activity on (±)-1-phenyl-1-propanol and its *ortho*-chloro derivative, and *para*-halogenated 1-phenylethanols. However, SaADH2 showed a relatively high activity with 1-indanol and α-tetralol, but a poor activity on the β-hydroxy ester ethyl (*R*)-4-chloro-3-hydroxybutyrate.

The enzyme was not active on aliphatic and aromatic aldehydes, and on aliphatic linear, and branched ketones (data not shown). However, it was active on aliphatic cyclic and bicyclic ketones such as cyclohexanone, methyl-substituted cyclohexanones and decalone (Table 2). Two aryl diketones, 1-phenyl-1,2-propanedione and benzil were good substrates of SaADH2 which also showed a relatively high reduction rate with 2,2-dichloro- and 2,2,2-trifluoroacetophenone and penta-substituted fluoro-acetophenone (Table 2). The electronic factor accounts for the relatively high activity measured with the

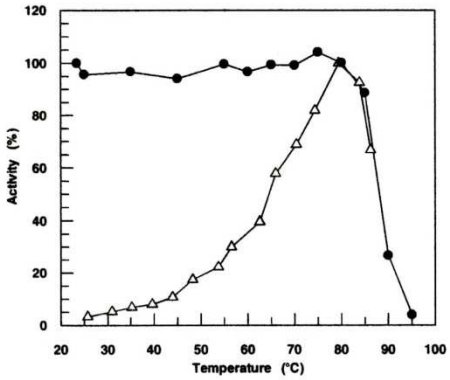

Fig. 2 Effect of temperature on activity and stability of SaADH2 monitored by dehydrogenase activity. The assays at the increasing temperature values (*triangles*) were carried out as described in Materials and methods, using cycloheptanol as the substrate. The thermal stability (*circles*) was studied by incubating 0.2 mg ml^{-1} protein samples in 50 mM Tris–HCl, pH 9.0 for 30 min at the indicated temperatures. Activity measurements were carried out under the conditions of the standard assay using cycloheptanol as the substrate. The assay temperature was 65 °C. The percentage of residual activity was obtained by the ratio to the activity without heating

Table 2 Substrate specificity of SaADH2 in the oxidation and reduction reactions[a]

Substrate	Relative activity (%)[b]	Substrate	Relative activity (%)[b]
Alcohols			
2-Propyn-1-ol	5	1-(2-Chlorophenyl)-1-propanol[c]	2
4-Methyl-1-pentanol	2	(±)-1-Indanol[d]	26
(*S*)-2-Butanol	3	(±)-α-Tetralol[c]	51
(*R*)-2-Butanol	0	(±)-1-(2-Naphthyl)ethanol	2
2,3-Butanediol	2	(*S*)-1-(2-Naphthyl)ethanol	3
(±)-2-Pentanol	2	(*R*)-1-(2-Naphthyl)ethanol	2
(*S*)-2-Pentanol	7	Benzoin	0
(*R*)-2-Pentanol	0	*trans*-1,3-Diphenyl-2-propen-1-ol	5
3-Pentanol	1	Ethyl (*R*)-4-chloro-3-hydroxybutyrate	2
2-Hexanol[c]	2	Methyl (*S*)-(−)-mandelate	4
2-Heptanol[c]	2	Methyl (*R*)-(+)-mandelate	3
6-Methyl-5-hepten-2-ol[c]	3	Ethyl (*S*)-(−)-mandelate	2
1-Octanol	1	Ethyl (*R*)-(+)-mandelate	2
Geraniol	2	Ketones[c]	
Cyclopentanol	2	Cyclohexanone	13
Cyclohexanol	6	2-Methylcyclohexanone	33
3-Methylcyclohexanol[c]	10	3-Methylcyclohexanone	60
Cycloheptanol	55	4-Methylcyclohexanone	41
Cyclohexylmethanol[c]	2	Cycloheptanone	0
2-Cyclohexylethanol	1	1-Decalone	85
Chrysanthemyl alcohol	1	(±)-Camphor	0
cis-Decahydro-1-naphthol	3	Acetophenone	0
Isoborneol	100	2,2-Dichloroacetophenone	30
Benzyl alcohol	7	2,2,2-Trifluoroacetophenone	35
2-Methoxybenzyl alcohol	5	2′,3′,4′,5′,6′-Pentafluoroacetophenone	45
3-Methoxybenzyl alcohol	6	1-Phenyl-1,2-propanedione	100
4-Methoxybenzyl alcohol	3	1-Indanone[d]	0
4-Bromobenzyl alcohol[c]	9	α-Tetralone	0
(*R*,*S*)-1-Phenylethanol[c]	2	Benzil	62
(*S*)-(−)-1-Phenylethanol	6	2,2′-Dichlorobenzil	0
(*R*)-(+)-1-Phenylethanol	0	Chalcone	0
(*R*,*S*)-α-(Trifluoromethyl)benzyl alcohol	2	Keto esters[c]	
(*S*)-α-(Trifluoromethyl)benzyl alcohol	2	Ethyl pyruvate	16
(*R*)-α-(Trifluoromethyl)benzyl alcohol	2	Ethyl 3-methyl-2-oxobutyrate	100
1-(4-Fluorophenyl)ethanol[c]	5	Ethyl 4-chloroacetoacetate	0
1-(4-Chlorophenyl)ethanol[c]	2	Methyl benzoylformate	8
(±)-1-Phenyl-1-propanol[c]	2	Methyl *o*-chlorobenzoylformate	5
trans-Cinnamyl alcohol[c]	2	Ethyl benzoylformate	23

[a] The activity was measured at 65 °C as described in Materials and methods. The concentration of each substrate was 5 mM

[b] The percent values refer to cycloheptanol for alcohols, benzil for ketones and to ethyl 3-methyl-2-oxobutyrate for keto esters

[c] The substrates were dissolved in 100 % 2-propanol

[d] The substrate was dissolved in 100 % acetonitrile

halogenated acetophenones, as compared to the apparent zero activity observed with acetophenone. The electron withdrawing character of fluorine (or chlorine) favours hydride transfer, inductively decreasing electron density at the acceptor carbon C1. On the other hand, the corresponding ketones of cycloheptanol and isoborneol, cycloheptanone and camphor did not show any apparent activity due to the deactivating effect exerted by the

electron donating alkyl groups on the acceptor carbon C1. SaADH2 was also active on aliphatic and aryl α-keto esters but not on β-ketoesters (Table 2).

Kinetic studies

The kinetic parameters of SaADH2 determined for the most active substrates are shown in Table 3. Based on the specificity constant (k_{cat}/K_m), isoborneol is the best substrate in the oxidation reaction; compared to the alicyclic cycloheptanol and aromatic bicyclic alcohols, it displays a higher affinity to the active site probably due to its alicyclic bridged structure. However, the enzyme shows a 6-fold greater preference for (*S*)- than (*R*)-1-indanol and a 23-fold greater preference for (*S*)- than (*R*)-α-tetralol. In the reduction reaction, 2,2-dichloroacetophenone was preferred 22-fold more than 2,2,2-trifluoroacetophenone and 2′,3′,4′,5′,6′-pentafluoroacetophenone, and 1.6- and 6-fold more than the two diketones, benzil and 1-phenyl-1,2-propanedione, respectively, due to its higher affinity. Ethyl 3-methyl-2-oxobutyrate shows the highest turnover among the carbonyl compound tested, although it binds to the catalytic site with relatively low affinity. Moreover, the specificity constant value is 6-fold higher for NADH than NAD^+.

Effects of various compounds

The effects of salts, ions and reagents on SaADH2 activity were studied by adding each compound to the standard assay mixture. The enzyme activity in the presence of 1 mM of the Li^+, Na^+, K^+, Ca^{++}, Mg^{++} and Mn^{++} chlorides was 115, 113, 102, 101, 101 and 110 %, respectively, and in the presence of 1 mM of the sulphate of heavy metal ions such as Fe^{++}, Co^{++}, Ni^{++}, Cu^{++} and Zn^{++} was 93, 108, 104, 102 and 107 %, correspondingly, when compared to the enzyme activity measured in the absence of additional metal ions. The presence of 5 % ionic liquid (BMIMBF4) inactivated by 50 % the enzyme presumably due to a competition of the BF_4^- ion with the coenzyme phosphate moiety for the anion-binding site of the enzyme.

The addition of 4 mM iodoacetate and 1 mM Hg^{++} had no significant influence on the enzyme activity, which resulted in 101 and 113 % of the control activity, respectively, suggesting that the only Cys residue per monomer, C90, has no functional role. Even the metal-chelating agents did not affect enzyme activity. The enzyme activity in the presence of either 1 mM *o*-phenanthroline, or 10 mM EDTA was 98 and 87 %, respectively, suggesting that either the protein does not require metals for its activity or the chelating molecule was not able to remove the metal under the assay conditions. Furthermore, the enzyme showed no loss in activity following exhaustive dialysis against EDTA. The EDTA-dialysed enzyme turned out to be quite stable at 70 °C for 5 h, both in the absence and the presence of EDTA (data not shown).

Stability in organic solvents

The effects of common organic solvents, such as acetonitrile, DMSO, 1,4-dioxane and ethyl acetate on SaADH2 were investigated at 50 °C, at two different time points and 18 % concentration (Fig. 3). SaADH2 activated after 6 and 24 h incubation in aqueous buffer (120 and 105 % the initial values, respectively), and inactivated by 15 and 30 % in the presence of 18 % acetonitrile following incubation for 6 and 24 h,

Table 3 Steady-state kinetic constants of SaADH2

Substrate	k_{cat} (s^{-1})	K_m (mM)	k_{cat}/K_m (s^{-1} mM^{-1})
Cyclohepthanol	7.0	5.1	1.37
Isoborneol	16.6	0.81	20.5
(±)-1-Indanol	6.2	8.7	0.71
(*R*)-Indanol	2.7	15.3	0.18
(*S*)-Indanol	10.6	10.0	1.06
α-Tetralol	9.6	8.5	1.13
(*R*)-α-Tetralol	1.15	9.2	0.13
(*S*)-α-Tetralol	6.0	2.0	3.0
NAD^+	19.3	0.18	107
Benzil	1.6	0.43	3.72
1-Phenyl-1,2-propanedione	5.3	5.0	1.06
2,2-Dichloroacetophenone	0.65	0.11	5.91
2,2,2-Trifluoroacetophenone	1.7	6.3	0.27
2′,3′,4′,5′,6′-Pentafluoroacetophenone	3.2	11.9	0.27
Ethyl 3-methyl-2-oxobutyrate	26	16.6	1.57
Ethyl benzoylformate	1.9	4.2	0.45
NADH	26.2	0.04	655

The activity was measured at 65 °C as described in Materials and methods. Kinetic constants for NAD^+ and NADH were determined with 15 mM isoborneol and 30 mM ethyl 3-methyl-2-oxobutyrate, respectively

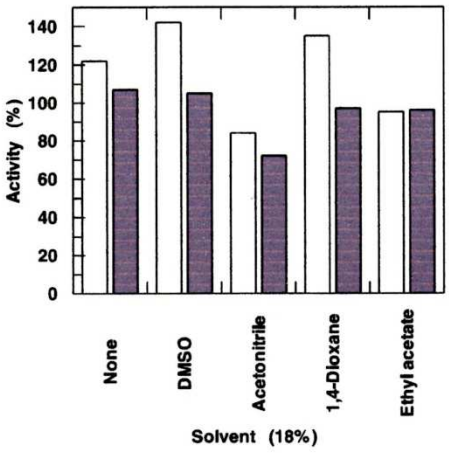

Fig. 3 Effects of various solvents on SaADH2. Samples of enzyme (0.20 mg/ml) were incubated at 50 °C in the absence and presence of the organic solvents at 18 % concentrations, and the assays were performed after 6 h (*white bars*) and 24 h (*grey bars*). The activity assays were performed at 50 °C as described in Materials and methods using cycloheptanol as the substrate. The data obtained in the absence and presence of organic solvents are expressed as percentage of activity relative to the value determined prior to incubation

respectively. A slightly reduced activity (~95 %) remained after 6 and 24 h incubation in aqueous solution containing 18 % ethyl acetate. Interestingly, significant increases in enzyme activity occurred after 6 h incubation in the presence of 18 % DMSO (>140%) and 1,4-dioxane (135 %). After 24 h incubation in the presence of these two solvents, the enzyme activity remained nearly unchanged with respect to the initial value.

Enantioselectivity

The enantioselectivity of SaADH2 was tested on benzil using an NADH recycling system consisting of thermophilic NAD(H)-dependent BsADH (Fig. 4). The latter enzyme is mainly active on aliphatic and aromatic primary and secondary alcohols and aldehydes (Guagliardi et al. 1996), but not on aliphatic and aromatic ketones, nor on the carbonyl substrates of SaADH2 and corresponding alcohols (data not shown). Since 2-propanol is not a substrate of SaADH2, it may be a suitable substrate for BsADH in NADH recycling, as well as being used as a co-solvent. Bioconversions were carried out for 24 h using 5 mM benzil as substrate and 2-propanol at three different concentrations. Sodium phosphate buffer, pH 7.0 and 50 °C was chosen as a compromise between cofactor stability and catalytic activity of the two ADHs at suboptimal pH (Pennacchio et al. 2008, 2011). Chiral HPLC analysis of the extracts obtained from the bioconversions showed that benzil

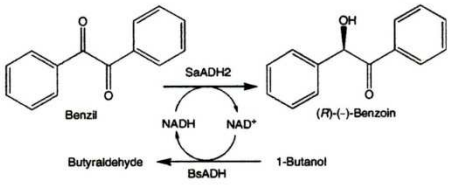

Fig. 4 Coenzyme recycling in the production of chiral diaryl alcohol with SaADH2 utilizing *B. stearothermophilus* ADH (BsADH) and 1-butanol

was reduced by the archaeal enzyme to the (*R*)-enantiomer of benzoin with a level of conversion of 35, 100 and 99 % and an enantiomeric excess (*ee*) of 85, 82 and 80 % using 4, 14 and 18 % (*v*/*v*) 2-propanol as ancillary substrate, respectively.

In addition to 2-propanol (k_{cat}/K_m=9 s^{-1} mM^{-1}), BsADH oxidizes other alcohols with even greater efficiency such as ethanol (k_{cat}/K_m=64 s^{-1} mM^{-1}), 1-propanol (286 s^{-1} mM^{-1}), 1-butanol (437 s^{-1} mM^{-1}), 1-pentanol (64 s^{-1} mM^{-1}) and 1-hexanol (64 s^{-1} mM^{-1}; Raia, unpublished data). We therefore tested these alcohols as alternative hydride source for NADH recycling and also to improve the solubility of the substrate in the aqueous phase. Moreover, these alcohols and the respective aldehydes are not substrates of SaADH2. Thus, only the cofactor is the co-substrate of SaADH2 and BsADH.

Figure 5 summarizes the results of the bioconversions carried out using different alcohol substrates at 18 % concentrations. As for the case of 2-propanol, benzil was reduced to the (*R*)-alcohol with excellent conversion (>99 %) but modest enantioselectivity using ethanol and 1-propanol. However, in the presence of 1-butanol, 1-pentanol and 1-hexanol excellent optical purity (98–99 % *ee*) and levels of conversion decreasing from 98 to 93 % and 66 %, respectively, were obtained. This suggests that ethanol and linear/branched propanol acted as good substrates and solvents for the bioconversion system, but negatively affected the prochiral selectivity of SaADH2 that was instead enhanced by longer chain-linear alcohols (four to six carbons). The decrease in conversion rate with 1-pentanol and 1-hexanol could be due to different effects: (1) substrate excess inhibition, (2) BsADH deactivation and (3) reduced substrate solubility.

The SaADH2 enantioselectivity was further examined with other aromatic ketones using the system BsADH/1-butanol. Table 4 shows that SaADH2 preferably reduced benzil to (*R*)-benzoin with an *ee* of 98 % and 98 % conversion after 24 h of reaction, and that the selectivity was reduced when 2-propanol instead of 1-butanol was used. However, 2,2′-dichlorobenzil was reduced to (*R*)-1,2-bis(2-chlorophenyl)-2-hydroxyethanone with lower conversion (33 %) and *ee* of 91 %, despite the apparent inactivity under different assay conditions (Table 2). Presumably, the presence of chlorine, a bulky

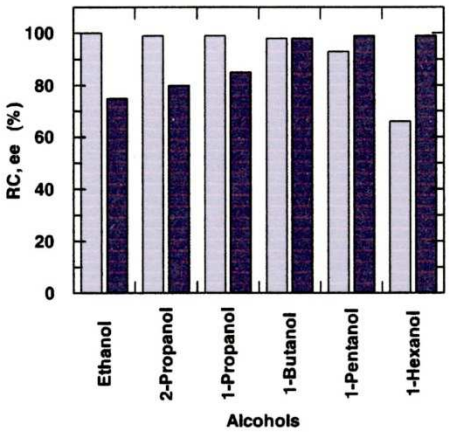

Fig. 5 Reduction of benzil catalyzed by SaADH2. Biotransformations were carried out at 50 °C with different alcohols at 18 % (*w/v*) concentrations. The reactions were stopped after 24 h by addition of ethyl acetate. The dried extracts were analysed by chiral HPLC to determine the relative conversion (*RC*, *grey bars*) and the enantiomeric excess (*ee*, *dark grey bars*). Error limit, 2 % of the stated values. The alcohols are plotted according to increasing log *P* (*P*=partition coefficient) values; from *left to right*: log *P*=−0.24, 0.07, 0.28, 0.8, 1.3 and 1.8. Log *P* values were from Laane et al. (1987)

atom with electron-withdrawing properties, disturbs the fitting of the diketone molecule in the substrate-binding pocket as well as the interactions that stabilize the transition state. Acetophenone was reduced to (*S*)-1-phenylethanol with a 4 % conversion and an *ee* of 92 %, while no conversion was observed for camphor, the ketone corresponding to the highly preferred alcohol isoborneol (Table 3). Kinetic tests showed that neither racemic benzoin nor (*R*)-benzoin was oxidized in the presence of NAD^+ as well as both were not reduced in the presence of NADH. Accordingly, the HPLC analysis indicated that no further reduction of benzoin occurred since no trace of hydrobenzoin could be found within the detection limits (data not shown).

Structural characterization

The determined crystal structure reveals a tetrameric organization similar to other members of the short-chain dehydrogenase/reductase (SDR) family. Although SaADH2 has low sequence similarities with other SDR proteins, it shares common structural features with them (Kallberg et al. 2002; Kavanagh et al 2008). The overall structure is typical of SDRs that is an α/β fold with characteristic Rossmann-fold motifs for the binding of the dinucleotide cofactor at the N-terminal region of the chain. Indeed, the structure confirmed that SaADH2 is a NAD-dependent enzyme with a cofactor-binding domain composed of a seven-stranded parallel sheet flanked by helices on each side.

Overall tertiary and quaternary structure

The structural comparison of SaADH2 with other SDRs demonstrated that SaADH2 exhibits a high degree of overall structural homology. Indeed, when aligning the monomeric structures by the DALI server the first 100 best superimpositions showed RMS deviations on C^{α} atoms ranging from 1.5 to 2.5 Å (with a minimum of 222/255 aligned residues). Some structural neighbours are superimposed onto a single chain of SaADH2 in Fig. S3. Major conformational differences are found on the molecular surface and at the terminal region of the polypeptide chain.

Analysis of the crystal packing (using PISA server:http://www.ebi.ac.uk/pdbe/prot_int/pistart.html), indicates that the tetramer is the biologically active form. The tetramer shows 222 point group symmetry and approximate dimensions of 80×70×55 Å (Fig. S4). The largest dimeric interface is the one involving AB or CD assemblies (~1,630 $Å^2$). The central elements in this interface are the long α6 helices (residues 156–179, Fig. S5) facing each other from adjacent subunits. Other segments involved in this interface are α4 and α5 helices (Fig. S5). The second large interface involving AC or BD assemblies (~1,250 $Å^2$) mainly comprises the C-terminal regions (residues 216–255) of the two subunits. The very terminal segment (residue 253–255) also

Table 4 Asymmetric reduction of carbonyl compounds by SaADH2

Substrate	Product	Conversion (%)	ee (%)	*R/S*
Benzil	Benzoin	98 (99)	98 (80)	*R*
2,2'-Dichlorobenzil	1,2-Bis(2-chlorophenyl)-2-hydroxyethanone	33	91	*R*
Acetophenone	1-Phenylethanol	4	92	*S*

Reactions were performed at 50 °C for 24 h as described in Materials and methods, using 18 % 1-butanol as ancillary substrate. Conversion and enantiomeric excess were determined by chiral HPLC analysis. Configuration of product alcohol was determined by comparing the retention time with that of standard samples as described in Material and methods. Values in parentheses refer to data obtained with 18 % 2-propanol as ancillary substrate

contributes to the smallest interface involving AD or BC assemblies (~445 Å^2); indeed, this segment forms inter-subunit interactions with residues belonging to 150–153 segment. It is worth noting that residues from the 209–218 region of the structure also mediate inter-subunit interactions in this interface.

Cofactor-binding site

A highly defined electron density was observed for the whole NAD(H) molecule thus allowing unambiguous identification of the positions of the cofactor in all the four molecules of the asymmetric unit (Fig. S6). The cofactor-binding site is located at the C-terminal end of the central parallel β-sheet.

The NAD(H) cofactor specificity is explained by the presence of Glu39 whose side chain oxygen atoms form hydrogen bonds with two oxygen atoms of the adenosine ribose of NAD(H).

The adenine ring of NAD binds in a hydrophobic pocket on the enzyme surface formed by the side chains of Val116, Leu40, Val66, Ala93 and Gly15. Hydrogen bonds are formed by N6 of adenine and the Asp65 side chain and by N1 and the peptide nitrogen of Val66. The segment 14-TGAGSGIG-21 corresponds to the glycine-rich sequence (TGxxx[AG]xG) present in NAD-binding site of "classical" SDR (Kavanagh et al 2008). This region interacts with the adenine ribose and the diphosphate moiety of NAD(H). The phosphate groups also interact with Thr193-Ala194. The 2′- and 3′-hydroxyls of the second ribose, attached to the nicotinamide ring, form a bifurcated hydrogen bond with Lys162. The 3′-hydroxyl is also hydrogen bonded to the active site Tyr158. The *syn* face of the nicotinamide ring displays vdW contacts with the hydrophobic side-chains of Ile20, Pro188 and Val191. The amide part of the nicotinamide portion is anchored to the protein by hydrogen bonds to Thr193 and Val191.

Substrate-binding site

The SaADH2 contains the conserved catalytic residues, Ser145, Tyr158 and Lys162, located in the active-site cleft with a spatial arrangement that is common to that found in other SDRs. SaADH2 also shows the conserved Asn residue (Asn117) which has been suggested as a key residue in a catalytic mechanism based on a tetrad instead of a triad (Filling et al. 2002). Its side chain atoms form hydrogen bonds with main chain atoms of Ile95.

In many SDRs the substrate-binding site is a deep cleft with a floor created by the NADH molecule and the right-side and left-side walls formed by the substrate-binding region (residues 193-221 in SaADH2 numbering) and the loop between β5 and β6 strands (Fig. 6).

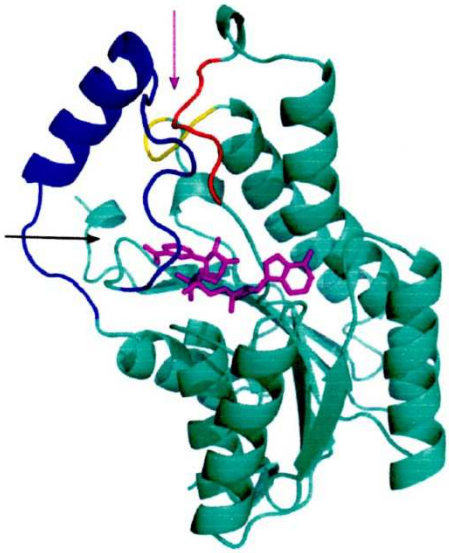

Fig. 6 Overall tertiary structure of one of the subunits of SaADH2. Bound NADH is shown in stick representation (*magenta*). The substrate-binding loop, the stretches 152–155 and 96–101 are highlighted in *blue*, *yellow* and *red*, respectively. The *arrows* point toward the substrate-binding cleft; the directions of approach are shown in *magenta* and *black* (see the text for details)

In three out of four subunits of the asymmetric unit there is a glycerol molecule occupying the position that is approximately suited for the binding of substrate. Indeed, the glycerol O2 and O3 oxygen atoms are hydrogen bonded to the oxygen of the NAD carboxamide and to the oxygen of Tyr158 side chain, respectively. Glycerol was used as cryoprotectant agent and therefore diffused through the water channels of the crystals up to the binding site. The lacking of glycerol binding in one of the subunits (chain B) of the tetramer is due to crystal packing which restricts the access to NADH in subunit B. Indeed, a nearby symmetric molecule (#B) inserts its 50–57 region into the substrate-binding region (residues 193–221) that covers the access to the NADH site. On the other hand, the other subunits of the tetramer do not show direct interactions with adjacent symmetric molecules through the substrate-binding loop.

It is worth noting that, despite the different crystal environments experienced by the four molecules of the asymmetric unit, the substrate-binding loops adopt similar conformations in the four subunits of the tetramer with pairwise RMSDs calculated on C^{α} atoms lying in the range 0.36–0.68 Å.

Furthermore, the structure of the loop (in blue in Fig. 6) represents the most significant difference between SaADH2 and the other SDR structures aligned with it. Indeed, as can be seen in Fig. S3, this loop (in cyan) is remarkably different from the other structures. In most of SDR structures the substrate-binding loop contains two segments of α-helix on opposite sides of the loop. In addition, part of the loop is often disordered thus revealing a considerable mobility. In SaADH2 the loop shows the following features: (1) it is well defined in the electron density; (2) it contains only one stretch of α-helix lacking the one usually present at the C-terminal end and (3) it partially obstructs the access to the substrate-binding cleft indicated with a magenta arrow in Fig. 6. Indeed, a detailed comparison with other SDR aligned structures reveals that three stretches (193–221, 96–101 and 152–155) of SaADH2 structure adopt a different conformation by getting closer to the NADH nicotinamide ring which becomes inaccessible to solvent/substrate from the top of the molecule (magenta arrow in Fig. 6). The cofactor ring is, however, still accessible to ligands through a side cavity (black arrow in Fig. 6) lined by residues Met96, Ser145, Ile146, Ala147, Phe153, Ala154, Tyr158, Gly189, Thr190, Ile195, Gly196, Leu197, Leu210 and Met214 (Fig. S7). The mouth of the cavity is composed of atoms from residues 190, 195–197, 210 and 214, as confirmed by CastP server (http://sts.bioengr.uic.edu/castp/calculation.php).

The benzil molecule is an interesting substrate of the enzyme that reduces it to *R*-benzoin in the presence of NADH with excellent conversion (>99 %). Several attempts were performed to crystallize a ternary complex of the enzyme bound to a benzil molecule, but they were unsuccessful. To envision how the enzyme binds the substrate and to probe the stereoselectivity of the hydride transfer we have manually modelled the benzil molecule in the active site.

The starting structure for the alpha-diketone modelling was the crystal structure present in the small molecule structure database (Allen 2002). This structure shows a conformation of the molecule with the two aromatic rings forming a dihedral angle of 114° around the diketo bond. A single benzil carbonyl group is bonded to two substituents: a smaller phenyl group and a larger carbophenyl group. In order to obtain a (*R*)-alcohol, the hydride has to be added to the *Si* face of the carbonyl ketone and this means that the smaller group is located opposite to the bulky carboxamide group of NADH.

A rigid docking of the benzil compound performed by the patchdock server identifies an orientation in the substrate site which is consistent with the stereoselectivity of the reduction reaction leading to (*R*)-benzoin. However, it has to be noted that in the best docked conformational ensemble of benzil, the carbonyl C atom, to be attacked by hydride, is still rather far from the hydrogen at the NADH C4 position (>5.5 Å). In addition, the oxygen atom of the carbonyl is not hydrogen bonded to the catalytic Tyr158 side chain (4.7 Å apart) as expected in case of a fully productive state of the enzyme–substrate complex.

Due to the steric hindrance of the benzil molecule an efficient accommodation in the substrate site would require a structural rearrangement of residues from the three segments (193–221, 96–101, and 152–155) which line the site and/or a change in the conformation of the diketone. A better packing of benzil in the site can be indeed obtained when the torsional angle around the carbon–carbon bond linking the two carbonyl moieties is reduced to values around 80–90°. Although approximate, this manually docked substrate position identifies a small pocket deep into the active site (Fig. 7) which is lined by Ser145, Leu146, Ala147, Tyr158, Phe153, Ala154 and Gly189. This pocket can accommodate the small phenyl group of benzil. Indeed, this phenyl ring would display mostly favourable contacts with Phe153, Ile146 and Ala147; the phenyl ring lies with its ring between two main-chain oxygen atoms from residues Phe153 and Glu189. On the other hand, the large carbophenyl group of benzil would point toward the channel opened to the solvent and lined by Met96, Thr190, Ile195, Gly196, Leu197, Leu210 and Met214. However, this bulky carbophenyl group would display steric clashes with the NADH and Thr190 when the intercarbonyl dihedral angle is about 80°. Some bad contacts can be relieved by a deviation of the phenyl group from the plane defined by the carbonyl moiety as well as by small rearrangements of the carboxyamide group of the nicotinamide ring (Fig. 7).

Conformational rearrangements with respect to the crystal structure of benzil can be accessible at a reasonable energetic cost since both experimental and theoretical studies have indicated a significant flexibility of the molecular structure even depending on the environmental conditions (Pawelka et al. 2001; Lopes et al. 2004).

The presence of the deep pocket in the active site, well suited for an aromatic ring, also explains why, in the case of acetophenone and its derivatives, the alcohol obtained by the reduction reaction is the (*S*)-enantiomer.

Discussion

In search of novel dehydrogenase/reductases that are both stable and NAD^+ dependent, a short-chain dehydrogenase (SDR) from *S. acidocaldarius* was identified and overexpressed. The enzyme was successfully purified and functionally/structurally characterized.

The enzyme is endowed with a high thermal stability showing a $T_{1/2}$ value of ~88 °C. It is rather stable in common organic solvents also exhibiting an increased activity in presence of DMSO and 1,4-dioxane. The activation

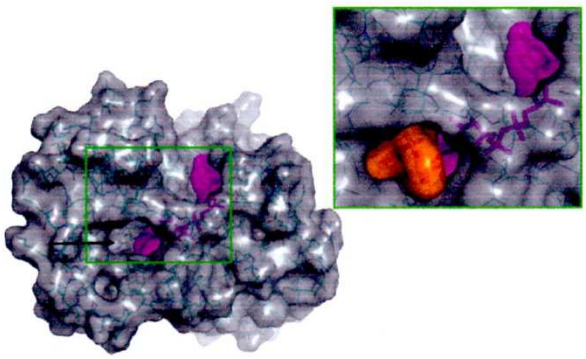

Fig. 7 Surface representation of a single chain of SaADH2. The NADH molecule is highlighted in *magenta*, as both stick and surface representations. The *black arrow* indicates the channel by which the nicotinamide ring is accessible. The *green box* is a close-up view of the binding site with the benzil molecule (in *orange*) manually docked into it. The figure was prepared using the PyMOL software (www.pymol.org)

of thermophilic enzymes by loosening of their rigid structure in the presence of protein perturbants is a well-documented phenomenon (Fontana et al. 1998; Liang et al. 2004). The two organic solvents discussed above (Fig. 3) may induce a conformational change in the protein molecule to a more relaxed and flexible state that is optimal for activity.

The analysis of the effects of ions reveals that SaADH2 does not require metals for its activity or structural stabilization; this is typical of non-metal SDR enzymes, although the well-known LB-RADH shows strong Mg^{++} dependency (Niefind et al. 2003).

Kinetic data show that SaADH2 is a strictly NAD(H)-dependent oxidoreductase with discrete substrate specificity. SaADH2 is more similar to the archaeal thermophilic TtADH and SaADH (Pennacchio et al. 2008; 2010a, b), than to the two representative SDR mesophilic ADHs, i.e. LB-RADH (Schlieben et al. 2005) and LSADH (Inoue et al. 2006), which are active on a variety of aliphatic as well as aromatic alcohols, ketones, diketones and keto esters. Indeed, the SaADH2 catalytic activity against various putative substrates was checked. Poor activity was observed on aliphatic linear and branched alcohols as well as on most of cyclic and bicyclic alcohols with the exception of cycloheptanol and isoborneol (Tables 2 and 3). Significant activity was found on alicyclic alcohols fused to an aromatic ring such as tetralol and indanol substrates. The kinetic data show that for most of chiral substrates SaADH2 is (*S*)-stereospecific and that the physiological direction of the catalytic reaction is reduction rather than oxidation (Table 3). The enzyme was active on aliphatic cyclic and bicyclic ketones such as cyclohexanone, methyl-substituted cyclohexanones and decalone (Table 2). It also showed a good reduction rate on halogenated acetophenone derivatives (Table 2) probably due to the electron withdrawing character of halogens which favours hydride transfer by decreasing electron density at the carbonyl carbon.

Interestingly, two aryl diketones, 1-phenyl-1,2-propanedione and benzil are good substrates of SaADH2. Although the natural substrates and function of SaADH2 remain unknown, the catalyzed reduction of the benzil α-diketone to (*R*)-benzoin with high yield and optical purity makes SaADH2 an interesting and biotechnologically relevant enzyme. Bioconversion studies have shown that SaADH2 can be conveniently coupled with a thermophilic bacillar ADH (BsADH) resulting in an efficient regeneration of NADH. Moreover, it is noteworthy that the SaADH2 enantioselectivity changes from moderate to excellent on going from ethanol to 1-hexanol (Fig. 5), i.e. that enantioselectivity increases as the hydrophobicity of the medium increases. The finely tuned solvent dependence of the prochiral selectivity shown by SaADH2 is remarkable and agrees with the general observation that enzyme selectivity (enantiomeric, prochiral and regiomeric) can change, or even reverse, from one solvent to another (Carrea and Riva 2000; Klibanov 2001). Overall, the solvent enantioselectivity study emphasizes the versatility and high efficiency of the BsADH/alcohol substrate system in recycling the reduced cofactor.

α-Hydroxy ketones are highly valuable building blocks for many applications for the fine chemistry sector as well as pharmaceuticals (Hoyos et al. 2010). It is noteworthy that optically pure (*R*)-benzoin is useful as urease inhibitor (Tanaka et al. 2004), and to prepare amino alcohols used as important chiral synthons (Aoyagi et al. 2000), or to synthesize different heterocycles (Wildemann et al. 2003). Many examples of stereoselective reduction of several benzils to the corresponding benzoins using whole microbial cells have been recently reviewed (Hoyos et al. 2010). The microorganisms *Bacillus cereus*, *Pichia glucozyma*, *Aspergillus oryzae*, *Fusarium roseum*, *Rhizopus oryzae* (at pH 4.5–5.0) and *B. cereus* Tm-r01 were reported to give (*S*)-benzoin while the microorganisms *R. oryzae* (at pH 6.8–8.5) and *Xanthomonas oryzae* were reported to transform benzil to (*R*)-benzoin with different yields and optical purity

(Hoyos et al. 2010 and references therein). However, recombinant *B. cereus* NADPH-dependent benzil reductase belonging to SDR superfamily which reduces benzil to 97 % optically pure (*S*)-benzoin in vitro was characterized (Maruyama et al. 2002). To our knowledge, this study represents the first biochemical characterization of an NAD(H)-dependent archaeal short-chain ADH reducing the diketone compound benzil to (*R*)-benzoin with high yield and optical purity.

The functional characterization of SaADH2 was complemented by the determination of the crystal structure of SaADH2–NADH complex at 1.75 Å resolution.

The determined crystal structure reveals a tetrameric organization that corroborates the results obtained by sucrose density gradient centrifugation. The structural comparison of SaADH2 with other SDRs demonstrated that SaADH2 exhibits a high degree of overall structural homology despite the low sequence similarities. The largest differences with other SDR structures are on the surface and at the C-terminal region of the polypeptide chain which contributes to the shaping of the active site.

The reductase activity measurements showed that the protein is not active with NADP(H), having a definite preference for NAD(H) cofactor. This cofactor specificity is consistent with structural results. Indeed, the side chain oxygen atoms of Glu39 form hydrogen bonds with two oxygen atoms of the adenosine ribose of NAD(H), thus hampering the binding of NADP(H). Therefore, the Glu residue plays the same role of the corresponding Asp residue found in many SDR structures.

The active site of SaADH2 structure contains the conserved catalytic residues, Ser145, Tyr158 and Lys162, which adopt position and orientation similar to those found in other SDRs (Schlieben et al. 2005). Besides the catalytic triad, also Asn117 is structurally conserved; this residue has been suggested to play a role in maintaining the active-site architecture and the building up of a proton-relay system in SDR structures (Filling et al. 2002; Schlieben et al. 2005).

A comparison with other structures of the SDR superfamily reveals that the substrate-binding loop (residues 193–221) is the most different region of the subunit structure (Fig. S3). This is not unexpected since the conformation, the length and the composition of the substrate-binding loop are rather variable in SDR proteins thus conferring different substrate specificity. Besides this loop, also the segment 152–155 shows a different conformation by getting closer to the NADH nicotinamide ring (Fig. 6). Interestingly, this region contains a Phe residue (Phe153) which points deep into the active site and can play a relevant role for substrate specificity. The region 96–101 is also closer to the nicotinamide ring thus contributing to the reduced accessibility of the site where hydride transfer has to occur (Fig. 6). As a consequence, the manual modelling of the bulky benzil molecule in the active site, guided by the position of glycerol molecule bound and by preliminary results of rigid docking, cannot avoid the presence of unfavourable contacts. However, it can be suggested that minor changes in the three segments of the protein structure discussed above as well as in the conformation of the benzil α-diketone may well accommodate this substrate in the site (Fig. 7).

The elucidation of the ternary complex structure will ultimately provide details of the conformational changes in both the enzyme and the substrate necessary to obtain a fully productive state which guarantees high enantioselectivity. Nonetheless, the modelling explains the enantioselectivity of the benzil reduction. The (*R*)-benzoin is obtained since the hydride transfer occurs on the *Si*-face of the carbonyl ketone attacked. There is a deep pocket in the active site which can accommodate the small phenyl group of benzil (Fig. 7). Indeed, this phenyl ring would display mostly favourable contacts with Phe153, Ile146 and Ala147. On the other hand, the large carbophenyl group of benzil would point toward the channel opened to the solvent (Fig. 7) and lined with hydrophobic residues (Fig. S7).

Furthermore, the modelling of benzil provides clues on the different stereoselective course of the reduction reaction for other substrates such as acetophenone and its derivatives. Indeed, the deep pocket in the active site, well suited for an aromatic ring, can efficiently accommodate the phenyl group of the acetophenone whereas the methyl group can point toward the channel; this orientation of the substrate in the site leads to the (*S*)-1-phenylethanol product (Table 4).

In conclusion, a new short-chain dehydrogenase from *S. acidocaldarius* was identified and overexpressed. The purified enzyme was shown to possess remarkable thermal resistance as well as high enantioselectivity on the aryl diketone benzil molecule. It shows many advantages with regard to its preparative application: ease of purification, preservability of the biocatalyst and absolute preference for NAD(H). It is also amenable for coupling with a thermophilic bacillar ADH (BsADH) in an efficient and sustainable bioconversion process based on coenzyme recycling, where both enzymes have only the coenzyme as co-substrate. The remarkable resistance of SaADH2 to organic solvents proves the sturdiness of this biocatalyst and suggests exploratory investigations on conversions of poorly water-soluble prochiral substrates. In addition, the availability of the crystal structure of the enzyme provides the opportunity to rationalize the stereospecificity and stereoselectivity of the enzyme and to design proper mutations to broaden the scope of possible substrates.

Acknowledgments This work was funded by FIRB (Fondo per gli Investimenti della Ricerca di Base) RBNE034XSW and by the ASI project MoMa n. 1/014/06/0.

Atomic coordinates as well as structure factors have been deposited within the PDB under the accession code 4FN4.

References

Allen FH (2002) The Cambridge Structural Database: a quarter of a million crystal structures and rising. Acta Crystallogr B 58:380–388

Aoyagi Y, Agata N, Shibata N, Horiguchi M, Williams RM (2000) Lipase TL-mediated kinetic resolution of benzoin: facile synthesis of (1R,2S)-erythro-2-amino-1,2-diphenylethanol. Tetrahedron Lett 41:10159–10162

Carrea G, Riva S (2000) Properties and synthetic applications of enzymes in organic solvents. Angew Chem Int Ed Engl 39:2226–2254

Ceccarelli C, Liang ZX, Strickler M, Prehna G, Goldstein BM, Klinman JP, Bahnson BJ (2004) Crystal structure and amide H/D exchange of binary complexes of alcohol dehydrogenase from *Bacillus stearothermophilus*: insight into thermostability and cofactor binding. Biochemistry 43:5266–5277

Chen L, Brügger K, Skovgaard M, Redder P, She Q, Torarinsson E, Greve B, Awayez M, Zibat A, Klenk HP, Garrett RA (2005) The genome of *Sulfolobus acidocaldarius*, a model organism of the *Crenarchaeota*. J Bacteriol 187:4992–4999

Filling C, Berndt KD, Benach J, Knapp S, Prozorovski T, Nordling E, Ladenstein R, Jörnvall H, Oppermann U (2002) Critical residues for structure and catalysis in short-chain dehydrogenases/reductases. J Biol Chem 277:25677–25684

Fiorentino G, Cannio R, Rossi M, Bartolucci S (1998) Decreasing the stability and changing the substrate specificity of the *Bacillus stearothermophilus* alcohol dehydrogenase by single amino acid replacements. Protein Eng 11:925–930

Fontana A, De Filippis V, Polverino de Laureto P, Scaramella E, Zambonin M (1998) Rigidity of thermophilic enzymes. In: Ballestreros A, Plou FJ, Iborra JL, Halling PJ (eds) Stability and stabilization in biocatalysis, vol 15. Elsevier Sciences, Amsterdam, pp 277–294

Friest JA, Maezato Y, Broussy S, Blum P, Berkowitz DB (2010) Use of a robust dehydrogenase from an archael hyperthermophile in asymmetric catalysis–dynamic reductive kinetic resolution entry into (S)-profens. J Am Chem Soc 132:5930–5931

Giordano A, Febbraio F, Russo C, Rossi M, Raia CA (2005) Evidence for co-operativity in coenzyme binding to tetrameric *Sulfolobus solfataricus* alcohol dehydrogenase and its structural basis: fluorescence, kinetic and structural studies of the wild-type enzyme and non-co-operative N249Y mutant. Biochem J 388:657–667

Goldberg K, Schroer K, Lütz S, Liese A (2007) Biocatalytic ketone reduction—a powerful tool for the production of chiral alcohols—part I: processes with isolated enzymes. Appl Microbiol Biotechnol 76:237–248

Guagliardi A, Martino M, Iaccarino I, De Rosa M, Rossi M, Bartolucci S (1996) Purification and characterization of the alcohol dehydrogenase from a novel strain of *Bacillus stearothermophilus* growing at 70 °C. Int J Biochem Cell Biol 28:239–246

Guy JE, Isupov MN, Littlechild JA (2003) The structure of an alcohol dehydrogenase from the hyperthermophilic archaeon *Aeropyrum pernix*. J Mol Biol 331:1041–1051

Hoyos P, Sinisterra JV, Molinari F, Alcántara AR, Domínguez de María P (2010) Biocatalytic strategies for the asymmetric synthesis of alpha-hydroxy ketones. Acc Chem Res 43:288–299

Huisman GW, Liang J, Krebber A (2010) Practical chiral alcohol manufacture using ketoreductases. Curr Opin Chem Biol 14:122–129

Hummel W (1999) Large-scale applications of NAD(P)-dependent oxidoreductases: recent developments. Trends Biotechnol 17:487–492

Inoue K, Makino Y, Dairi T, Itoh N (2006) Gene cloning and expression of *Leifsonia* alcohol dehydrogenase (LSADH) involved in asymmetric hydrogen–transfer bioreduction to produce (*R*)-form chiral alcohols. Biosci Biotechnol Biochem 70:418–426

Jones JB, Beck JF (1976) Applications of biochemical systems in organic chemistry. In: Jones JB, Sih CJ, Perlman D (eds) Techniques of chemistry series, part I, vol 10. Wiley, New York, pp 248–401

Jörnvall H (2008) Medium- and short-chain dehydrogenase/reductase gene and protein families: MDR and SDR gene and protein superfamilies. Cell Mol Life Sci 65:3873–3878

Kallberg Y, Oppermann U, Jörnvall H, Persson B (2002) Short-chain dehydrogenases/reductases (SDRs). Eur J Biochem 269:4409–4417

Kavanagh KL, Jörnvall H, Persson B, Oppermann U (2008) The SDR superfamily: functional and structural diversity within a family of metabolic and regulatory enzymes. Cell Mol Life Sci 65:3895–3906

Keinan E, Hafeli EK, Seth KK, Lamed R (1986) Thermostable enzymes in organic synthesis. 2. Asymmetric reduction of ketones with alcohol dehydrogenase from *Thermoanaerobium brockii*. J Am Chem Soc 108:162–169

Klibanov AM (2001) Improving enzymes by using them in organic solvents. Nature 409(6817):241–246

Korkhin Y, Kalb(Gilboa) AJ, Peretz M, Bogin O, Burstein Y, Frolow F (1998) NADP-dependent bacterial alcohol dehydrogenases: crystal structure, cofactor-binding and cofactor specificity of the ADHs of *Clostridium beijerinckii* and *Thermoanaerobacter brockii*. J Mol Biol 278:967–981

Kroutil W, Mang H, Edegger K, Faber K (2004) Recent advances in the biocatalytic reduction of ketones and oxidation of sec-alcohols. Curr Opin Chem Biol 8:120–126

Laane C, Boeren S, Hilhorst R, Veeger C (1987) Optimization of biocatalysis in organic media. In: Laane C, Tramper J, Lilly MD (eds) Biocatalysis in organic media, vol 29. Elsevier, Amsterdam, pp 65–84

Laemmli UK (1970) Cleavage of structural proteins during the assembly of the head of bacteriophage T4. Nature 227:680–685

Leatherbarrow RJ (2004) *GraFit* version 5.0.11. Erithacus Software Ltd, Horley

Liang ZX, Lee T, Resing KA, Ahn NG, Klinman JP (2004) Thermal-activated protein mobility and its correlation with catalysis in thermophilic alcohol dehydrogenase. Proc Natl Acad Sci U S A 101:9556–9561

Lopes S, Gòmez-Zavaglia A, Lapinski L, Chattopadhyay N, Fausto R (2004) Matrix-isolation FTIR spectroscopy of benzil: probing the flexibility of the C–C torsional coordinate. J Phys Chem A 108:8256–8263

Machielsen R, Uria AR, Kengen SW, van der Oost J (2006) Production and characterization of a thermostable alcohol dehydrogenase that belongs to the aldo-keto reductase superfamily. Appl Environ Microbiol 72:233–238

Machielsen R, Leferink NG, Hendriks A, Brouns SJ, Hennemann HG, Daussmann T, van der Oost J (2008) Laboratory evolution of *Pyrococcus furiosus* alcohol dehydrogenase to improve the production of (2S,5S)-hexanediol at moderate temperatures. Extremophiles 12:587–594

Maruyama R, Nishizawa M, Itoi Y, Ito S, Inoue M (2002) The enzymes with benzil reductase activity conserved from bacteria to mammals. J Biotechnol 94:157–169

Müller M, Wolberg M, Schubert T, Hummel W (2005) Enzyme-catalyzed regio- and enantioselective ketone reductions. Adv Biochem Eng Biotechnol 92:261–287

Nie Y, Xu Y, Mu XQ, Wang HY, Yang M, Xiao R (2007) Purification, characterization, gene cloning, and expression of a novel alcohol dehydrogenase with anti-prelog stereospecificity from *Candida parapsilosis*. Appl Environ Microbiol 73:3759–3764

Niefind K, Müller J, Riebel B, Hummel W, Schomburg D (2003) The crystal structure of R-specific alcohol dehydrogenase from *Lactobacillus brevis* suggests the structural basis of its metal dependency. J Mol Biol 327:317–328

Pawelka Z, Koll A, Zeegers-Huyskens Th (2001) Solvent effect on conformation of benzil. J Mol Struct 597:57–66

Pennacchio A, Pucci B, Secundo F, La Cara F, Rossi M, Raia CA (2008) Purification and characterization of a novel recombinant highly enantioselective, short-chain NAD(H)-dependent alcohol dehydrogenase from *Thermus thermophilus*. Appl Environ Microbiol 74:3949–3958

Pennacchio A, Giordano A, Pucci B, Rossi M, Raia CA (2010a) Biochemical characterization of a recombinant short-chain NAD (H)-dependent dehydrogenase/reductase from *Sulfolobus acidocaldarius*. Extremophiles 14:193–204

Pennacchio A, Giordano A, Esposito L, Langella E, Rossi M, Raia CA (2010b) Insight into the stereospecificity of short-chain *Thermus thermophilus* alcohol dehydrogenase showing pro-S hydride transfer and prelog enantioselectivity. Protein Pept Lett 17:437–443

Pennacchio A, Giordano A, Rossi M, Raia CA (2011) Asymmetric reduction of α-keto esters with *Thermus thermophilus* NADH-dependent carbonyl reductase using glucose dehydrogenase and alcohol dehydrogenase for cofactor regeneration. Eur J Org Chem 23:4361–4366

Persson B, Kallberg Y, Bray JE, Bruford E, Dellaporta SL, Favia AD, Duarte RG, Jörnvall H, Kavanagh KL, Kedishvili N, Kisiela M, Maser E, Mindnich R, Orchard S, Penning TM, Thornton JM, Adamski J, Oppermann U (2009) The SDR (short-chain dehydrogenase/reductase and related enzymes) nomenclature initiative. Chem Biol Interact 178:94–98

Radianingtyas H, Wright PC (2003) Alcohol dehydrogenases from thermophilic and hyperthermophilic archaea and bacteria. FEMS Microbiol Rev 27:593–616

Raia CA, Giordano A, Rossi M (2001) Alcohol dehydrogenase from *Sulfolobus solfataricus*. Methods Enzymol 331:176–195

Sambrook J, Fritsch EF, Maniatis T (1989) Molecular cloning: a laboratory manual, 2nd edn. Cold Spring Harbor Laboratory, New York

Schlieben NH, Niefind K, Muller J, Riebel B, Hummel W, Schomburg D (2005) Atomic resolution structures of R-specific alcohol dehydrogenase from *Lactobacillus brevis* provide the structural bases of its substrate and cosubstrate specificity. J Mol Biol 349:801–813

Tanaka T, Kawase M, Tani S (2004) Alpha-hydroxyketones as inhibitors of urease. Bioorg Med Chem 12:501–505

van der Oost J, Voorhorst WG, Kengen SW, Geerling AC, Wittenhorst V, Gueguen Y, de Vos WM (2001) Genetic and biochemical characterization of a short-chain alcohol dehydrogenase from the hyperthermophilic archaeon *Pyrococcus furiosus*. Eur J Biochem 268:3062–3068

Wildemann H, Dünkelmann P, Müller M, Schmidt B (2003) A short olefin metathesis-based route to enantiomerically pure arylated dihydropyrans and alpha, beta-unsaturated delta-valero lactones. J Org Chem 68:799–804

Zhu D, Malik HT, Hua L (2006) Asymmetric ketone reduction by a hyperthermophilic alcohol dehydrogenase. The substrate specificity, enantioselectivity and tolerance of organic solvents. Tetrahedron-Asymmetry 17:3010–3014

Zhu D, Hyatt BA, Hua L (2009) Enzymatic hydrogen transfer reduction of α-chloro aromatic ketones catalyzed by a hyperthermophilic alcohol dehydrogenase. J Mol Catal B: Enzym 56:272–276

DOI: 10.1002/ejoc.201100107

Asymmetric Reduction of α-Keto Esters with *Thermus thermophilus* NADH-Dependent Carbonyl Reductase using Glucose Dehydrogenase and Alcohol Dehydrogenase for Cofactor Regeneration

Angela Pennacchio,[a] Assunta Giordano,[b] Mosè Rossi,[a] and Carlo A. Raia*[a]

Keywords: Asymmetric catalysis / Enzymes / Biotransformations / Ketones / Reduction

The enantioselective synthesis of methyl (*R*)-mandelate and methyl (*R*)-*o*-chloromandelate was investigated using an NADH-dependent carbonyl reductase from *Thermus thermophilus* (TtADH) and, separately, archaeal glucose dehydrogenase and *Bacillus stearothermophilus* alcohol dehydrogenase (BsADH) for NADH regeneration. Optimal reaction times and substrate concentrations in the absence and presence of organic solvents were determined. The enantiofacial selectivity of TtADH was shown to be inversely proportional to the hydrophobicity of the short-chain linear alcohols employed as co-substrates of the bacillar ADH. The bioreduction of methyl benzoylformate yielded the (*R*)-alcohol with a 77% yield (*ee* = 96%) using glucose dehydrogenase and glucose, and 81% yield (*ee* = 94%) applying BsADH and ethanol. The bioreduction of methyl *o*-chlorobenzoylformate yielded the halogenated (*R*)-alcohol with 95% and 92% *ee*, and 62% and 78% yield using glucose dehydrogenase and BsADH, respectively.

Introduction

Optically active hydroxy esters provide very versatile building blocks widely used as chiral intermediates for the synthesis of pharmaceuticals and other fine chemicals.[1] Among them, methyl (*R*)-mandelate (**1a**) and methyl (*R*)-*o*-chloromandelate (**2a**) are valuable synthons used in organic synthesis (Scheme 1). *O*-protected **1a** is used as an intermediate for the synthesis of pharmaceuticals[2] and **2a** is an intermediate for the *anti*-thrombotic agent, (*S*)-clopidogrel, commercialized under the brand name Plavix (clopidogrel sulfate).[3] Compound **1a** has been obtained by reduction of methyl benzoylformate (**1**) using resting cells of *Rhodotorula* sp. AS2.2241[4a] and more recently on lab-scale using *Saccharomyces cerevisiae* AS2.1392 whole cells with 85.8% isolated yield and *ee* = 96.6%.[4b] However, several methods for the preparation of the key enantiomer for clopidogrel, **2a** have been developed, including (i) preparation of the corresponding (*R*)-carboxylic acid through fractional crystallization after diastereomeric salt formation of (*R*,*S*)-*o*-chloromandelic acid,[3] (ii) asymmetric reduction of the corresponding α-keto acid,[5] (iii) asymmetric hydrocyanation of the corresponding *o*-chlorobenzaldehyde using (*R*)-selective oxynitrilase,[6] and (iv) direct reduction of methyl *o*-chlorobenzoylformate (**2**) by Ru-catalyzed asymmetric hydrogenation.[7] A process has also been reported for resolution of racemic methyl *o*-chloromandelate using *Candida antarctica* lipase A-mediated transesterification which produces **2a** in 99% *ee* and 41% yield.[8] More recently, Ema and co-workers[9] reported the efficient and environmentally friendly chemoenzymatic synthesis of **2a** from **2** in >99% *ee* on a 15-g scale using recombinant *Escherichia coli* overproducing a carbonyl reductase from baker's yeast. Moreover, Jeong and co-workers have also reported the reduction of **2a** from **2** in 96.1% *ee* and 100% conversion using whole cells of baker's yeast.[10]

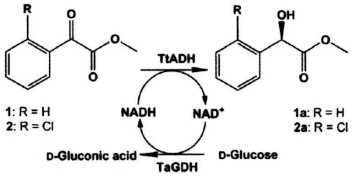

Scheme 1. Reduction of methyl benzoylformate (**1**) and methyl *o*-chlorobenzoylformate (**2**) catalyzed by *T. thermophilus* ADH (TtADH) coupled with *T. acidophilum* glucose dehydrogenase (TaGDH) for NADH regeneration.

A number of carbonyl reductases from different sources have been described which catalyze the direct asymmetric reduction of **1** to **1a** with high yields and high *ee*, such as NADH-dependent alcohol dehydrogenase (ADH) from *Pyrococcus furiosus*,[11] NADH-dependent α-keto ester reductase from the actinomycete *Streptomices coelicolor* A3(2),[12] and NADH-dependent ADH from *Leifsonia* sp. S749.[13]

[a] Istituto di Biochimica delle Proteine, CNR,
Via P. Castellino 111, 80131 Naples, Italy
Fax: +39-081-613-2277
E-mail: ca.raia@ibp.cnr.it
[b] Istituto di Chimica Biomolecolare, CNR,
Via Campi Flegrei 34, 80078 Pozzuoli, Naples, Italy
Supporting information for this article is available on the WWW under http://dx.doi.org/10.1002/ejoc.201100107.

More recently, an NADH-dependent, highly enantioselective ADH (TtADH), identified from the thermophilic, halotolerant gram-negative eubacterium *Thermus thermophilus* HB27, has been purified and characterized in our laboratory.[14] The thermophilic enzyme catalyses the reduction of α-methyl and α-ethyl benzoylformate to methyl (*R*)-mandelate (*ee* = 91%) and ethyl (*R*)-mandelate (*ee* = 95%), respectively, by way of an in situ NADH-recycling system involving 2-propanol and *Bacillus stearothermophilus* ADH (BsADH).[14]

This paper reports the enzymatic synthesis of **1a** and **2a** by TtADH and the evaluation of glucose dehydrogenase as well as BsADH for achieving cofactor regeneration. The work describes the determination of the optimal reaction time and substrate concentration in the absence and presence of organic solvents and the choice of the alcohol which is most suitable co-substrate for the TtADH/BsADH system.

Results and Discussion

Process Development using Glucose Dehydrogenase for Cofactor Regeneration

Previous studies showed that the *E. coli* expression system developed for TtADH is quite efficient, producing ca. 30 mg protein per litre of culture, and that this enzyme shows potential for applications involving bioconversions of substituted acetophenones and aromatic α-keto esters such as **1**.[14] Kinetic studies showed that this latter compound was a better substrate when halogenated at the *ortho* position of the benzene ring. The k_{cat}, K_m and k_{cat}/K_m values determined for the reduction of **1** were $38.1 \pm 3.7\ s^{-1}$, 2.7 ± 0.6 mM, and $14.1\ s^{-1}\ mM^{-1}$, respectively and those for **2** were $7.1 \pm 0.2\ s^{-1}$, 0.32 ± 0.1 mM, and $22.2\ s^{-1}\ mM^{-1}$, respectively. This indicates that the electronic properties of the halogen rather than its steric effects determine the efficiency of the reaction.

Glucose dehydrogenase from *Thermoplasma acidophilum* (TaGDH), a thermophilic and stable enzyme possessing dual cofactor-specificity,[15] was chosen for the in situ NADH-regeneration system utilizing glucose as the hydride source (Scheme 1). Experimental conditions including buffer, pH, temperature, reaction time and organic solvent were considered in order to optimise bioconversion of **1**. The optimal pH for the reduction reaction catalyzed by TtADH is approximately 6.0[14] and that for glucose oxidation catalysed by TaGDH is 7.0.[16] Due to the instability of the reduced cofactor under acidic conditions, neutral pH was chosen as a compromise taking into account cofactor stability and TtADH activity at suboptimal pHs. Nevertheless, TaGDH retains full catalytic activity after 9 h at 55 °C,[17] while TtADH is highly efficient and selective at 50 °C.[14] To establish the optimal reaction time the conversion of **1** was carried out at 50 °C, at low substrate concentration (1 $g\,L^{-1}$, 6.2 mM) in aqueous solution and by letting the reactions proceed for 1, 3, 6 and 24 h. The conversion of **1** proceeded in 99% after 6 h, affording the (*R*)-α-hydroxy ester **1a** with 95% *ee*; the yield and *ee* obtained using BsADH were 99% and 91%, respectively (see the Supporting Information).[14] The degree of conversion and *ee* of the biotransformation was unchanged at reaction times as long as 24 h, as already observed for the BsADH/2-propanol system.[14] The high conversion is noteworthy, considering that TaGDH has a marked preference for NADP(H) over NAD(H).[15]

Bioconversions were then carried out using increasingly higher concentrations of **1** for a reaction time of 24 h. The conversion proceeded with >99% at 1 to 10 $g\,L^{-1}$ **1**, but decreased to ca. 10% and ca. 1% yields at 30 and 50 $g\,L^{-1}$ substrate, respectively. However, the *ee* of **1a** was 95% over the whole range of concentrations for **1** that were examined (see Supporting Information for more details). The decrease in conversion could be due to a decrease in solubility of the substrate, enzyme inactivation by substrate or product, or both factors. The next step was to develop a suitable solvent system to improve bioconversions at higher substrate concentrations. TtADH possesses a remarkable tolerance to common organic solvents. Indeed, it even showed a significant increase in activity in the presence of various organic solvents, reaching 150% and 180% of the initial value with 5% v/v acetonitrile and 10% v/v 2-propanol, respectively, after 24 h of incubation at 50 °C and 182% with 10% v/v hexane after 65 h at 25 °C.[14] The stability of the archaeabacterial glucose dehydrogenase in the presence of organic solvents was investigated to evaluate its tolerance to organic solvents (see the Supporting Information). TaGDH was inactivated by 34% and 28% following 24 h incubation at 50 °C, in the absence and presence of 20% v/v hexane, respectively. Moreover, the enzyme was inactivated by over 50% in the presence of 5% v/v and 10% v/v DMSO, 10% v/v acetonitrile or 10% v/v methanol. However, incubation in the presence of 5% and 10% v/v 2-propanol, 5% v/v methanol or 5% v/v acetonitrile resulted in activities that were similar to those measured in aqueous buffer after 6 h and 24 h. Therefore, bioconversions were carried out at different concentrations of **1** in the presence of acetonitrile or hexane at concentrations of 5% and 20% v/v, respectively; these concentrations fulfilled the majority of the criteria for a solvent system in which both enzymes retained activity. As shown in the Supporting Information, the presence of water-miscible or immiscible organic solvents did not improve conversion at concentrations of **1** higher than 10 $g\,L^{-1}$, since the profiles of the conversion with acetonitrile and hexane were similar to those obtained in aqueous buffer (Figure S2). Nevertheless, the good levels of conversion obtained between 1 and 10 $g\,L^{-1}$substrate was accompanied by a slight decrease in enantioselectivity in the presence of acetonitrile (*ee* = 85%–89%) as well as in the presence of hexane (*ee* = 92–93%) compared to the 95% *ee* obtained in aqueous buffer. The decrease in enantioselectivity could be related to the solvent-mediated enhancement of catalysis as a result of increased flexibility of the enzyme active site.[14] However, an increase in *ee* from 37% in phosphate buffer up to 43% in the presence of ace-

tonitrile was observed for the 2-butanone to (*R*)-2-butanol reduction catalyzed by *L. brevis* ADH.[18]

In light of our findings related to enantioselectivity and concentration, optimum conditions for the bioconversion of **1** as well as **2** were determined to involve a temperature of 50 °C, substrate concentrations up to 10 gL^{-1}, in the presence of 1 mM NAD^+ in pH 7.0 aqueous buffer. Table 1 summarizes the results of a study carried out for the two α-hydroxy esters. The bioreduction of 100 mg of **1** at 50 °C for 24 h gave 74 mg of **1a** with *ee* = 95% (Table 1, Entry 1). The same reaction carried out in 6 h with a 5-fold lower substrate and 2-fold higher TtADH concentrations yielded slightly better results (Table 1, Entry 2). However, the conversion and optical purity of **2a** were somewhat lower when the concentration of **2** was 10 gL^{-1} (Table 1, Entry 3). Nevertheless, the bioreduction of 100 mg of **2** gave 86 and 62 mg of **2a** with similar *ee* (Table 1, Entries 4 and 5) at substrate concentrations of 2 and 5 gL^{-1}, respectively. This suggests that greater insolubility of the halogenated keto ester and/or enzyme inactivation alters the efficiency of the biotransformation. It is noteworthy that, although the affinities of the two substrates are quite different, the presence of the halogen in substrate **2** did not affect TtADH enantioselectivity.

Table 1. Reduction of **1** and **2** to **1a** and **2a** with TtADH by the TaGDH/glucose-NADH regeneration system.[a]

Entry	**1** [mg]	[**1**] [gL^{-1}]	TtADH [$mgmL^{-1}$]	TaGDH [$mgmL^{-1}$]	Conv.[b] [%]	*ee*[b] [%]
1	100	10	0.05	0.010	100 (74) [d]	95
2[c]	100	2	0.10	0.010	78 (77) [d]	96
	2 [mg]	[**2a**] [gL^{-1}]				
3	100	10	0.125	0.0275	28 (n.d.) [d]	88
4	100	2	0.100	0.020	96 (86) [d]	93
5	100	5	0.125	0.0275	100 (62) [d]	95

[a] Reactions were carried out for 24 h at 50 °C. [b] Determined by HPLC {Chiralcel OD-H, hexane/*i*PrOH [(9:1)]}. [c] The reaction was carried out in 6 h. [d] Isolated yield in parentheses; n.d.: not determined.

Process Development using BsADH for Cofactor Regeneration

Early bioconversion processes performed to establish TtADH enantioselectivity were carried out on analytical scale by way of an in situ NADH-recycling system involving a second thermophilic NAD-dependent ADH, the recombinant ADH from *Bacillus stearothermophilus* (BsADH).[14] The bacillary enzyme is active with 2-propanol which was therefore used as both co-solvent and substrate. The enzyme is inactive on aliphatic and aromatic ketones, including the carbonyl substrates of TtADH and the corresponding alcohols. However, TtADH does not accept 2-propanol or acetone as substrates. These features allowed the reaction to proceed almost to completion for reduction of 3 mg of **1** to **1a** with 99% conversion and *ee* = 91%, in 24 h at 50 °C, and in the presence of 2% v/v 2-propanol.[14] The scaled-up bioreduction of **1** involving 100 mg of substrate was performed by increasing the amount of 2-propanol to 4% v/v and using different enzyme concentrations. The data summarized in Table 2 indicate that the improved conversion was obtained either in a short reaction time (6 h) using higher amounts of the two enzymes (Table 2, Entry 3) or using lower amounts of enzymes at a reaction time which was four times longer (Table 2, Entry 2). Notably, the yields of 96–97% were similar to those obtained from bioreductions using 3 mg substrate,[14] but with a lower optical purity (86–87% *ee* relative to 91% *ee*), suggesting that the change in TtADH selectivity could be related to 2-propanol concentrations.

Table 2. Asymmetric reduction of **1** with TtADH by the BsADH/2-propanol-NADH regeneration system.[a]

Entry	TtADH [$mg\,mL^{-1}$]	BsADH [$mgmL^{-1}$]	Time [h]	2-Propanol (% v/v)	Conv.[b] [%]	*ee*[b] [%]
1	0.050	0.010	6	4	81	84
2	0.050	0.010	24	4	97	86
3	0.265	0.024	6	4	96	87

[a] Conditions: concentration of **1**: 10 gL^{-1}; TtADH and BsADH at the indicated concentrations; 1 mM NAD^+; buffer, 0.1 M sodium phosphate, pH 7.0, 0.1 M KCl, 5 mM 2-mercaptoethanol. Reaction volume, 10 mL; T = 50 °C. [b] Determined by HPLC {Chiralcel OD-H, hexane/*i*PrOH [(9:1)]}.

In addition to 2-propanol (k_{cat}/K_m = 9 $s^{-1}\,mM^{-1}$), BsADH oxidizes other alcohols with even greater efficiency. Examples include ethanol (k_{cat}/K_m = 64 $s^{-1}\,mM^{-1}$), 1-propanol (286 $s^{-1}\,mM^{-1}$), 1-butanol (437 $s^{-1}\,mM^{-1}$), 1-pentanol (64 $s^{-1}\,mM^{-1}$), and 1-hexanol (64 $s^{-1}\,mM^{-1}$) (Raia, unpublished data) and these were therefore tested as alternative hydride sources for NADH recycling. Moreover, these alcohols and their respective aldehydes are not substrates of TtADH.[14] Thus, only the cofactor is the co-substrate of TtADH and BsADH.

Bioreductions of 100 mg of **1** were carried out in the presence of each alcohol at a concentration of 4% v/v, which corresponds to 700 mM for ethanol down to 310 mM for 1-hexanol. All values were over-saturating for the bacillar ADH. The data obtained were plotted against the respective log*P* values to correlate conversions and the TtADH enantioselectivity with the hydrophobicity of the alcohol added (see Supporting Information). The TtADH enantioselectivity decreased as the hydrophobicity of the medium increased. However, the level of conversion remained high and near constant for all of the alcohols tested, emphasizing the versatility and high efficiency of the BsADH/alcohol substrate system in recycling the reduced cofactor. An increase in conversion rate with increasing log*P* with no effect on enantioselectivity was recently reported for the 2-octanone to (*R*)-2-octanol reduction with *Oenococcu oeni* cells in a biphasic system.[19] Moreover, *Lactobacillus brevis* ADH enantioselectivity was recently shown not to be altered by the presence of an organic phase.[20] Instead, *Thermoanaerobium brockii* ADH enantioselectivity was seen to increase proportionally to increasing

Table 3. Asymmetric reduction of **1** with the TtADH/BsADH system at different ethanol and cofactor concentrations.[a]

Entry	Ethanol (% v/v)	NAD^+ [mM]	TtADH [mg mL^{-1}]	BsADH [mg mL^{-1}]	Conversion [%]	*ee* [%]	Isolated yield [%]
1	0.6	1 (2)	0.05	0.01	60 (89)	90 (90)	n.d.
2	1	1 (2)	0.05	0.01	79 (98)	89 (92)	n.d.
3	2	1 (2)	0.05	0.01	92 (98)	90 (93)	n.d.
4	3	1 (2)	0.05	0.01	91 (98)	92 (92)	n.d.
5	4	1 (2)	0.05	0.01	91 (99)	91 (93)	n.d.
6	4	2	0.10	0.02	99	94	81

[a] Conditions reaction and chiral analysis as in Table 1. Amount of **1**: 100 mg. **1** concentration, 10 g L^{-1}, except for #6: 2 g L^{-1}. Values in parentheses refer to data obtained with 2 mM NAD^+. n.d.: not determined.

water composition.[21] In general terms, the stereoselectivity of enzymes decreased as solvent hydrophobicity increased[22] and enantiofacial selectivity was also significantly affected by the reaction medium.[23] Although the examples mentioned describe biphasic systems, including high concentrations of an apolar solvent, the effect of relatively low concentrations of polar protic solvents on the TtADH enantiofacial selectivity is rather remarkable. Docking calculations using the TtADH structure explain the selective formation of the methyl (*R*)-mandelate **1a**[24] by showing that the methyl benzoylformate molecule assumes the lowest energy orientation by fitting the phenyl ring into a hydrophobic pocket, with the two carbonyl groups staggered by about 78° and the methoxy group pointing toward the carboxyamide group of the cofactor. Moreover, the docking analysis showed that the keto ester molecule can also assume another conformation, less energetically favourable compared to that described above, which has the opposite face of the carbonyl group directed to the nicotinamide ring, and therefore leading to the (*S*)-enantiomer of the alcohol product. Importantly, there is no major steric constraint preventing the positioning of this alternative conformation in the enzyme active site.[24] A change in polarity occurring in the active site may induce a structural rearrangement that facilitates the positioning of this alternative conformation.

Since the TtADH/BsADH system showed higher enantioselectivity with ethanol than with 2-propanol, the next step was to examine the synthesis of **1a** using concentrations of ethanol lower than 4% v/v (Table 3). The keto ester reduction was limited by the cofactor recycling rate when the ethanol percentage was 0.6% or 1% v/v and the cofactor concentration was 1 mM (Table 3, Entries 1 and 2). This concentration is much lower than the cofactor K_m (13 ± 2 mM) and is therefore far below that required for saturation of the BsADH active sites. However, by doubling the cofactor concentration, the conversion increased from 60 to 89% (Table 3, Entry 1) and from 79 to 98% (Table 3, Entry 2) in the presence of 0.6% and 1% v/v ethanol, respectively. Conditions employing 4% v/v ethanol and 2 mM NAD (Table 3, Entries 5 and 6) and a substrate concentration of 2 g L^{-1} (as in Table 1, Entry 2) were shown to be ideal for achieving asymmetric reduction of 100 mg of **1** with 81% isolated yield and *ee* = 94% (Table 3, Entry 6). The bioconversion of **2** to **2a** occurred with the same enantioselectivity as the non-halogenated compound and with good productivity (Table 4). Using relatively low substrate concentrations 78 mg of **2a** (*ee* = 92%) was obtained from 100 mg of **2** in 24 h at 50 °C (Table 3, Entry 3). As in the case for the TtADH/TaGDH system (Table 1, Entry 3) the substrate concentration of 2 g L^{-1} was found to be optimal for scaling up production of **2a**. However, the formation of the more reactive acetaldehyde could limit the use of ethanol as a regeneration reductant. Nevertheless, new applications for ethanol as a tunable nicotinamide reductant under four-electron redox conditions for the chemoenzymatic synthesis of important synthons,[25a] as well as solvent and reductant in the enantioselective synthesis of (*S*)-profens using *Sulfolobus solfataricus* ADH[25b] and (2*S*)-2-arylpropanols using horse liver and yeast ADHs[25c] have been recently reported.

Table 4. Reduction of **2** to **2a** with TtADH by the BsADH/ethanol-NADH regeneration system.[a]

Entry	**2** [mg]	[**2**] [g L^{-1}]	TtADH [mg mL^{-1}]	BsADH [mg mL^{-1}]	Conv.[b] [%]	*ee*[b] [%]
1	1	1	0.05	0.01	100	91
2	2	2	0.05	0.01	100	92
3	100	2	0.10	0.02	98 (78)[c]	92

[a] The reactions were carried out for 24 h at 50 °C. Ethanol, 4% v/v. [b] Determined by HPLC {Chiralcel OD-H, hexane/*i*PrOH [(9:1)]}. [c] Isolated yield in parentheses.

Conclusions

The enzymatic synthesis of methyl (*R*)-mandelate (**1a**) and methyl (*R*)-*o*-chloromandelate (**2a**), two important pharmaceutical building blocks, has been developed in a one-phase system, using a carbonyl reductase and two different dehydrogenases to recycle the NADH. The two regeneration modes gave similar yields and optical purities. BsADH displayed two distinct advantages: feasibility of purification and high efficiency at suboptimal pH. For the TaGDH method, the hydride source was glucose, which constitutes cheap biomass whereas for the BsADH method, ethanol was the cheap sacrificial substrate. Both methods are characterized by favourable thermodynamics since alcohol/aldehyde, and glucose/gluconic acid do not interfere with the synthesis reaction. Only a few examples are known for enzyme-coupled cofactor regeneration involving a second ADH[26] and the present study represents a successful application of the bacillary ADH.

Experimental Section

Chemicals: NAD(P)$^+$ and NAD(P)H were obtained from AppliChem. (Darmstadt, Germany). Methyl benzoylformate **1** and methyl (*S*)- and (*R*)-mandelate were obtained from Sigma–Aldrich. Methyl *o*-chlorobenzoylformate **2** was obtained from Ricci Chimica (Perugia, Italy). Other chemicals were A grade substances from Applichem. Solutions of NAD(P)H and NAD$^+$ were prepared as previously reported.[14] All solutions were made up with MilliQ water.

Enzymes and Kinetic Assays: Recombinant *Thermus thermophilus* ADH (TtADH) and recombinant *Bacillus stearothermophilus LLD-R strain* (BsADH) were prepared as described previously.[14] Glucose dehydrogenase from *Thermoplasma acidophilum* (TaGDH) was from Sigma, St. Luis, MO. TtADH activity was assayed spectrophotometrically at 65 °C by measuring the change in absorbance of NADH at 340 nm using a Cary 1E spectrophotometer equipped with a Peltier effect-controlled temperature cuvette holder. The kinetic parameters of TtADH for α-keto esters were determined as described previously.[14] TaGDH was assayed at 50 °C by measuring the change in absorbance of NADPH at 340 nm. The standard assay was performed by adding 0.25 μg of enzyme to 1 mL of preheated assay mixture containing 50 mM glucose and 0.4 mM NADP in 50 mM sodium phosphate, pH 7.0.

The effect of organic solvents on TaGDH was investigated by incubating 0.025 mg mL^{-1} protein in 50 mM sodium phosphate, pH 7.0, at 50 °C, in the absence and presence of organic solvents. At specific time intervals, the samples were centrifuged and small aliquots were withdrawn and assayed. The volume of solution in the tight capped test tube did not change during incubation.

Procedure for Bioreduction: Bioreduction of α-keto esters was performed at 50 °C using two NADH regeneration systems. The first consisted of TaGDH and glucose. For analytical biotransformation the reaction mixture contained 6.2 mM carbonyl compound, 1 mM NAD$^+$, 50 mM glucose, 25 μg TtADH, and 5.5 μg TaGDH in 0.2 mL of 100 mM sodium phosphate, pH 7.0. Semi-preparative reactions were performed on a 0.1 g scale in a reaction volume up to 10 mL, using 0.05 mg mL^{-1} TtADH, and 0.01 mg mL^{-1} TaGDH. During the reaction the pH was maintained at pH 6.5–7.0 with the addition of a 2 M NaOH solution.

The second NADH regeneration system consisted of BsADH and 2-propanol or different linear alcohols as described previously[14] with some modifications. The reaction mixture contained 6.2 mM carbonyl compound, 1 mM NAD$^+$, 15 μg of BsADH, 0.6 to 4% v/v alcohol substrate, and 125 μg TtADH in 1 mL of 100 mM sodium phosphate, pH 7.0, 5 mM 2-mercaptoethanol and 100 mM KCl. Semi-preparative reactions were performed on a 0.1 g scale in a reaction volume up to 10 mL, using 0.05 mg mL^{-1} TtADH, and 0.01 mg mL^{-1} BsADH. In both systems the mixtures were shaken at 160 rpm for different reaction times in a temperature-controlled water bath. Upon termination of the reaction, the mixtures were extracted twice with ethyl acetate, dried with anhydrous Na_2SO_4 and concentrated under reduced pressure. The samples were prepared in hexane/2-propanol (9:1) for HPLC analysis.

To determine the isolated yield of the semi-preparative reactions carried out using the two NADH regeneration systems, the ethyl acetate extracts were dried with anhydrous Na_2SO_4, filtered, and concentrated under reduced pressure. Purification by silica gel column chromatography (hexane/ethyl acetate, 9:1) gave **1a** or **2a** as colourless oils; yield: 77 mg (77% isolated yield; conversion: 78%) and 81 mg (81%; 99%) of **1a** produced by the TtADH/TaGDH and TtADH/BsADH system, respectively; 86 mg (86% isolated yield; conversion: 96%) and 78 mg (78%; 98%) of **2a** produced by TtADH/TaGDH and TtADH/BsADH system, respectively. For details on the NMR and optical rotation analyses, see the Supporting Information.

The degree of conversion and enantiomeric purity of the products were determined on the basis of the peak areas of ketone substrates and alcohol products separated and visualized by HPLC, on a Chiralcel OD-H column (Daicel Chemical Industries, Ltd., Osaka, Japan). The absolute configuration of product alcohols was determined by comparing the HPLC data with standard samples. Products were analyzed with isocratic elution under the following conditions: hexane/2-propanol (9:1) (mobile phase), flow rate of 1 mL min^{-1}, detection for bioconversions of **1** and **2** at 210 nm. At this wavelength, both **1** and **1a** as well as **2** and **2a** have the same molar extinction coefficient values, so that areas of substrates and products are equally proportional to concentrations. Retention times were as follows: 6.14, 8.82 and 14.15 min for **1**, methyl (*S*)-mandelate and methyl (*R*)-mandelate, respectively; 6.92, 10.12 and 17.16 min for **2**, methyl (*S*)-*o*-chloromandelate and methyl (*R*)-*o*-chloromandelate, respectively. The absolute stereochemistry of the two halogenated alcohol enantiomers were assigned by comparison to the values described in the literature for methyl *o*-chloromandelates.[9] The log*P* values were obtained from Laane and coworkers.[27]

Supporting Information (see footnote on the first page of this article): Time course of the bioreduction of **1** by TtADH. Production of methyl (*R*)-mandelate **1a** at different concentrations of **1**. Effects of organic solvents on TaGDH. Production of methyl (*R*)-mandelate (**1a**) at different concentrations of **1** in the presence of the water-miscible or immiscible organic solvents. Effect of the BsADH alcohol substrates on the enantioselectivity and efficiency of the reduction catalysed by TtADH. NMR spectra and spectroscopic analyses. Optical rotation analyses.

Acknowledgments

This work was funded by Fondo per gli Investimenti della Ricerca di Base (FIRB) n. RBNE034XSW, and by the Agenzia Spaziale Italiana (ASI), project "From Molecules to Man" (MoMan), 1/014/06/0. We thank Prof. Tadashi Ema for the generous gift of methyl *o*-chlorobenzoylformate at an early stage of the work.

[1] a) D. Zhu, Y. Yang, L. Hua, *J. Org. Chem.* **2006**, *71*, 4202–4205; b) T. Ema, H. Yagasaki, N. Okita, K. Nishikawa, T. Korenaga, T. Sakai, *Tetrahedron: Asymmetry* **2005**, *16*, 1075–1078; c) C. He, D. Chang, J. Zhang, *Tetrahedron: Asymmetry* **2008**, *19*, 1347–1351; d) R. Kratzer, M. Pukl, S. Egger, B. Nidetzky, *Microb. Cell Fact.* **2008**, *7*, 37; e) K. Nakamura, R. Yamanaka, T. Matsuda, T. Harada, *Tetrahedron: Asymmetry* **2003**, *14*, 2659–2681.

[2] a) Y. Kobayashi, Y. Takemoto, Y. Ito, S. Terashima, *Tetrahedron Lett.* **1990**, *31*, 3031–3034; b) C. Pousset, M. Haddad, M. Larchevêque, *Tetrahedron* **2001**, *57*, 7163–7167.

[3] A. Bousquet, A. Musolino, PCT Int. Appl., WO9918110 A1; *Chem. Abstr.* **1999**, *130*, 296510e.

[4] a) W. Yang, J.-H. Xu, Y. Xie, Y. Xu, Zh. Gang, G.-Q. Lin, *Tetrahedron: Asymmetry* **2006**, *17*, 1769–1774; b) J. L. Guo, X. Q. Mu, Y. Xu, *Bioprocess Biosyst. Eng.* **2010**, *33*, 797–804.

[5] K. Mitsuhashi, H. Yamamoto, *Eur. Pat. Appl.* **2003**, EP1316613 A2.

[6] L. M. van Langen, R. P. Selassa, F. van Rantwijk, R. A. Sheldon, *Org. Lett.* **2005**, *7*, 327–329.

[7] a) Y. Sun, X. Wan, J. Wang, Q. Meng, H. Zhang, I. Jiang, Z. Zhang, *Org. Lett.* **2005**, *7*, 5425–5427; b) L. Yin, W. Shan, X.

Jia, X. Li, A. S. C. Chan, *J. Organomet. Chem.* **2009**, *694*, 2092–2095.
[8] K.-N. Uhm, S.-J. Lee, H.-K. Kim, H.-Y. Kang, Y. Lee, *J. Mol. Catal. B* **2007**, *45*, 34–38.
[9] T. Ema, S. Ide, N. Okita, T. Sakai, *Adv. Synth. Catal.* **2008**, *350*, 2039–2044.
[10] M. Jeong, Y. M. Lee, S. H. Hong, S. Y. Park, I. K. Yoo, M. J. Han, *Biotechnol. Lett.* **2010**, *32*, 1529–1531.
[11] D. Zhu, H. T. Malik, L. Hua, *Tetrahedron: Asymmetry* **2006**, *17*, 3010–3014.
[12] K. Ishihara, H. Yamaguchi, T. Omori, T. Uemura, N. Nakajima, N. Esaki, *Biosci. Biotechnol. Biochem.* **2004**, *68*, 2120–2127.
[13] K. Inoue, Y. Makino, N. Itoh, *Tetrahedron: Asymmetry* **2005**, *16*, 2539–2549.
[14] A. Pennacchio, B. Pucci, F. Secundo, F. La Cara, M. Rossi, C. A. Raia, *Appl. Environ. Microbiol.* **2008**, *74*, 3949–3958.
[15] J. John, S. J. Crennell, D. W. Hough, M. J. Danson, G. L. Taylor, *Structure* **1994**, *2*, 385–393.
[16] J. Woodward, K. A. Cordray, R. J. Edmonston, M. Blanco-Rivera, S. M. Mattingly, B. R. Evans, *Energy Fuels* **2000**, *14*, 197–201.
[17] L. D. Smith, N. Budgen, S. J. Bungard, M. J. Danson, D. W. Hough, *Biochem. J.* **1989**, *261*, 973–977.
[18] J. Shumacher, M. Eckstein, U. Kragl, *Biotechnol. J.* **2006**, *1*, 574–581.
[19] J. Hu, Y. Xu, *Biotechnol. Lett.* **2006**, *28*, 1115–1119.
[20] M. Villela Filho, T. Stilliger, M. Müller, A. Liese, C. Wandrey, *Angew. Chem. Int. Ed.* **2003**, *4*, 2993–2996.
[21] Å. Jönsson, E. Wehtje, P. Adlercreutz, B. Mattiasson, *Biochim. Biophys. Acta* **1999**, *1430*, 313–322.
[22] G. Carrea, S. Riva, *Angew. Chem.* **2000**, *39*, 2226–2254.
[23] A. M. Klibanov, *Nature* **2001**, *409*, 241–246.
[24] A. Pennacchio, A. Giordano, L. Esposito, E. Langella, M. Rossi, C. A. Raia, *Protein Pept. Lett.* **2010**, *17*, 437–444.
[25] a) S. Broussy, R. W. Cheloha, D. B. Berkowitz, *Org. Lett.* **2009**, *11*, 305–308; b) J. A. Friest, Y. Maezato, S. Broussy, P. Blum, D. B. Berkowitz, *J. Am. Chem. Soc.* **2010**, *132*, 5930–5931; c) P. Galletti, E. Emer, G. Gucciardo, A. Quintavalla, M. Pori, D. Giacomini, *Org. Biomol. Chem.* **2010**, *8*, 4117–4123.
[26] K. Goldberg, K. Schroer, S. Lütz, A. Liese, *Appl. Microbiol. Biotechnol.* **2007**, *76*, 237–248.
[27] C. Laane, S. Boeren, R. Hilhorst, C. Veeger, *Optimization of Biocatalysis in Organic Media*, in: *Biocatalysis in Organic Media* (Eds.: C. Laane, J. Tramper, M. D. Lilly), Elsevier, Amsterdam, **1987**, vol. 29, pp. 65–84.

Received: January 25, 2011
Published Online: June 1, 2011

Extremophiles (2010) 14:193–204
DOI 10.1007/s00792-009-0298-3

ORIGINAL PAPER

Biochemical characterization of a recombinant short-chain NAD(H)-dependent dehydrogenase/reductase from *Sulfolobus acidocaldarius*

Angela Pennacchio · Assunta Giordano · Biagio Pucci · Mosè Rossi · Carlo A. Raia

Received: 8 October 2009 / Accepted: 16 December 2009 / Published online: 6 January 2010

Abstract The gene encoding a novel alcohol dehydrogenase that belongs to the short-chain dehydrogenases/reductases (SDRs) superfamily was identified in the aerobic thermoacidophilic crenarchaeon *Sulfolobus acidocaldarius* strain DSM 639. The *saadh* gene was heterologously overexpressed in *Escherichia coli*, and the protein (SaADH) was purified to homogeneity and characterized. SaADH is a tetrameric enzyme consisting of identical 28,978-Da subunits, each composed of 264 amino acids. The enzyme has remarkable thermophilicity and thermal stability, displaying activity at temperatures up to 75°C and a 30-min half-inactivation temperature of ~90°C, and shows good tolerance to common organic solvents. SaADH has a strict requirement for NAD(H) as the coenzyme, and displays a preference for the reduction of alicyclic, bicyclic and aromatic ketones and α-keto esters, but is poorly active on aliphatic, cyclic and aromatic alcohols, and shows no activity on aldehydes. The enzyme catalyses the reduction of α-methyl and α-ethyl benzoylformate, and methyl *o*-chlorobenzoylformate with 100% conversion to methyl (*S*)-mandelate [17% enantiomeric excess (ee)], ethyl (*R*)-mandelate (50% ee), and methyl (*R*)-*o*-chloromandelate (72% ee), respectively, with an efficient in situ NADH-recycling system which involves glucose and a thermophilic glucose dehydrogenase. This study provides further evidence supporting the critical role of the D37 residue in discriminating NAD(H) from NAD(P)H in members of the SDR superfamily.

Keywords Alcohol dehydrogenase · *Sulfolobus acidocaldarius* · Short-chain dehydrogenases/reductases · Archaea · Bioreduction

Communicated by H. Santos.

A. Pennacchio · M. Rossi · C. A. Raia (✉)
Istituto di Biochimica delle Proteine, CNR, Via P. Castellino 111, 80131 Naples, Italy
e-mail: ca.raia@ibp.cnr.it

A. Giordano
Istituto di Chimica Biomolecolare, CNR, Via Campi Flegrei 34, 80078 Pozzuoli, Naples, Italy

B. Pucci
Centro Ricerche Oncologiche Mercogliano (CROM), Via A. Bianco, 83013 Mercogliano, Avellino, Italy

Introduction

Dehydrogenases/reductases are enzymes which are found throughout across a wide range of organisms, where they are involved in a broad spectrum of metabolic functions (Jörnvall 2008). A system of short-, medium- and long-chain dehydrogenase/reductases has been recently identified based on molecular size, sequence motifs, mechanistic features and structural comparisons (Kavanagh et al. 2008; Persson et al. 2009). Many studies have been addressed to characterize alcohol dehydrogenases (ADHs) from thermophiles and hyperthermophiles, mainly to understand their evolution and structure/function/stability relationship (Radianingtyas and Wright 2003) and develop their biotechnological potential mainly in the synthesis of chiral alcohols (Hummel 1999; Kroutil et al. 2004). Early applications in asymmetric reduction involved horse liver and yeast ADHs (Jones and Beck 1976), followed by *Thermoanaerobacter brockii* ADH (TbADH) (Keinan et al. 1986). Since then, new ADHs from various species of microorganisms displaying distinct substrate specificity, good efficiency and high enantioselectivity have been described.

Representative examples include the NADP-dependent (*R*)-specific ADH from *Lactobacillus brevis* (LB-RADH) (Schlieben et al. 2005), the NAD-dependent (*S*)-specific 1-phenylethanol dehydrogenase from the denitrifying bacterium strain EbN1 (PED) (Höffken et al. 2006), the NAD-dependent ADH from *Leifsonia* sp. strain S749 (LSADH) (Inoue et al. 2006), and the NADP-dependent carbonyl reductase from *Candida parapsilosis* (Nie et al. 2007). These enzymes originate from mesophilic microorganisms and belong to the short-chain dehydrogenases/reductases (SDRs) superfamily (Kavanagh et al. 2008) which is characterized by ~250 residue subunits, a Gly-motif in the coenzyme-binding regions, and a catalytic tetrad (Filling et al. 2002; Schlieben et al. 2005; Persson et al. 2009).

Representative examples of ADHs from thermophilic microorganisms are medium-chain enzymes, including TbADH (Korkhin et al. 1998), the ADH from *Bacillus stearothermophilus* (Ceccarelli et al. 2004) and two archaeal enzymes, the ADH from *Aeropyrum pernix* (Guy et al. 2003) and *Sulfolobus solfataricus* (Giordano et al. 2005). However, two archaeal short-chain ADHs have been identified in *Pyrococcus furiosus*, an NADP(H)-dependent SDR (AdhA) (van der Oost et al. 2001; Machielsen et al. 2008), and an NAD(H)-preferring ADH, that belongs to the aldo–keto reductase superfamily (Persson et al. 2009), recently characterized (Machielsen et al. 2006; Zhu et al. 2006, 2009). Furthermore, an NAD(H)-dependent ADH (TtADH) that belongs to the SDR superfamily, identified in *Thermus thermophilus* HB27, has been purified and characterized (Pennacchio et al. 2008).

In order to find a dehydrogenase/reductase that is both stable and NAD^+ dependent, we have focused our attention on the genomes of thermophilic organisms containing genes encoding putative ADHs belonging to the SDR superfamily, and applied the criteria used for TtADH to select enzymes with a high probability of being NAD^+-dependent (Pennacchio et al. 2008). An open reading frame coding for a protein belonging to the SDR superfamily with relatively high sequence identity to that of most representative ADHs (PED, LSADH and TtADH) was found in the genome of *Sulfolobus acidocaldarius*, an aerobic thermoacidophilic crenarchaeon which grows optimally at 80°C and pH 2 (Chen et al. 2005). Noteworthy, the amino acid sequence revealed the presence of an aspartate residue at position 42. This residue plays a critical role in determining the preference of SDRs for NAD(H) (Schlieben et al. 2005). Further evidence of this role is provided by LSADH (Inoue et al. 2006), PED (Höffken et al. 2006) and TtADH (Pennacchio et al. 2008), since these three SDRs are strictly NAD-dependent and have an aspartate residue at the same position within the sequence. Therefore, the putative dehydrogenase/reductase from *S. acidocaldarius* (SaADH) was expected to display a preference for NAD(H) rather than the more expensive NADP(H). This preference as well as an intrinsic thermostability and tolerance of organic solvents are the features that make an oxidoreductase more attractive from an application perspective (Hummel 1999; Kroutil et al. 2004; Zhu et al. 2006).

The current report describes the cloning and heterologous expression of the *S. acidocaldarius saadh* gene, which encodes the SDR SaADH. The purified and characterized enzyme was found to be a thermophilic and thermostable NAD(H)-dependent archaeal short-chain ADH tolerant to organic solvents and active on alicyclic alcohols, aromatic ketones, diketones, and α- and β-keto esters.

Materials and methods

Chemicals

$NAD(P)^+$ and NAD(P)H were obtained from AppliChem (Darmstadt, Germany). Alcohols, aldehydes, ketones and keto esters were obtained from Sigma-Aldrich. MES {2-(*N*-morpholino)ethanesulfonic acid} was obtained from Sigma Chemical Co. (St. Louis, MO). Aldolase was obtained from Amersham Biosciences. Dimethylsuberimidate (DMS) and dimethyladipimate (DMA) chemical cross-linkers were from Pierce. Methyl *o*-chlorobenzoylformate was a kind gift from Tadashi Ema. 1-Phenylethanol-d_9 [$C_6D_5CD(OH)CD_3$] was obtained from Ricci Chimica (Perugia, Italy). Other chemicals were A grade substances from AppliChem. Solutions of NADH and NAD^+ were prepared as previously reported (Raia et al. 2001). All solutions were made up with MilliQ water.

Amplification and cloning of the *saadh* gene

Chromosomal DNA was extracted by caesium chloride purification as described by Sambrook et al. (1989). Ethidium bromide and caesium chloride were removed by repeated extraction with isoamyl alcohol and extensive dialysis against 10 mM Tris–HCl pH 8.0, 1 mM EDTA, respectively. DNA concentration was determined spectrophotometrically at 260 nm, and the molecular weight was checked by electrophoresis on 0.8% agarose gel in 90 mM Tris–borate pH 8.0, 20 mM EDTA, using DNA molecular size markers. The *saadh* gene was amplified by polymerase chain reaction (PCR) using oligonucleotide primers based on the *saadh* sequence of *Sulfolobus acidocaldarius* strain DSM 639 (GenBank accession no. YP_256716.1). The following oligonucleotides were used: 5′-GGTTGG CATATGGACATTGATAGGCTCTTTTCAGTA-3′ as the forward primer (the *Nde*I restriction site is underlined in the sequence) and the oligonucleotide 5′-GGTTGG GAATTCCTACACCTTTGGGTCATATCTACCATCTA-3′

as the reverse primer. This latter oligonucleotide introduces a translational stop following the last codon of the ADH gene, followed by an *Eco*RI restriction site, which is underlined in the sequence shown. The PCR product was cloned into the expression vector pET29a (Novagen, Madison, WI, USA) and digested with the appropriate restriction enzymes to create pET29a-*sa*ADH. The insert was sequenced in order to verify that mutations had not been introduced during PCR.

Expression and purification of recombinant SaADH

Recombinant protein was expressed in *E. coli* BL21(DE3) cells (Novagen) transformed with the corresponding expression vector. Cultures were grown at 37°C in 2 l of LB medium containing 30 μg ml^{-1} kanamycin. When the A_{600} of the culture reached 1.4, protein expression was induced by addition of isopropyl β-D-1-thiogalactopyranoside (IPTG) to a concentration of 1.0 mM. The bacterial culture was incubated at 37°C for a further 24 h. Cells were harvested by centrifugation, and the pellet was stored at −20°C until use. The cells obtained from 2 l of culture were suspended in 20 mM Tris–HCl buffer (pH 7.5) containing 0.1 mM phenylmethylsulfonyl fluoride (PMSF) and were lysed using a French pressure cell (Aminco Co., Silver Spring, MD) at 2,000 psi (1 psi = 6.9 kPa). The lysate was centrifuged, and the supernatant was incubated in the presence of DNase I (50 μg per ml of solution) and 5 mM $MgCl_2$ for 30 min at 37°C, followed by protamine sulphate (1 mg per ml of solution) at 4°C for 30 min. The nucleic acid fragments were removed by centrifugation, and the supernatant was incubated at 75°C for 15 min. The host protein precipitate was removed by centrifugation. The supernatant was dialysed overnight at 4°C against 20 mM Tris–HCl, pH 8.4 (buffer A) containing 1 mM PMSF. The dialysed solution was applied to a DEAE-Sepharose Fast Flow (1.6 × 12 cm) column equilibrated in buffer A. After washing with 1 bed volume of the same buffer, elution was performed with a linear gradient of 0–0.06 M NaCl (80 ml of each concentration) in buffer A, at a flow rate of 60 ml h^{-1}. The active pool was dialysed against buffer A, concentrated fivefold with a 30,000 MWCO centrifugal filter device (Millipore), and applied to a Sephadex G-75 (1.6 × 30 cm) column equilibrated in buffer A containing 0.15 M NaCl. The active pool was dialysed against buffer A and concentrated to obtain 2.5 mg protein ml^{-1} as described previously. SaADH was stored at −20°C, without loss of activity following several months of storage. SDS-PAGE and non-denaturing PAGE were carried out according to the Laemmli method (1970), with minor modifications (Raia et al. 2001). The subunit molecular mass value was determined by electrospray ionization mass spectrometry (ESI-MS) with a QSTAR Elite instrument (Applied Biosystems, USA).

The protein concentration was determined with a Bio-Rad protein assay kit using BSA as a standard.

Size-exclusion chromatography

Molecular masses were determined by size-exclusion chromatography using a Superdex 200 10/300 GL column (Amersham Biosciences), equilibrated with 50 mM Tris–HCl, pH 9.0, containing 0.15 M NaCl, at a flow rate of 0.5 ml min^{-1}. The following molecular mass standards were used for calibration: vitamin B_{12} (1,350 Da), horse myoglobin (17.5 kDa), chicken ovalbumin (44 kDa), beef γ-globulin (158 kDa), and thyroglobulin (670 kDa) from Bio-Rad. In order to calculate the distribution coefficient, the void and total volumes of the column were determined with blue dextran and tryptophan, respectively.

Chemical cross-linking

Cross-linking reactions of SaADH with DMA and DMS were conducted for 1 h at 25°C in a 25-μl volume of 0.1 M triethanolamine–HCl, pH 8.5 at 0.20 mg ml^{-1} protein, and 0.1 mg ml^{-1} bifunctional reagent. The molecular mass of cross-linked SaADH species was estimated by SDS-PAGE according to the procedure described by Davies and Stark (1970).

Enzyme assay

SaADH activity was assayed spectrophotometrically at 65°C by measuring the change in absorbance of NADH at 340 nm using a Cary 1E spectrophotometer equipped with a Peltier effect-controlled temperature cuvette holder. The standard assay for the reduction reaction was performed by adding 5–25 μg of the enzyme to 1 ml of preheated assay mixture containing 25 mM ethyl benzoylformate (EBF) and 0.3 mM NADH in 37.5 mM MES–NaOH, pH 5.5. The standard assay for the oxidation reaction was performed using a mixture containing 25 mM cycloheptanol and 5 mM NAD^+ in 25 mM sodium phosphate, pH 8.0. Screening of the substrates was performed using 1 ml of assay mixture containing either 10 mM alcohol and 5 mM NAD^+ in 25 mM sodium phosphate, pH 8.0, or 10 mM carbonyl compound and 0.1 mM NADH in 37.5 mM MES–NaOH, pH 5.5. One unit of SaADH represented 1 μmol of NADH produced or utilized per min at 65°C, on the basis of an absorption coefficient of 6.22 mM^{-1} cm^{-1} for NADH at 340 nm.

Effect of pH on activity

The optimum pH values for the reduction and oxidation reactions were determined at 65°C under the conditions

used for EBF and cycloheptanol, respectively, except that different buffer systems were used. The pH was controlled in each assay mixture at 65°C.

Kinetics

The SaADH kinetic parameters were calculated from measurements determined in duplicate or triplicate and by analysing the kinetic results using the program GraFit (Leatherbarrow 2004). The turnover value (k_{cat}) for SaADH was calculated on the basis of a molecular mass of 29 kDa, assuming that the four subunits are catalytically active.

Thermophilicity and thermal stability

SaADH was assayed in a temperature range of 30–95°C using standard assay conditions and 22 μg of protein ml^{-1} of assay mixture. The stability at various temperatures was studied by incubating 0.2–mg ml^{-1} protein samples in 50 mM Tris–HCl, pH 9.0 at temperatures between 25 and 95°C for 30 min. Each sample was then centrifuged at 5°C, and the residual activity was assayed as described above. Long-term stability was studied by incubating protein samples (0.2 mg ml^{-1}) in 50 mM Tris–HCl, pH 9.0, at 50 and 70°C, or in 50 mM Tris–H_3PO_4, pH 7.0 at 50 and 60°C and the residual activity was assayed after 6 and 24 h as described above.

The effect of chelating agents on enzyme stability was studied by measuring the activities before and after exhaustive dialysis of the enzyme against buffer A, containing 1 mM EDTA, and then against buffer A alone. An aliquot of the dialysed enzyme was then incubated at 70°C in the absence and presence of 1 mM EDTA or *o*-phenanthroline, and the activity was assayed at different times.

Effects of compounds on enzyme activity

The effects of salts, metal ions, and chelating agents on SaADH activity were investigated by assaying the enzyme in the presence of an appropriate amount of each compound in the standard assay mixture used for the oxidation reaction.

The effects of organic solvents were investigated by measuring the activity in enzyme samples (0.5 mg ml^{-1} in 100 mM MES, pH 6.0, 5 mM 2-mercaptoethanol) immediately after the addition of organic solvents at different concentrations, and 6 and 24 h of incubation at 50°C. The percentage activity for each sample was calculated by comparison with the value measured prior to incubation. The volume of the solution in a tightly capped test tube did not change during incubation.

Enantioselectivity

The enantioselectivity of SaADH was determined by examining the reduction of bicyclic ketones and α-keto esters using an NADH regeneration system consisting of glucose and glucose dehydrogenase from *Thermoplasma acidophilum* (TaGDH) (Sigma, St. Louis, MO). The reaction mixture contained 1 mM NAD^+, 5–10 mM carbonyl compound, 50 mM glucose, 125 μg SaADH, and 25 μg of TaGDH in 1 ml of 50 mM Tris–H_3PO_4, pH 7.0. The reactions were carried out at 50°C at different times in a temperature-controlled water bath. Upon termination of the reaction, the reaction mixture was extracted twice with ethyl acetate. The conversion yield and enantiomeric purity of the product were determined on the basis of the peak areas of ketone substrates and alcohol products by HPLC, on a Chiralcel OD-H column (Daicel Chemical Industries Ltd., Osaka, Japan). The absolute configuration of product alcohols was identified by comparing the chiral HPLC data with the standard samples. Products were analysed with isocratic elution, under the following conditions: hexane/2-propanol (9:1) (mobile phase), flow rate of 1 ml min^{-1}, detection at 210 nm for bioconversions of methyl and ethyl benzoylformate and for methyl *o*-chlorobenzoylformate; hexane/2-propanol (95:5), flow rate of 1 ml min^{-1}, detection at 217 nm for 1-indanone. Retention times were the following: 5.7, 8.1 and 13.4 min for methyl benzoylformate, methyl (*S*)-mandelate and methyl (*R*)-mandelate; 5.5, 7.4 and 12.1 min for ethyl benzoylformate, ethyl (*S*)-mandelate and ethyl (*R*)-mandelate; 6.9, 8.8 and 9.7 min for methyl *o*-chlorobenzoylformate, methyl (*R*)-*o*-chloromandelate and methyl (*S*)-*o*-chloromandelate; 8.8, 9.7, 10.8 min for 1-indanone and (*S*)- and (*R*)-1-indanol, respectively.

Coenzyme stereospecificity determination

The SaADH stereospecificity was investigated by NMR analysis of NADD obtained from the reaction of NAD^+ with 1-phenylethanol-d_9. The reaction mixture contained 2.0 mmol 1-phenylethanol-d_9, 30 μmol NAD^+, 26 units of SaADH and 0.25 mmol sodium phosphate buffer (pH 8.0) in a total volume of 5 ml. The reaction proceeded at 50°C while monitoring at 340 nm. When the A_{340} of the mixture reached a maximum (after 4 h), the solution was cooled and then applied to a DEAE-FF Sepharose column (1.6 × 8 cm) previously equilibrated with 10 mM sodium phosphate buffer (pH 8.0). The column was washed enough with the same buffer and then NADD was eluted with 20 mM sodium phosphate buffer (pH 8.0) containing 20 mM NaCl. Fractions with value of A_{260}/A_{340} ratio ≤2.3 were collected and the pool (8.2 μmol of NADD) was lyophilized for ^{1}H-NMR analysis. ^{1}H-NMR spectra were

Table 1 Purification of recombinant SaADH

Step	Total protein (mg)	Total activity (U)	Specific activity (U/mg)	Yield (%)	Purification (fold)
Crude extract	294	750	2.5	100	1
Thermal step	184	618	3.3	82.4	1.3
DEAE-FF	119	578	4.8	77.0	1.9
Gel filtration	68	452	6.6	60.3	2.6

The data are for a 2-l culture. Activities were measured at 65°C as described in "Materials and methods", using cycloheptanol as substrate

recorded on a Bruker cryoprobe™ Avance DRX instrument operating at 600 MHz. Samples were dissolved in 0.5 ml of D_2O. Chemical shifts were given in ppm (δ) scale; the HDO signal was used as the internal standard (δ 4.68).

Results and discussion

Expression and protein purification

Analysis of the *Sulfolobus acidocaldarius* genome (Chen et al. 2005) for genes encoding short-chain ADHs resulted in identification of a putative oxidoreductase gene. The oxidoreductase protein, named SaADH, was expected to be NAD(H)-dependent on the basis of the presence of an aspartic residue at position 42, whose critical role in determining the preference for NAD(H) (Kallberg et al. 2002) has been shown through kinetic and structural studies of the LB-RADH G37D mutant (Schlieben et al. 2005), and recently supported by kinetic studies (Pennacchio et al. 2008) and structural characterization of TtADH (Asada et al. 2009).

SaADH is a 28,978-Da protein whose sequence shows the greatest identity to four typical SDRs, LB-RADH (30% identity), LSADH (29%), PED (28%), and TtADH (27%), as well as the archaeal AdhA (25% identity). The *saadh* gene was successfully expressed in *E. coli* cells, yielding an active enzyme accounting for more than 20% of the total protein content of the cell extract (Table 1). Host protein precipitation at 75°C was found to be the most effective purification step. An overall purification of 2.6-fold was achieved from crude, cell-free extracts with an overall yield of 60%. The enzyme was shown to be homogeneous by denaturing and non-denaturing PAGE (data not shown).

Protein separation by SDS-PAGE resulted in a single band corresponding to a molecular mass of ~30 kDa (see below). Gel filtration performed in 50 mM Tris–HCl buffer, pH 9.0 containing 150 mM NaCl yielded a profile consisting of a single peak corresponding to molecular mass ~65 kDa (data not shown). The quaternary structure

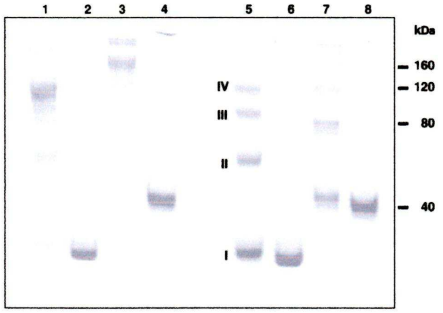

Fig. 1 SDS-PAGE analysis of cross-linked SaADH. *Lanes 1* and *5* DMS- and DMA-cross-linked and denatured enzyme, respectively. *Lanes 2* and *6* non-cross-linked denatured enzyme. *Lanes 3* and *7* DMS- and DMA-cross-linked and denatured aldolase, respectively. *Lanes 4* and *6* non-cross-linked denatured aldolase. The kDa values refer to Mr of monomer, dimer, trimer, and tetramer of cross-linked aldolase, used as molecular mass markers. *I*, *II*, *III*, and *IV* indicate the monomer, dimer, trimer, and tetramer of DMS-cross-linked SaADH. Cross-linking reaction and SDS-PAGE were carried out as described in "Materials and methods"

of SaADH was further investigated by chemical cross-linking using dimethyladipimate (DMA, N–N distance 8.6 Å) and dimethylsuberimidate (DMS, N–N distance 11.0 Å) as bifunctional reagents. SDS-PAGE of the DMA-cross-linked enzyme resulted in the appearance of four bands decreasing in intensity from monomer to tetramer (Fig. 1). However, the longer cross-linking reagent, DMS, resulted in a pattern predominantly consisting of cross-linked tetramer and smaller amounts of the other species (Fig. 1). These data suggest that SaADH has a tetrameric structure which adopts a more compact structure in the presence of salt, resulting in greater permeation into the packing pores of the gel matrix. However, it is not excluded that a tetramer to dimer dissociation occurs in the presence of relatively high salt concentration.

The molecular mass of the subunit determined by ESI-MS analysis proved to be 28,978.0 Da (average mass), in agreement with the theoretical value of the sequence.

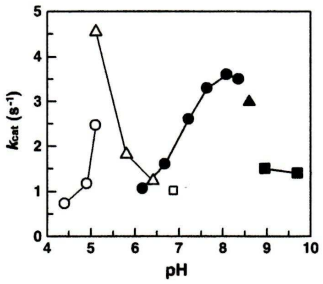

Fig. 2 SaADH activity as a function of pH in the reduction and oxidation reactions. The following 50 mM buffer solutions were used: sodium acetate (*open circles*), MES (*open triangles*), and sodium phosphate (*open square*) in the reduction reaction, and sodium phosphate (*filled circles*), Tris–HCl (*filled triangle*), and glycine–NaOH (*filled squares*) in the oxidation reaction. The mixture for the reduction reaction contained 25 mM methyl benzoylformate and 0.1 mM NADH, and the mixture for the oxidation reaction contained 25 mM cycloheptanol and 5 mM NAD^+. The assays were performed at 65°C under the conditions described in "Materials and methods"

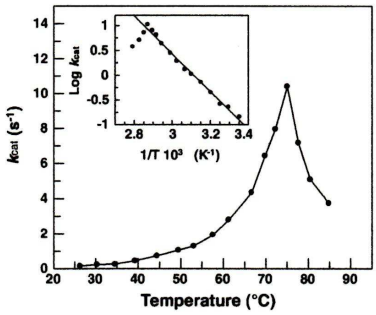

Fig. 3 Temperature dependence of the SaADH activity. The assay was carried out as described in "Materials and methods", using cycloheptanol as the substrate. The *inset* shows the Arrhenius plot from the same data. The value of the activation energy was 72.8 ± 2.0 kJ mol^{-1}

Optimal pH and thermophilicity

Figure 2 shows the pH dependence of SaADH in the reduction and oxidation reactions. The SaADH activity was found to be closely dependent on pH in the reduction reaction, displaying a narrow peak of maximum activity at approximately pH 5.1. The oxidation reaction showed a less marked dependence on pH, displaying a peak with a maximum at around pH 8.2.

The effect of temperature on SaADH activity is shown in Fig. 3. The reaction rate increases up to 75°C and then decreases rapidly due to thermal inactivation. This optimal temperature value is similar to that of TtADH (73°C) (Pennacchio et al. 2008), lower than that of thermophilic medium-chain, zinc-containing ADHs such as SsADH (88°C) (Raia et al. 2001) and TbADH (85°C) (Korkhin et al. 1998), and significantly lower than that of *Pyrococcus furiosus* aldo–keto reductase (100°C) (Machielsen et al. 2006). The activation energy for oxidation is 72.8 ± 2.0 kJ mol^{-1}, which is higher than that determined for TtADH (62.9 ± 2.6 kJ mol^{-1}) (Pennacchio et al. 2008) or SsADH (46.7 kJ mol^{-1}) (Raia et al. 2001), and lower than that reported for TbADH (94.1 kJ mol^{-1}) (Korkhin et al. 1998).

Coenzyme and substrate specificity

The enzyme showed no activity with NADP(H) and full activity with NAD(H). This coenzyme preference further supports the evidence that an aspartate residue at position 37 of an SDR enzyme (numbering of LB-RADH) plays a critical role in discriminating NAD(H) from NADP(H) (Filling et al. 2002; Kallberg et al. 2002, Pennacchio et al. 2008). The specificity of SaADH for various alcohols, aldehydes and ketones was examined (Table 2). The enzyme showed no activity on aliphatic linear and branched alcohols (not shown), except for a poor activity on 2-propyn-1-ol, 3-methyl-1-butanol and 2-pentanol; however, it showed a discrete activity on aliphatic cyclic and bicyclic alcohols. Benzyl alcohol and 4-bromobenzyl alcohol were not found to be substrates. In contrast, in view of the great influence that the strong electron-donating methoxy group exerts on the *para* position of the benzene ring, only the 4-methoxybenzyl alcohol was found to be an active substrate. (*S*)-1-Phenylethanol was also found to be an active substrate, whereas the *S* and *R* enantiomers of α-(trifluoromethyl)benzyl alcohol and methyl and ethyl mandelates showed no apparent activity with SaADH (data not shown). Moreover, the enzyme showed relatively poor activity on (±)-1-phenyl-1-propanol, 1-(1-naphthyl)ethanol and the two enantiomers of 1-(2-naphthyl)ethanol. However, SaADH showed highest activity with 1-indanol and α-tetralol (Table 2).

The enzyme was not active on aliphatic and aromatic aldehydes, and on aliphatic linear, branched and cyclic ketones (data not shown) except for 3-methylcyclohexanone (Table 2). However, the enzyme showed a relatively high reduction rate with isatin, 2,2,2-trifluoroacetophenone, and with an aryl diketone such as 1-phenyl-1,2-propanedione, and a bicyclic ketone such as 1-decalone (Table 2). The electronic factor accounts for the discrete activity measured with (*S*)-1-phenylethanol and 2,2,2-trifluoroacetophenone, as compared to the apparent catalytic inactivity observed with acetophenone and (*S*)-α-(trifluoromethyl)benzyl

Table 2 Substrate specificity of SaADH in the oxidation and reduction reactions

Substrate	Relative activity (%)	Substrate	Relative activity (%)
Alcohols[a]		Ketones[b]	
2-Propyn-1-ol	6	Cyclohexanone	0
3-Methyl-1-butanol	4	2-Methylcyclohexanone	0
(±)-2-Pentanol	5	3-Methylcyclohexanone	29
(*S*)-2-Pentanol	11	4-Methylcyclohexanone	0
(*R*)-2-Pentanol	0	2,6-Dimethylcyclohexanone	0
Cyclopentanol	5	Cycloheptanone	0
Cyclohexanol	8	1-Decalone	14
Cycloheptanol	37	Acetophenone	0
Cyclohexylmethanol[c]	0	2,2,2-Trifluoroacetophenone	100
2-Cyclohexylethanol	0	1-Indanone	0
3-Methylcyclohexanol[c]	14	α-Tetralone	0
3-Cyclohexyl-1-propanol[c]	0	1-phenyl-1,2-propanedione	70
cis-Decahydro-1-naphthol	11	Isatin[d]	300
Benzyl alcohol	0	2-Acetonaphthone	0
2-Methoxybenzyl alcohol	0	Keto esters[b]	
3-Methoxybenzyl alcohol	0	Ethyl pyruvate	43
4-Methoxybenzyl alcohol	5	Methyl benzoylformate	100
(*R*,*S*)-1-Phenylethanol[c]	6	Methyl *o*-chlorobenzoylformate	160
(*S*)-(−)-1-Phenylethanol	8	Ethyl benzoylformate	88
(*R*)-(+)-1-Phenylethanol	0	Ethyl 4-chloroacetoacetate	27
(±)-1-Phenyl-1-propanol[c]	8		
1-(1-Naphthyl)ethanol	5		
(±)-1-(2-Naphthyl)ethanol	6		
(*R*)-1-(2-Naphthyl)ethanol	5		
(*S*)-1-(2-Naphthyl)ethanol	5		
(*R*)-3-Chloro-1-phenyl-1-propanol	5		
(*R*)-1-Indanol[e]	62		
(*S*)-1-Indanol[e]	100		
(*R*)-α-Tetralol[c]	58		
(*S*)-α-Tetralol[c]	12		

[a] The assays were performed using 1 ml of mixture containing 10 mM alcohol and 5 mM NAD^+ in 25 mM sodium phosphate, pH 8.0, at 65°C for 1 min. Relative rates were calculated by setting the activity to be 100 for (*S*)-1-indanol

[b] The assays were performed using 1 ml of mixture containing 10 mM carbonyl compound and 0.1 mM NADH in 37.5 mM MES–NaOH, pH 5.5, at 65°C for 1 min. Substrates were dissolved in 2-propanol and added to the reaction mixture (10 mM in 2% (v/v) 2-propanol). The percent values refer to 2,2,2-trifluoroacetophenone for ketones, and to methyl benzoylformate for ketoesters

[c] Substrates were dissolved in 100% 2-propanol

[d] Substrate concentration, 1 mM; solvent, acetonitrile; the enzyme was present at a sevenfold lower concentration

[e] Substrate was dissolved in 100% acetonitrile

alcohol. In fact, although the CF_3 group is sterically more demanding than the CH_3 group (van der Waals volume = 42.7 and 24.5 $Å^3$, respectively) (Zhao et al. 2003), the electron-withdrawing character of fluorine favours hydride transfer, inductively decreasing electron density at the acceptor carbon C1. It is noteworthy that SaADH proved to be very effective in reducing aliphatic and aryl α-keto esters, halogenated aryl α-keto esters, and halogenated β-keto esters (Table 2).

These data show that SaADH is a strictly NAD(H)-dependent oxidoreductase that has discrete substrate specificity. As such, SaADH is more similar to the thermophilic TtADH (Pennacchio et al. 2008), than to the three SDR superfamily mesophilic ADHs (i.e., LSADH, LB-RADH, and PED) which are active on a variety of aliphatic as well as aromatic alcohols, ketones, diketones and keto esters.

Kinetic studies

The kinetic parameters of SaADH determined for the most active substrates are shown in Table 3. Based on the specificity constant (k_{cat}/K_m), this enzyme shows a fivefold greater preference for (*R*)- than (*S*)-α-tetralol, but a similar preference for the enantiomers of 1-indanol. (*R*)- and (*S*)-1-(2-naphthyl)ethanol are very poor substrates and display similar specificity constants. Alicyclic alcohols such as 3-methylcyclohexanol, cycloheptanol and *cis*-decahydro-1-naphthol were oxidized with relatively low efficiency. In the reduction reaction, isatin was preferred more than

Table 3 Steady-state kinetic constants of SaADH

Substrate	k_{cat} (s^{-1})	K_m (mM)	k_{cat}/K_m (s^{-1} mM^{-1})
3-Methylcylohexanol	3.4 ± 0.2	9.9 ± 0.5	0.34
Cycloheptanol	4.4 ± 0.1	9.3 ± 0.3	0.47
(±)-1-Indanol	6.6 ± 0.2	2.30 ± 0.02	2.86
(*R*)-Indanol	7.1 ± 0.2	2.39 ± 0.01	2.98
(*S*)-Indanol	13.7 ± 0.4	6.4 ± 0.3	2.14
cis-Decahydro-1-naphthol	0.98 ± 0.04	4.2 ± 0.3	0.23
α-Tetralol	1.2 ± 0.1	0.48 ± 0.09	2.5
(*R*)-α-Tetralol	13.5 ± 0.5	1.28 ± 0.03	10.5
(*S*)-α-Tetralol	2.1 ± 0.2	1.05 ± 0.08	2.0
(±)-1-(2-Naphthyl)ethanol	0.43 ± 0.01	3.7 ± 0.4	0.11
(*R*)-(+)-1-(2-Naphthyl)ethanol	0.54 ± 0.06	5.3 ± 0.7	0.10
(*S*)-(−)-1-(2-Naphthyl)ethanol	0.48 ± 0.01	5.4 ± 0.5	0.09
NAD^+	3.7 ± 0.1	0.44 ± 0.04	8.4
3-Methylcyclohexanone	3.8 ± 0.03	66.0 ± 3.1	0.06
2,2,2-Trifluoroacetophenone	10.0 ± 0.6	23.5 ± 1.3	0.42
1-Phenyl-1,2-propanedione	3.1 ± 0.3	12.1 ± 2.2	0.25
Methyl benzoylformate	6.2 ± 0.21	6.5 ± 0.4	0.95
Methyl *o*-chlorobenzoylformate	9.2 ± 0.9	2.8 ± 0.2	3.3
Ethyl benzoylformate	2.35 ± 0.07	5.3 ± 0.4	0.44
Isatin	22.0 ± 2.5	0.71 ± 0.11	31
NADH	28.0 ± 2.5	0.16 ± 0.02	175

The activity was measured at 65°C as described in "Materials and methods". Kinetic constants for NAD^+ and NADH were determined with 25 mM cycloheptanol and 5 mM isatin, respectively. The k_{cat} and K_m data are the mean ± standard deviations

methyl and ethyl benzoylformate, and the halogenated acetophenones as well as the aryl diketone 1-phenyl-1,2-propanedione. It is noteworthy that a chlorine substituent at position 2 of the phenyl ring of methyl benzoylformate enhances the reaction rate to 150%, due to the electron-withdrawing character of halogen; it also increases the affinity of the substrate, reflecting the hydrophobic character of the environment surrounding the phenyl group. Moreover, the specificity constant value is 21-fold higher for NADH than NAD^+.

These results suggest that the physiological direction of the catalytic reaction is reduction rather than oxidation. However, the natural substrate and function of SaADH are unknown. As far as the substrate stereospecificity of SaADH is concerned the enzyme does not seem discriminate between the enantiomer *S* and *R* of 1-indanol, α-tetralol and 1-(2-naphthyl)ethanol, based on the similarity in the K_m values.

Coenzyme stereospecificity

The ^1H NMR spectrum of the deuterium-labelled NADD obtained by the reaction of SaADH with 1-phenylethanol-d_9 and NAD^+ shows a single peak at 2.68 ppm corresponding to the *pro-R* hydrogen at the C-4 position of NADD in place of a double doublet centered at 2.62 ppm present in the NADH spectrum (data not shown). The presence of a *pro-S* deuterium atom at C-4 of the pyridine ring of the NADD produced indicates that SaADH transfers the deuteride to the *Si*-face of NAD^+, as illustrated in Fig. 4. Therefore, SaADH is a B-type (*pro-S* specific) dehydrogenase in agreement with the classification proposed by Schneider-Bernlöhr et al. (1986) that the SDRs enzymes are *pro-S*, whereas the medium-chain ADHs are *pro-R*, recently substantiated by the structural studies of Kwiecień et al. (2009). SaADH shares the same coenzyme stereospecificity with few other short-chain ADHs such as the thermophilic *T. thermophilus* ADH and the mesophilic enzymes *Leifsonia* sp. strain S749 ADH, 1-phenylethanol dehydrogenase from the denitrifying bacterium strain EbN1, and *Mucor javanicus* and *Drosophila* ADH (Pennacchio et al. 2009 and references therein).

Thermal stability

The thermal stability of SaADH was determined by measuring the residual enzymatic activity after 30 min of incubation over a temperature range from 25 to 95°C (Fig. 5). SaADH was shown to be quite stable up to a temperature of 80°C, above which its activity decreased abruptly, resulting in a $T_{1/2}$ value (the temperature of 50% inactivation) of ~88°C.

The residual activity measured after 24 h incubation in 50 mM Tris–HCl, pH 9.0, at 50 and 70°C was 109 and 76%, respectively. In 50 mM Tris–H_3PO_4, pH 7.0, i.e., the buffer used for the bioconversion studies, the residual

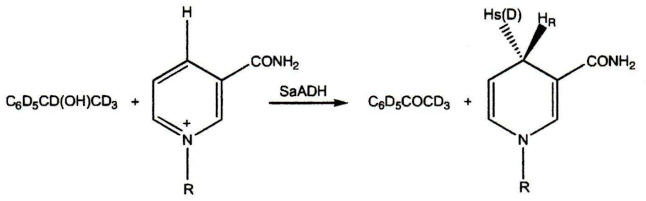

Fig. 4 Stereospecificity of hydrogen transfer catalysed by SaADH. *R* adenosine diphosphate ribose

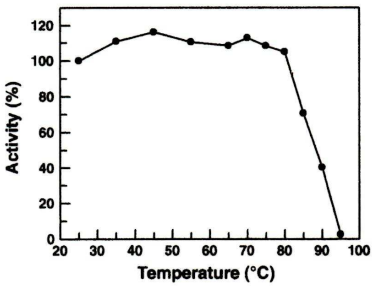

Fig. 5 Thermal denaturation of SaADH monitored by dehydrogenase activity. The stability was studied by incubating 0.2 mg ml^{-1} protein samples in 50 mM Tris–HCl, pH 9.0 for 30 min at the indicated temperatures. Activity measurements were carried out under the conditions of the standard assay using cycloheptanol as the substrate. The assay temperature was 65°C

activity measured after 6 and 24 h incubation at 50°C was 105 and 107%, respectively.

Effects of various compounds

The effects of salts, ions and reagents on SaADH activity were studied by adding each compound to the standard assay mixture (Table 4). The chlorides of Li^+, Na^+, K^+, Ca^{2+}, Mg^{2+}, and Mn^{2+} did not affect the enzyme's activity, whereas the sulphate of heavy metal ions such as Fe^{2+}, Co^{2+}, and Cu^{2+} caused a slight inactivation. Iodoacetate and Hg^{2+} did, to some extent, affect the activity, indicating that the only Cys residue per monomer, C67, may have a functional role.

The presence of metal-chelating agents did not affect enzyme activity, suggesting that either the protein does not require metals for its activity or the chelating molecule was not able to remove the metal under the assay conditions. Furthermore, the enzyme showed no loss in activity following exhaustive dialysis against EDTA. The EDTA-dialysed enzyme turned out to be quite stable at 70°C for 6 h, both in the absence and the presence of EDTA or *o*-phenanthroline (data not shown). These results suggest that SaADH does not require metals for its activity or structural stabilization. This is usual for the typically non-metal SDRs enzymes, although the well-known LB-RADH shows strong Mg^{2+} dependency (Niefind et al. 2003).

Stability in organic solvents

The effects of common organic solvents, such as 2-propanol, ethyl acetate, acetonitrile, *n*-hexane, *n*-heptane, *tert*-butylmethyl ether (TBME), methanol, and 1,4-dioxane, on SaADH were investigated at 50°C and at two different time points (Fig. 6). SaADH was activated up to 115% after incubation for 6 h in aqueous buffer and up to 120–125% after incubation for 25 h in the presence of 17% 2-propanol or 17% acetonitrile. Significant increases in enzyme activity occurred after 25 h incubation when ethyl acetate, *n*-hexane, *n*-heptane, TBME, and 1,4-dioxane were present at 30% concentration. Activity values ranged from 170 to 210% of the values determined prior to incubation. However, the presence of 2-propanol, acetonitrile, and 1,4-dioxane at a high concentration (30%) resulted in enzyme inactivation to 5–30% of the initial values following 5 h incubation at 50°C.

Standard assays performed in the presence of 0.1–0.5% 2-propanol and 0.15% TBME did not affect enzyme activity, suggesting that the enhancement in activity was not due to an immediate effect of solvent on the protein structure. A considerable body of literature exists which describes the activation of thermophilic enzymes by loosening of their rigid structure in the presence of protein perturbants (Fontana et al. 1998; Liang et al. 2004). To account for the observed enhancements of SaADH activity, the organic solvent is proposed to induce a conformational change in the protein molecule to a more relaxed and flexible conformation that is optimal for activity. Analogously, the activating effect following heating of SaADH in aqueous buffer at 50°C over a short period (Fig. 6) may be due to partial loosening of the overall structure, inducing an increased flexibility at the active site, and consequently an increased turnover.

Enantioselectivity

The enantioselectivity of SaADH was tested using α-methyl and α-ethyl benzoylformate, methyl *o*-chlorobenzoylformate,

Table 4 Effect of various compounds on SaADH

Compound	Concentration (mM)	Relative activity (%)
None		100
LiCl	1	110
NaCl	1	88
	10	95
KCl	1	99
	10	97
$MgCl_2$	1	94
	10	98
$CaCl_2$	1	100
	10	99
$MnCl_2$	1	95
$FeSO_4$	1	80
$CoSO_4$	1	89
$NiSO_4$	1	106
$CuSO_4$	1	89
$ZnSO_4$	1	91
$Hg(CH_3COO)_2$	1	63
2-Mercaptoethanol	5	112
Iodoacetate	4	88
o-Phenanthroline	1	110
EDTA	1	93
	10	107

Each compounds was added to the reaction mixture at the indicated concentration. The enzyme activity was measured at 65°C using cycloheptanol as substrate

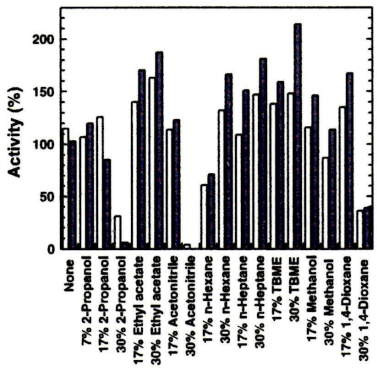

Fig. 6 Effect of organic solvents on SaADH. Samples of enzyme (0.5 mg ml^{-1}) were incubated at 50°C in the absence and presence of the organic solvents at the concentrations indicated, and assays were performed after 6 h (*white bars*) and 25 h (*grey bars*). The activity assays were performed as described in "Materials and methods" using (*R*)-α-tetralol as the substrate. The data obtained in the absence and presence of organic solvents are expressed as percentage of activity relative to the value determined prior to incubation

and 1-indanone as substrates, and an NADH regeneration system consisting of glucose and glucose dehydrogenase from *Thermoplasma acidophilum* (TaGDH), a thermophilic enzyme with dual coenzyme specificity, but with a marked preference for NADP(H) over NAD(H) (John et al. 1994). Tris–phosphate buffer pH 7.0 and 50°C was chosen as the pH and temperature conditions suitable for catalysis by the two archaeal enzymes. Thermal stability studies indicated that TaGDH activity dropped to ~70 and 35% following 24 h incubation at 50°C in Tris–phosphate buffer, pH 7.0, in the absence and presence of 10% acetonitrile, respectively (data not shown).

Bioconversions of EBF were carried out allowing the reactions to proceed for 1, 3, 6 and 24 h at 50°C. Figure 7 shows that conversion of EFB was completed in 6 h. However, reaction times as long as 24 h did not improve the enantiomeric excess (ee) of the biotransformation. SaADH preferably reduced this keto ester to ethyl (*R*)-mandelate with an ee of 50%, after 6 h of reaction. Methyl benzoylformate was reduced by SaADH to methyl (*S*)-mandelate with 100% conversion after 6 h of reaction and an ee of 17%, and methyl *o*-chlorobenzoylformate was reduced to methyl (*R*)-*o*-chloromandelate with >99% conversion and an ee of 72% (Table 5). These results show that enantioselectivity of SaADH is dependent upon the structure of both the phenyl group and alkyl substituent of the ester group of the substrate. 1-Indanone was reduced to the corresponding (*S*)-alcohol following a 6-h reaction at 50°C, with a conversion of 6% and an ee of 25%, reflecting the apparent inactivity under different assay conditions (see Table 2). It is noteworthy that the optically active alcohols produced are used as chiral building blocks in organic synthesis. Methyl (*R*)-*o*-chloromandelate is an intermediate

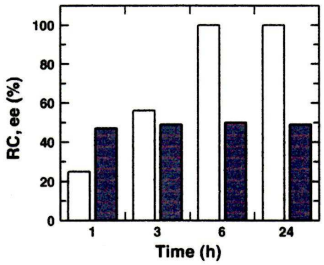

Fig. 7 Reduction of ethyl benzoylformate catalysed by SaADH. Biotransformations were carried out at 50°C at different reaction times as described in "Materials and methods". The reactions were stopped by addition of ethyl acetate at the times indicated. The dried extracts were analysed by chiral HPLC to determine the relative conversion (RC, *open bars*) and the enantiomeric excess (ee, *grey bars*)

Table 5 Asymmetric reduction of carbonyl compounds by SaADH

Substrate	Product	Conversion[a] (%)	ee[a] (%)	*R/S*
Methyl benzoylformate	Methyl mandelate	100	17	*S*
Ethyl benzoylformate	Ethyl mandelate	100	50	*R*
Methyl *o*-chlorobenzoylformate	Methyl *o*-chloromandelate	100	72	*R*

Reactions were performed at 50°C for 6 h as described in "Materials and methods"

[a] Conversion yields and enantiomeric excesses were determined by chiral HPLC analysis. Configuration of product alcohol was determined by comparing the retention time with that of standard samples as described in "Materials and methods"

for the platelet aggregation inhibitor clopidogrel (Ema et al. 2008), and (*R*)-ethyl mandelate is precursor for the synthesis of cryptophycins (Gardinier and Leahy 1997).

To our knowledge, this study represents the first biochemical characterization of an NAD(H)-dependent archaeal short-chain ADH. The remarkable activation of SaADH by organic solvents constitutes evidence of the sturdiness of this biocatalyst, and suggests exploratory investigations on conversions of poorly water-soluble prochiral substrates in a biphasic reaction media. Moreover, the importance of the critical role of the above-mentioned D37 in SDRs in discriminating NAD(H) from NADP(H) is further supported by this study.

Acknowledgments This work was funded by FIRB (Fondo per gli Investimenti della Ricerca di Base) RBNE034XSW, and by the ASI project MoMa n. 1/014/06/0.

References

Asada Y, Endo S, Inoue Y, Mamiya H, Hara A, Kunishima N, Matsunaga T (2009) Biochemical and structural characterization of a short-chain dehydrogenase/reductase of *Thermus thermophilus* HB8: a hyperthermostable aldose-1-dehydrogenase with broad substrate specificity. Chem Biol Interact 178:117–126

Ceccarelli C, Liang ZX, Strickler M, Prehna G, Goldstein BM, Klinman JP, Bahnson BJ (2004) Crystal structure and amide H/D exchange of binary complexes of alcohol dehydrogenase from *Bacillus stearothermophilus*: insight into thermostability and cofactor binding. Biochemistry 43:5266–5277

Chen L, Brügger K, Skovgaard M, Redder P, She Q, Torarinsson E, Greve B, Awayez M, Zibat A, Klenk HP, Garrett RA (2005) The genome of *Sulfolobus acidocaldarius*, a model organism of the Crenarchaeota. J Bacteriol 187:4992–4999

Davies GE, Stark GR (1970) Use of dimethyl suberimidate, a cross-linking reagent, in studying the subunit structure of oligomeric proteins. Proc Natl Acad Sci USA 66:651–656

Ema T, Ide S, Okita N, Sakai T (2008) Highly efficient chemoenzymatic synthesis of methyl (*R*)-*o*-chloromandelate, a key intermediate for clopidogrel, via asymmetric reduction with recombinant *Escherichia coli*. Adv Synth Catal 350:2039–2044

Filling C, Berndt KD, Benach J, Knapp S, Prozorovski T, Nordling E, Ladenstein R, Jörnvall H, Oppermann U (2002) Critical residues for structure and catalysis in short-chain dehydrogenases/reductases. J Biol Chem 277:25677–25684

Fontana A, De Filippis V, Polverino de Laureto P, Scaramella E, Zambonin M (1998) Rigidity of thermophilic enzymes. In: Ballestreros A, Plou FJ, Iborra JL, Halling PJ (eds) Stability and stabilization in biocatalysis, vol 15. Elsevier, Amsterdam, The Netherlands, pp 277–294

Gardinier KM, Leahy JW (1997) Enantiospecific total synthesis of the potent antitumor macrolides cryptophycins 1 and 8. J Org Chem 62:7098–7099

Giordano A, Febbraio F, Russo C, Rossi M, Raia CA (2005) Evidence for co-operativity in coenzyme binding to tetrameric *Sulfolobus solfataricus* alcohol dehydrogenase and its structural basis: fluorescence, kinetic and structural studies of the wild-type enzyme and non-co-operative N249Y mutant. Biochem J 388:657–667

Guy JE, Isupov MN, Littlechild JA (2003) The structure of an alcohol dehydrogenase from the hyperthermophilic archaeon *Aeropyrum pernix*. J Mol Biol 331:1041–1051

Höffken HW, Duong M, Friedrich T, Breuer M, Hauer B, Reinhardt R, Rabus R, Heider J (2006) Crystal structure and enzyme kinetics of the (*S*)-specific 1-phenylethanol dehydrogenase of the denitrifying bacterium strain EbN1. Biochemistry 45:82–93

Hummel W (1999) Large-scale applications of NAD(P)-dependent oxidoreductases: recent developments. Trends Biotechnol 17:487–492

Inoue K, Makino Y, Dairi T, Itoh N (2006) Gene cloning and expression of *Leifsonia* alcohol dehydrogenase (LSADH) involved in asymmetric hydrogen-transfer bioreduction to produce (*R*)-form chiral alcohols. Biosci Biotechnol Biochem 70:418–426

John J, Crennell SJ, Hough DW, Danson MJ, Taylor GL (1994) The crystal structure of glucose dehydrogenase from *Thermoplasma acidophilum*. Structure 2:385–393

Jones JB, Beck JF (1976) Applications of biochemical systems in organic chemistry. In: Jones JB, Sih CJ, Perlman D (eds) Techniques of chemistry series, part I, vol 10. Wiley, New York, NY, pp 248–401

Jörnvall H (2008) Medium- and short-chain dehydrogenase/reductase gene and protein families: MDR and SDR gene and protein superfamilies. Cell Mol Life Sci 65:3873–3878

Kallberg Y, Oppermann U, Jörnvall H, Persson B (2002) Short-chain dehydrogenases/reductases (SDRs). Eur J Biochem 269:4409–4417

Kavanagh KL, Jörnvall H, Persson B, Oppermann U (2008) Medium- and short-chain dehydrogenase/reductase gene and protein families: the SDR superfamily: functional and structural diversity within a family of metabolic and regulatory enzymes. Cell Mol Life Sci 65:3895–3906

Keinan E, Hafely EK, Seth KK, Lamed R (1986) Thermostable enzymes in organic synthesis. Asymmetric reduction of ketones with alcohol dehydrogenase from *Thermoanaerobium brockii*. J Am Chem Soc 108:162–169

Korkhin Y, Kalb(Gilboa) AJ, Peretz M, Bogin O, Burstein Y, Frolow F (1998) NADP-dependent bacterial alcohol dehydrogenases: crystal structure, cofactor-binding and cofactor specificity of the ADHs of *Clostridium beijerinckii* and *Thermoanaerobacter brockii*. J Mol Biol 278:967–981

Kroutil W, Mang H, Edegger K, Faber K (2004) Recent advances in the biocatalytic reduction of ketones and oxidation of sec-alcohols. Curr Opin Chem Biol 8:120–126

Kwiecień RA, Ayadi F, Nemmaoui Y, Silvestre V, Zhang BL, Robins RJ (2009) Probing stereoselectivity and pro-chirality of hydride transfer during short-chain alcohol dehydrogenase activity: a combined quantitative 2H NMR and computational approach. Arch Biochem Biophys 482:42–51

Laemmli UK (1970) Cleavage of structural proteins during the assembly of the head of bacteriophage T4. Nature 227:680–685

Leatherbarrow RJ (2004) GraFit Version 5.0.11. Erithacus Software Ltd., Horley, UK

Liang ZX, Lee T, Resing KA, Ahn NG, Klinman JP (2004) Thermal-activated protein mobility and its correlation with catalysis in thermophilic alcohol dehydrogenase. Proc Natl Acad Sci USA 101:9556–9561

Machielsen R, Uria AR, Kengen SW, van der Oost J (2006) Production and characterization of a thermostable alcohol dehydrogenase that belongs to the aldo–keto reductase superfamily. Appl Environ Microbiol 72:233–238

Machielsen R, Leferink NG, Hendriks A, Brouns SJ, Hennemann HG, Daussmann T, van der Oost J (2008) Laboratory evolution of *Pyrococcus furiosus* alcohol dehydrogenase to improve the production of (2*S*,5*S*)-hexanediol at moderate temperatures. Extremophiles 12:587–594

Nie Y, Xu Y, Mu XQ, Wang HY, Yang M, Xiao R (2007) Purification, characterization, gene cloning, and expression of a novel alcohol dehydrogenase with anti-Prelog stereospecificity from *Candida parapsilosis*. Appl Environ Microbiol 73:3759–3764

Niefind K, Müller J, Riebel B, Hummel W, Schomburg D (2003) The crystal structure of R-specific alcohol dehydrogenase from *Lactobacillus brevis* suggests the structural basis of its metal dependency. J Mol Biol 327:317–328

Pennacchio A, Pucci B, Secundo F, La Cara F, Rossi M, Raia CA (2008) Purification and characterization of a novel recombinant highly enantioselective, short-chain NAD(H)-dependent alcohol dehydrogenase from *Thermus thermophilus*. Appl Environ Microbiol 74:3949–3958

Pennacchio A, Giordano A, Esposito L, Langella E, Rossi M, Raia CA (2009) Insight into the Stereospecificity of Short-Chain Thermus thermophilus Alcohol Dehydrogenase Showing pro-S Hydride Transfer and Prelog Enantioselectivity. Protein Pept Lett (in press)

Persson B, Kallberg Y, Bray JE, Bruford E, Dellaporta SL, Favia AD, Duarte RG, Jörnvall H, Kavanagh KL, Kedishvili N, Kisiela M, Maser E, Mindnich R, Orchard S, Penning TM, Thornton JM, Adamski J, Oppermann U (2009) The SDR (short-chain dehydrogenase/reductase and related enzymes) nomenclature initiative. Chem Biol Interact 178:94–98

Radianingtyas H, Wright PC (2003) Alcohol dehydrogenases from thermophilic and hyperthermophilic archaea and bacteria. FEMS Microbiol Rev 27:593–616

Raia CA, Giordano A, Rossi M (2001) Alcohol dehydrogenase from *Sulfolobus solfataricus*. Methods Enzymol 331:176–195

Sambrook J, Fritsch EF, Maniatis T (1989) Molecular cloning: a laboratory manual, 2nd edn. Cold Spring Harbor Laboratory Press, Cold Spring Harbor, NY

Schlieben NH, Niefind K, Muller J, Riebel B, Hummel W, Schomburg D (2005) Atomic resolution structures of R-specific alcohol dehydrogenase from *Lactobacillus brevis* provide the structural bases of its substrate and cosubstrate specificity. J Mol Biol 349:801–813

Schneider-Bernlöhr H, Adolph H-W, Zeppezauer M (1986) Coenzyme stereospecificity of alcohol/polyol dehydrogenases: conservation of protein types vs. functional constraints. J Am Chem Soc 108:5573–5576

van der Oost J, Voorhorst WG, Kengen SW, Geerling AC, Wittenhorst V, Gueguen Y, de Vos WM (2001) Genetic and biochemical characterization of a short-chain alcohol dehydrogenase from the hyperthermophilic archaeon *Pyrococcus furiosus*. Eur J Biochem 268:3062–3068

Zhao YH, Abraham MH, Zissimos AM (2003) Fast calculation of van der Waals volume as a sum of atomic and bond contributions and its application to drug compounds. J Org Chem 68:7368–7373

Zhu D, Malik HT, Hua L (2006) Asymmetric ketone reduction by a hyperthermophilic alcohol dehydrogenase. The substrate specificity, enantioselectivity and tolerance of organic solvents. Tetrahedron: Asymmetry 17:3010–3014

Zhu D, Hyatt BA, Hua L (2009) Enzymatic hydrogen transfer reduction of α-chloro aromatic ketones catalyzed by a hyperthermophilic alcohol dehydrogenase. J Mol Catal B: Enzym 56:272–276

Abstracts

Angela Pennacchio, Mosè Rossi, and Carlo A. Raia

Practical synthesis of cinnamyl alcohol from cinnamaldehyde with *B. stearothermophilus* alcohol dehydrogenase as isolated enzyme and in recombinant *E. coli* cells, Oral Communication.

XI National Biotechnology Congress, Varese, 27-29 June 2012, P. W10

Angela Pennacchio, Mosè Rossi, and Carlo A. Raia

A recombinant short-chain NAD(H)-dependent dehydrogenase/reductase from *Sulfolobus acidocaldarius* highly enantioselective on diaryl diketone benzil.

Biotrans 2011, October 2-6, 2011, Giardini Naxos (ME) Sicilia, Abstr. PC 152.

Angela Pennacchio, Assunta Giordano, Mosè Rossi, and Carlo A. Raia

Asymmetric Reduction of alfa-Keto Esters with *Thermus thermophilus* NADH-Dependent Carbonyl Reductase using Glucose Dehydrogenase and Alcohol Dehydrogenase for Cofactor Regeneration.

Biotrans 2011, October 2-6, 2011, Giardini Naxos (ME) Sicilia, Abstr. PC 153.

Angela Pennacchio, Assunta Giordano, Mosè Rossi, and Carlo A. Raia

Asymmetric reduction of α-keto esters with thermophilic NADH-dependent carbonyl reductase.

International Conference on Enzyme Science and Technology **(**ICEST), 31 October – 4 November 2011, Kusadasi (Turkey), Abstr. PP 64.

A. Pennacchio, A. Giordano, M. Rossi, and C. A. Raia

Effective synthesis of methyl (*R*)-mandelate by asymmetric reduction with a thermophilic NADH-dependent alcohol dehydrogenase.

Proceedings of 14th International Biotechnology Symposium and Exhibition, IBS 2010, 14-18 September 2010, Rimini – Italy